

POLITECNICO DI TORINO

Chemical and Materials Engineering College

Master of Science in Chemical and Sustainable Processes Engineering

Master thesis

Mechanical pre-treatments and particle size distribution in Anaerobic Digestion



Relators

prof. Ruggeri Bernardo,

Ing. Carlos E. Gómez Camacho

Candidate

firma del candidato
Chiara Barilaro

September 2018

Sommario

Introduzione

I combustibili fossili, come suggerisce il nome, sono molto antichi. A causa di questo fatto e della quantità limitata disponibile di queste risorse, oltre che per gli effetti indesiderati sull'ambiente e sulla salute umana, è bene ridurre la dipendenza dal petrolio per un approvvigionamento futuro sostenibile dell'energia. In questo senso, i biocarburanti intervengono come alternativa ai combustibili fossili e sono principalmente raggruppati in quattro generazioni:

- prima generazione: biodiesel da oli vegetali e etanolo dalla fermentazione di canna da zucchero o amido e biogas;
- seconda generazione: biomassa lignocellulosica, residui agricoli o materiale vegetale di rifiuto (a differenza della prima generazione, le materie prime non sono destinate al consumo umano);
- terza generazione: viene sfruttata la coltivazione di alghe, le quali fissano la CO₂ e non sottraggono terreni alla coltivazione;
- quarta generazione: eletrocombustibili e combustibili solari fotobiologici (la biomassa non è coinvolta).

Il biogas è, quindi, un biocarburante di seconda generazione ed è prodotto attraverso la Digestione Anaerobica (DA) a partire da diversi materiali organici, come fanghi di depurazione, rifiuti zootechnici, biomasse agricole e altri rifiuti (Tabella 1.1). Il biogas è costituito principalmente da metano (50-70%) e anidride carbonica (30-50%). Il potere calorifico del biogas dipende solo dal contenuto di metano; per questo motivo, la CO₂ è rimossa e destinata ad altri scopi (Figura 1.1). Il numero di impianti di biogas in Europa è praticamente triplicato in soli 6 anni, raggiungendo il numero di 17.376 nel 2015. Con 1.550 impianti, l'Italia è solamente seconda alla Germania, la quale ne possiede c. 10.846 (Figura 1.2).

Dal punto di vista microbiologico, la digestione anaerobica rappresenta un processo catabolico, in cui i batteri degradano il substrato utilizzando degli enzimi; dei catalizzatori biochimici di natura proteica prodotti nella cellula e rilasciati (esoenzimi) o meno (endoenzimi) all'esterno della stessa (Figura 1.3). Siccome nessun batterio è in grado di produrre tutti gli enzimi necessari alla degradazione del substrato, una vasta e diversificata comunità di batteri si rende indispensabile (Tabella 1.2). L'attività batterica nella DA può essere, poi, obbligati o facoltativamente anaerobica, oppure strettamente aerobica. Gli aerobi ricavano l'energia biosintetica e producono metaboliti solo in presenza di ossigeno molecolare libero (e producono ATP attraverso la respirazione). Gli anaerobi stretti, d'altra parte, sono inattivi in presenza di ossigeno molecolare libero, in quanto mancano di determinati enzimi essenziali per la loro sopravvivenza in presenza di ossigeno. Questi, infatti, rimuovono le specie reattive dell'ossigeno, che derivano dalla riduzione dell'ossigeno molecolare e provocano danni intracellulari. Il termine anaerobico facoltativo, invece, fa riferimento a una condizione di crescita ideale in assenza di ossigeno. Il processo di DA è composto da diversi step, in seguito riassunti.

1. La prima fase della DA, detta *idrolisi*, comporta la disintegrazione delle materie prime da parte dei batteri anaerobi facoltativi e obbligati attraverso la produzione di esoenzimi (idrolase). I carboidrati (come la cellulosa) sono scomposti in zuccheri

semplici; le proteine diventano singoli amminoacidi; mentre i grassi, formati da glicerolo e tre catene di acidi grassi, vedono le ultime rimosse dal gruppo di testa. Quando il substrato è complesso, questo diventa il *rate-determining step*.

2. Durante la seconda fase, la *acidogenesi*, i monomeri formati nella fase di idrolisi vengono convertiti in acidi organici a catena corta (C1-C5), alcoli, pochi composti organici dell'azoto e dello zolfo, insieme a idrogeno e anidride carbonica. Questo step è comunemente chiamato *la prima fermentazione*. Un valore di pH inferiore a 5,5 induce la produzione di solventi (come alcoli e acetone) e, cioè, le cellule entrano nella fase, nota come *solventogenesi*; da evitare, se si desidera portare a termine la DA, poiché i metanogeni non sopravvivono a pH acidi.
3. Il terzo stadio, noto come *acetogenesi* o *seconda fermentazione*, comporta la conversione degli acidi grassi volatili e degli alcoli in acido acetico e gas idrogeno (1.1).
4. Nell'ultimo step si ha la produzione di metano dalla degradazione dell'acetato (1.1) e dalla riduzione del biossido di carbonio a opera dell'idrogeno (1.2) (quest'ultima via rappresenta circa il 27-30% della produzione di CH₄ nei reattori della DA). I metanogeni si dividono, quindi, rispettivamente in *acetoclastici* e *idrogenotropici*, pur essendo anaerobi obbligati in entrambi i casi.

I batteri acetogenici, produttori obbligati di H₂ e inibiti da una quantità eccessiva del prodotto devono, quindi, vivere in una relazione sintrofica con i metanogeni idrogenotropici [9]. Il sintrofismo è quel fenomeno per cui una specie vive dei prodotti di un'altra specie [9]. Infatti, i secondi rimuovono costantemente il prodotto del metabolismo dei primi dal substrato, mantenendo la pressione parziale dell'idrogeno a basso livello, adatta ai batteri acetogenici. Invece, i monomeri (ad esempio zuccheri) possono essere catabolizzati dai batteri *omoacetogenici* ad acetato, che funge, poi, da substrato per i metanogeni acetoclastici convertendoli in CH₄ e CO₂.

Se solamente il glucosio è considerato come substrato (sostanza più fermentabile), la reazione di combustione di quest'ultimo (1.4) rilascerebbe circa 2.870 kJ/mol C₆H₁₂O₆ (ΔG), mentre la reazione di conversione del glucosio a metano attraverso la DA (1.3) è 390 kJ/mol C₆H₁₂O₆ (ΔG). La restante energia si trova immagazzinata nel metano, infatti, nella DA i microorganismi sfruttano l'energia presente nei legami carbonio-carbonio, causando un cambiamento dello stato di ossidazione degli atomi da 0 (nel glucosio) a -4 nel metano. Questa energia immagazzinata può essere sfruttata in seguito, ad esempio attraverso la combustione. Ciò è vantaggioso, in quanto la biomassa può contenere un grande quantitativo d'acqua, che non è necessario vaporizzare, poiché il processo di DA avviene in presenza di acqua. Inoltre, per la presenza di biomassa, la temperatura di lavoro è relativamente bassa.

Il phylum di batteri responsabile della DA è Firmicutes. I Firmicutes sono i batteri fermentativi responsabili della digestione degli acidi grassi volatili. A causa della grande disponibilità di questi ultimi, i Firmicutes sono quantitativamente dominanti nel digestore. Il phylum Firmicutes è composto principalmente da due classi di microorganismi: Clostridia (13%) e Bacilli (76%) [11], entrambi Gram-positivi e in grado di produrre endospore (lo "stato dormiente" a cui i batteri possono ridursi in condizioni ambientali stressanti, anche per periodi molto lunghi). Inoltre, i Clostridi sono anaerobi o aerotolleranti, mentre i bacilli sono aerobi obbligati o anaerobi facoltativi e possono essere considerati i successori evolutivi dei Clostridi Firmicutes anaerobici.

In assenza di nutrienti essenziali, la crescita dei microorganismi si ferma. Pertanto, si rende spesso necessario fornire eventuali nutrienti essenziali insieme al substrato oppure fare codigestione di substrati che hanno proprietà diverse. I nutrienti essenziali possono essere

suddivisi in macronutrienti (fonte di carbonio e fonte di azoto) e micronutrienti (oligoelementi). Come fonte di carbonio, ad esempio, lo zucchero viene consumato molto velocemente, a differenza della lignocellulosa, che, in effetti, è costituita da tre tipi di polimeri (cioè cellulosa, emicellulosa e lignina) fortemente interconnessi da legami covalenti e forze non covalenti. In generale, comunque, ogni biomassa può essere utilizzata come substrato, se contiene carboidrati, proteine, grassi, cellulosa ed emicellulosa come componenti principali nel giusto rapporto C:N. A causa della presenza di matrici difficilmente degradabili nei substrati, come la lignocellulosa, l'idrolisi è stata identificata come il passaggio chiave nel determinare la velocità del processo di DA. Per questo motivo, diverse tecnologie di pretrattamento sono volte a semplificare questa fase. Pretrattare il substrato prima che entri nel digestore anaerobico significa rompere la lignina e l'emicellulosa, e ridurre la struttura cristallina della cellulosa. In questo modo, il substrato è più solubile e viene promossa una digestione più rapida. I pretrattamenti attualmente applicabili sono classificati in:

- meccanici;
- termici;
- chimici (attraverso l'uso di alcali, acidi, ozono, ecc.);
- biologici (attraverso specifici microrganismi o specifici enzimi).

In questo lavoro sono stati investigati i pretrattamenti meccanici. Essi portano a particelle più piccole o a pezzi di substrato schiacciati. Infatti, la dimensione delle particelle influenza la velocità della digestione anaerobica poiché agisce sull'areasuperficiale del substrato disponibile per le idrolasi. Inoltre, la viscosità nel digestore diminuisce con il diminuire della dimensione delle particelle, rendendo più facile la miscelazione, poiché il sistema risulta essere più omogeneo.

In particolare, sono stati studiati i seguenti pretrattamenti.

- I mulini con sfere abrasive, nei quali i campioni vengono mescolate con sfere di vetro e poi sottoposte a vigorosa agitazione. Le cellule risultano, così, frantumate dagli urti meccanici tra le microsfere.
- L'omogeneizzatore a rotore-statore, composto da un albero di metallo rotante (rotore) all'interno di un tubo stazionario aperto (statore), che è sagomato con fessure nella parte finale (Figura 1.11). La rotazione del rotore crea un effetto di aspirazione che trascina il liquido nello spazio tra il rotore e lo statore; qui il liquido è soggetto a forze di taglio elevate a causa dello spazio ridotto (Figura 1.12).
- Il sonicatore con ultrasuoni batch, il quale si basa sull'utilizzo di onde acustiche, che vengono propagate da una sonda nel liquido in contatto con essa. In particolare, le onde acustiche sono onde di rarefazione e compressione che, quando propagate ad alta intensità in un liquido, generano cicli alternati di bassa e alta pressione. Durante il ciclo di bassa pressione, il liquido raggiunge la tensione di vapore, dando vita a piccole bolle. Durante la fase di alta pressione le bolle non possono più mantenere l'equilibrio tra la pressione e le forze viscose, e implodono violentemente. Tale implosione distrugge le pareti delle particelle di substrato vicine, che rilasciano materiale intercellulare. La cavitazione è quindi il principio fisico che sta dietro l'ultrasonificazione (Figura 1.13). L'apparecchiatura è composta da quattro componenti: generatore, convertitore (o trasduttore), booster e sonda (Figura 1.14). Il generatore trasforma la potenza della linea AC in energia elettrica ad alta frequenza (20-100 kHz), che viene ulteriormente trasformata dal convertitore in vibrazione (l'energia elettrica viene convertita in energia meccanica), grazie al materiale piezoelettrico di cui è costituito. Il booster aumenta l'ampiezza delle onde e la sonda, infine, diffonde le onde acustiche nel mezzo.

- La sonicazione continua (Figura 1.15), dove il campione liquido viene pompato nella camera del sonicatore; viene sottoposto a sonificazione durante il suo attraversamento ed esce dall'unità da una porta di uscita.

I pretrattamenti possono avere un impatto non solo sul substrato, ma anche sui microrganismi della DA in caso di processi di DA umidi, dove alla materia prima fresca viene aggiunta dell'acqua per raggiungere le condizioni ottime del processo (i.e. concentrazione si sostanza secca circa 100-150 g/L). In questo caso, la deidratazione è la prima fase del processo di post-digestione; la frazione solida deidratata è destinata ad essere utilizzata come fertilizzante e l'acqua viene riciclata per alimentare l'impianto. In questo caso, i microrganismi della DA vengono pretrattati insieme al substrato. Chiaramente, l'effetto desiderato per il substrato (la sua rottura) non è auspicabile anche per i microrganismi, che devono essere in grado di portare a termine le diverse fasi della DA. L'evoluzione subita dallo specifico tipo di microorganismo e il dominio (vedi Figura 1.3) determinano la facilità con cui i microorganismi possono risultare seriamente danneggiati.

La costituzione della cellula differisce a seconda del dominio a cui i microorganismi appartengono. La cellula dei batteri Gram-positivi è racchiusa in una membrana cellulare, avvolta ulteriormente dalla parete cellulare. La membrana è elastica, interattiva e semi-permeabile, in quanto formata principalmente da fosfolipidi e proteine. La parete cellulare è, invece, costituita da peptidoglicano, che conferisce rigidità all'involucro cellulare, per via dei legami chimici che lo caratterizzano (residui di N-acetil-glucosamina e acido N-acetilmuramico tenuti insieme da legami β - (1-4) -glicosidici). I batteri Gram-positivi possiedono, quindi, una parete cellulare spessa e composta per il 50-80% da peptidoglicano. D'altra parte, i batteri Gram-negativi hanno una parete cellulare relativamente sottile e costituita da pochi strati di peptidoglicano (anche se questo è il principale responsabile della resistenza cellulare), ma circondata da una seconda membrana a doppio strato lipidico, che comprende proteine, lipopolisaccaridi e fosfolipidi. I Firmicutes (Clostridia e Bacilli) sono classificati come batteri Gram-positivi. I metanogeni presentano una parete cellulare diversa, dovuto alla mancanza di acido muramico, e la membrana cellulare non contiene un estere lipidico come suo costituente principale [7] (Figura 1.16). Quindi, è possibile concludere che i metanogeni saranno più influenzati dagli sforzi di taglio, a causa della costituzione sia della membrana cellulare che della parete cellulare, che mancano di alcuni componenti responsabili della resistenza e che, al contrario, sono presenti nei Gram-positivi.

Procedura sperimentale

I pretrattamenti meccanici e la distribuzione della dimensione delle particelle in fase liquida sono l'oggetto di studio di questo progetto di tesi sperimentale. Per valutare l'effetto del pretrattamento in relazione allo scopo, la distribuzione delle dimensioni delle particelle è stata analizzata prima e dopo ogni pretrattamento. La prestazione ottimale della fase di pretrattamento porta a un cambiamento nella distribuzione delle dimensioni delle particelle del substrato verso diametri inferiori senza danneggiare considerevolmente la biomassa. La biomassa, il substrato e il brodo di fermentazione (substrato contenente biomassa) sono stati studiati separatamente. La biomassa consiste nelle specie *B. subtilis*, appartenente alla classe dei Bacilli, (Tabella 3.1) e la specie *C. acetobutylicum*, appartenente alla casse dei Clostridi (Tabella 3.5), separatamente studiate. Il substrato consta di una miscela di fibre di erba, piccoli residui di arbusti e di terreno in parti uguali, diluita con acqua deionizzata risultante in circa il

20% (w/w) di biomassa secca (Figura 3.4). Il brodo di fermentazione è il risultato delle condizioni di fermentazione in Tabella 3.7, ma, più in generale, un brodo di fermentazione è un mezzo complesso in cui coesistono le seguenti fasi: substrati grezzi, microrganismi e loro componenti (cioè la fase biologica), additivi chimici, prodotti di fermentazione, gas come CO₂, H₂, CH₄.

Per quanto riguarda la coltura di *B. subtilis*, in primo luogo, è stato prodotto uno stock di glicerolo con il ceppo DSM 21393, geneticamente modificato con la capacità inibita di formare spore, da sfruttare per gli esperimenti. Trattandosi di una coltura batterica, il brodo Lysogeny (LB) è stato utilizzato come medium (Tabella 3.2) per l'inoculazione. Una beuta è stata riempita con un volume di 50 mL di LB, inoculata con 50 µL di inoculo e posta nello shaker a 200 rpm e 30°C. Il mattino seguente, un volume di 500 µL della coltura è stato unito allo stesso volume di una soluzione di glicerolo al 50%v/v in una provetta eppendorf da 2 mL per 16 volte (ottenendo 16 replicati), miscelando in seguito e conservando, quindi, a una temperatura di -80 °C. Per gli esperimenti la concentrazione desiderata della coltura pura di questo microrganismo era di circa 5 g/L (che corrisponde a una densità ottica misurata a 600 nm di 15), allo scopo di simulare le materie prime della DA, come i fanghi industriali. Il medium utilizzato è una variante di LB (Tabella 3.3), in grado di aumentare la crescita della biomassa, contenendo anche tiamina e biotina. La coltura veniva preparata in beute da 500 mL o da 2500 mL (in base alle esigenze dell'esperimento), riempiendole con un volume rispettivamente di 50 mL o 250 mL di medium sterilizzato e 250 µL o 1 mL di inoculo.

Per *C. acetobutylicum* il primo passo è stata l'inoculazione della cultura. Inizialmente 1 L di Clostridium Growth Medium (CGM) (Tabella 3.6) sterile è stato preparato. Successivamente, una bottiglia di vetro da 500 mL contenente il medium è stata flussata con azoto a 1,5 bar per circa 3 minuti per rimuovere l'ossigeno e garantire condizioni anaerobiche. A questo punto il medium è stato trasferito a cinque tubi di vetro con tappo a vite da 10 ml precedentemente sterilizzati per un volume di 5 ml ciascuno (Figura 3.2). Quattro di essi sono stati inoculati con 100 µL (0,02% v/v) di inoculo e uno con 500 µL (0,10% v/v). I tubi di vetro sono stati, quindi, chiusi in una scatola (Figure 3.1 e 3.2) collocata nell'incubatore a 37 °C. La scatola in questione è dotata di chiusure costituite di gomma butilica che prevengono l'aria ed è accompagnata da bustine che fissano l'ossigeno. Dopo due giorni, altri tre tubi id vetro con tappo a vite sono stati riempiti ciascuno con 5 mL di medium, sottoposti a un trattamento termico (70 °C per 10 minuti) e inoculati con 1 mL della coltura precedente. Una settimana dopo, ebbe luogo la fase di seminatura su piastrine di Agar, quindi collocate nella scatola anaerobica nell'incubatore. Dopo cinque settimane, un'aliquota di 450 ml di terreno è stata inoculata in una bottiglia di vetro da 500 mL, dopo che il medium è stato flussato con azoto. La cultura è stata considerata pronta, quando è stata osservata la flocculazione (Figura 3.3.)

Diversi esperimenti sono stati condotti a seconda del campione analizzato. La Tabella I illustra in modo semplificato quale pretrattamento è stato sottoposto ciascun tipo di campione.

Tabella I: Riassunto degli esperimenti.

	Mulin	Sonicatore	Rotore-Statore	Sonicatore continuo
<i>Clostridi</i>				×
<i>Bacilli</i>	×	×	×	×
Brodo				×
Substrato	×	×		

In maniera più dettagliata, la procedura sperimentale seguita per ogni pretrattamento.

- **Mulini con sfere abrasive.** Inizialmente, le sfere di vetro del diametro di 0,5 mm sono stati sterilizzati con una soluzione 70% v/v-etanolo, sfruttando un filtro di nylon da 125 µm. I contenitori di acciaio sono stati anche sterilizzati con la stessa soluzione. I contenitori sono, poi, stati riempiti con 4 mL di perle di vetro e la quantità desiderata di campione. I contenitori sono, quindi, stati bloccati ai bracci di scuotimento della macchina e la macchina accesa. Le impostazioni, che includono il tempo e la frequenza, sono state modificate alle condizioni desiderate (frequenza costante di 30 Hz in ogni esperimento e tempo variabile). Trascorso il tempo imposto, i contenitori sono stati rimossi dalla macchina e svuotati, filtrando il campione con un filtro di nylon da 125 µm collocato su un imbuto di plastica per separare le perle di vetro.
- **Sonicatore con ultrasuoni.** Prima di ogni esperimento, la sonda veniva sterilizzata con una soluzione al 70% v/v-etanolo. La macchina veniva quindi impostata secondo i valori di ampiezza e cicli desiderati per ciascun esperimento. La sonda veniva, infine, immersa nel campione. Il trattamento di ultrasonificazione è stato eseguito sul substrato (ampiezza pari a 50% per 6x20 sec) e sulla cultura di *B. subtilis* (Tabella 4.3). Dopo aver condotto una prima serie di esperimenti, nel secondo gruppo di esperimenti si è deciso di allungare il tempo di applicazione del trattamento.
- **Omogeneizzatore a rotore-statore.** Gli esperimenti sono stati condotti su una sospensione cellulare di *B. Subtilis* (10 ml di volume), contenuta in una provetta falcon da 50 ml. Prima dell'esperimento, lo statore è stato sterilizzato con una soluzione 70% v/v-etanolo. La singola impostazione richiesta dalla macchina è il valore di frequenza, che può essere scelto tra 4 diversi. La frequenza più alta (20500 min^{-1}) era quella desiderata, ma è stato possibile eseguire solo una serie di esperimenti in questo modo. In seguito, la macchina poteva essere utilizzata solamente alla frequenza più bassa. Pertanto, è stata eseguita un'altra serie di esperimenti utilizzando una frequenza di 800 min^{-1} . Sempre a causa di difficoltà tecniche, questo pretrattamento non è stato ulteriormente testato. Il protocollo degli esperimenti è riportato in Tabella 4.4.
- **Sonicazione continua.** Innanzitutto, è stato necessario costruire il set-up, per procedere con gli esperimenti (Figura 4.2). Dopo di che, per eseguire gli esperimenti è stato necessario seguire i seguenti passi: impostare l'ampiezza e i cicli nella macchina, aprire il rubinetto per fare fluire acqua fredda nella camicia del sonicatore, immergere il "sample-intube" nella beuta contenente il campione; accendere la pompa; avviare la sonicazione. Questo pre-trattamento è stato testato su tutti i tipi di campione (culture pure, substrato e brodo di fermentazione). Gli esperimenti riportati nelle Tabelle 4.5 e 4.6, sono stati eseguiti con una sospensione di *B. subtilis*. Gli esperimenti eseguiti su *C. acetobutylicum* sono riportati in tabella 4.7 e quelli eseguiti sul brodo di fermentazione in tabella 4.8.

Infine, l'analisi dei dati è stata effettuata sfruttando il software *Fiji (Image J)* per il conteggio delle cellule o sfruttando la tecnica di *in-situ* laser back reflection. Ogni volta che si è svolta la fase di plating (solo in alcuni esperimenti condotti sulla cultura di *B. subtilis*), le piastrine sono state fotografate dopo l'incubazione e le immagini sono state analizzate utilizzando il software Fiji. Prima di tutto, è stata impostata la scala, vale a dire la corrispondenza tra 1 pixel e 1 cm. La fotografia è stata tagliata fino ad avere un quadrato, i cui lati erano tangenti al cerchio della piastrina (Figura 5.1 A). I pixel dell'immagine (variabile da un'immagine all'altra) sono stati divisi per il diametro della piastrina (fisso e noto, cioè 5,2 cm) e la corrispondenza tra 1 pixel e 1 cm trovato. Nel caso di un quadrato non perfetto (un rettangolo), la media tra i lati è stata utilizzata come valore per il lato del quadrato corrispondente. I canali dell'immagine venivano quindi separati in blu, verde e rosso e veniva scelta solo una delle tre immagini risultanti.

Successivamente veniva selezionata solo la parte contenente le celle, ritagliando il resto dell'immagine. L'immagine veniva poi convertita in un formato in bianco e nero a 8 bit ei colori invertiti per ottenere le cellule in nero e lo sfondo in bianco (Figura 5.1, B). Infine, il calcolo dell'area (%) dell'immagine (riquadro rosso) occupata dalle cellule (Figura 5.2, B) veniva calcolata con il software. Tramite la scala impostata nella fase iniziale, il software era in grado di fornire anche l'area totale (cm^2) dell'immagine (quadrato rosso). Considerando quanto precedentemente affermato, l'area (%) è stata trasformata in area (cm^2) dell'immagine occupata dalle celle. Conoscendo anche l'area della piastrina attraverso il suo diametro (cioè $\pi d^2/4$) (Figura 5.2, A), l'area (%) della piastra occupata dalle celle è stata ottenuta dal rapporto matematico. Il numero di cellule sulla piastrina è stato anche calcolato con il software, ma il valore calcolato includeva molti punti piccoli e quindi il numero di celle risultava costantemente sovrastimato.

La tecnica di *in situ* laserback-reflection è stata utilizzata come metodo alternativo al plating per la sospensione di *B. subtilis* e, in generale, come metodo per analizzare la distribuzione delle dimensioni delle particelle prima e dopo il trattamento per tutti i substrati. L'analisi con la sonda è stata condotta come mostrato nella Figura 5.3. Il campione è stato sempre trasferito in un contenitore di vetro in particolare, in quanto questo era l'unico che consentisse di lavorare con un'inclinazione della sonda di circa 45°. Nel contenitore veniva inserito, poi, un piccolo magnete, per poter usare l'agitatore. La sonda Sequip è stata quindi collegata a un computer, dove è stato installato il software Sequip da utilizzare in combinazione con questa. Qui è stato possibile visualizzare gli histogrammi e le curve cumulative in tempo reale ed esportare i file excel dei dati raccolti durante la misurazione (Figura 5.4).

Risultati

L'analisi dei dati effettuata sfruttando il software *Fiji (Image J)* per il conteggio delle cellule ha portato ai seguenti risultati, raggruppati secondo il pretrattamento.

- Mulin con sfere abrasive. Una prima serie di esperimenti esplorativi è stata condotta allo scopo di ricavare le condizioni ottimali di pretrattamento, quali il tempo e il volume. Il tempo testato inizialmente per la crescita in vitro è 24 ore, che ha portato, però, a una crescita eccessiva della biomassa nelle piastrine di Petri. Con ciò, come si può notare in Figura 6.1, la corretta quantificazione delle colonie/granuli non è stata possibile e pertanto l'analisi con il software Fiji non è stata eseguita. Tuttavia, la semplice analisi visiva delle piastrine indica che la biomassa non è stata gravemente compromessa a causa della fase di pretrattamento, poiché le piastrine inoculate mostrano una buona crescita micrubbica. Negli esperimenti successivi il volume è stato assunto costante e pari a 8 ml. Inoltre, è stato scelto di considerare un tempo più lungo di applicazione del pretrattamento (20 min) per osservare se la biomassa sarebbe stata gravemente danneggiata e i risultati della seconda serie di esperimenti sono illustrati in Figura 6.2. I tempi di applicazione del trattamento sono: 0 min (prima che la sospensione cellulare sia stata sottoposta al trattamento), 5 min, 10 min, 20 min. Dall'osservazione dell'istogramma, è possibile concludere che, a differenza di 5 min, dove il numero di colonie diminuiva del 10%, per 10 min e 15 min la biomassa è risultata gravemente compromessa con significative riduzioni del, rispettivamente, 70% e 85%. La deviazione standard, in questo caso, rappresenta anche il grado di uniformità che può essere raggiunto con il pretrattamento. Per tempi più brevi (ovvero

5 minuti), le cellule sono danneggiate in modo non uniforme, mentre per periodi di esposizione più lunghi al pretrattamento l'effetto resulta più marcato sull'intera popolazione.

- Sonicatore con ultrasuoni. La prima serie di esperimenti esplorativi è stata condotta allo scopo di esaminare il tempo e l'ampiezza di pretrattamento ottimali; i risultati sono riportati in Figura 6.3. Osservando il grafico, è evidente che, passando da un tempo di applicazione di 30 s (3 volte 10 s) a uno di 2 min (3 volte 40 s), la biomassa non è stata danneggiata. Infatti, con il 50% di ampiezza dell'area occupata dalle colonie sulla piastrina aumenta leggermente del 20% circa da 30 sec a 3 min e rimane quasi costante da 1 min a 2 min. Lo stesso vale per il numero di colonie, che diventa il doppio da 30 sec a 2 min. È stato deciso, quindi, di mantenere solo il tempo più lungo di applicazione del pretrattamento (variabile costante pari a 2 min) e di eseguire l'esperimento con due diversi valori di ampiezza (50% e 25%). Nella Figura 6.4 sono illustrati i risultati. È possibile osservare che le cellule occupano un'area inferiore dopo il pretrattamento, che era la tendenza attesa. D'altra parte, il numero di cellule aumenta dopo il trattamento. Analizzando i risultati di tali esperimenti, si dovrebbe considerare che molti fattori possono influenzare i risultati, come ad esempio: il numero di cellule iniziali, le condizioni ambientali (nutrienti, pH, temperatura, concorrenti, composti inibitori), tra gli altri. Tuttavia, risulta evidente che a basse ampiezze (cioè il 25%), le cellule sono danneggiate in modo non uniforme mentre ad un'ampiezza di sonificazione più elevata (cioè il 50%) l'effetto del pre-trattamento è più marcato su tutta la popolazione.
- Omogeneizzatore a rotore-statore. La Figura 6.5 mostra i risultati ottenuti eseguendo esperimenti con l'omogeneizzatore a rotore-statore. La linea verde si riferisce alla frequenza più grande (20500 min^{-1}) e alla linea blu a quella più bassa (800 min^{-1}). Nel primo caso, la fase di pretrattamento ha comportato un declino lineare dell'area occupata dalle colonie sulla piastra con l'aumento del tempo di pretrattamento. D'altra parte, a bassa frequenza la biomassa non è stata gravemente colpita dal pretrattamento. Per quanto riguarda il numero di cellule, non è stato possibile effettuare una quantificazione corretta delle colonie. Tuttavia, la semplice analisi visiva delle piastre (Figura 6.7) indica che il numero di colonie diminuisce con l'aumento del tempo di applicazione del pre-trattamento, simile alla tendenza ottenuta per l'area.
- Sonicazione continua. I risultati sono riportati in Figura 6.8 e quanto emerge è che la biomassa non è stata gravemente colpita dal pretrattamento. In particolare, in ogni caso il numero di colonie sulla piastrina diminuisce dopo la fase di pre-trattamento (del 50% circa), mentre l'area occupata dalle colonie (in percentuale dell'area totale della piastrina) generalmente aumenta, tranne che per il 20% di amplitudine in cui rimane quasi costante. Rispetto all'effetto generalmente ottenuto, usando l'ultrasonificazione discontinua, il risultato è in questo caso il contrario, poiché è stato precedentemente rilevato che le cellule occupavano un'area inferiore dopo il pretrattamento, mentre il numero di cellule aumentava (dopo il pretrattamento). Mentre, lo stesso ragionamento sulla deviazione standard può essere fatto come per l'ultrasonificazione; ovvero la deviazione standard rappresenta anche il grado di uniformità che può essere raggiunto con il pretrattamento. Per ampiezze maggiori (vale a dire 20%), le cellule sono danneggiate in modo non uniforme, mentre a un'ampiezza di sonificazione inferiore l'effetto del pretrattamento è più marcato sull'intera popolazione.

L'analisi dei dati effettuata sfruttando la tecnica di *in-situ* laser back reflection ha condotto ai seguenti risultati, raggruppati secondo il tipo di campione utilizzato.

- *Clostridium acetobutylicum*. L'ultrasonificazione in continuo costituisce l'unico pre-trattamento testato e due diversi valori di ampiezza (50% e 20%) sono stati confrontati. Nel caso di 50% di ampiezza, l'istogramma in Figura 6.9 mostra che la distribuzione della dimensione delle particelle si sposta verso diametri maggiori dopo il primo pretrattamento per tornare a diametri più piccoli dopo il secondo pretrattamento, ma in ogni caso, maggiori del campione non-pretrattato. La stessa analisi può essere eseguita osservando le curve di distribuzione in Figura 6.10 e i relativi valori medi in Tabella 6.1. Il diametro medio delle particelle del campione non-pretrattato è 4,71 μm , diventa 6,21 μm con il primo trattamento e diminuisce leggermente con il secondo pretrattamento (6,07 μm), dove la deviazione standard è di circa 1. Lo stesso comportamento può essere osservato nelle curve cumulative (Figura 6.11) e nei valori risultanti di D50 e D90 (Tabella 6.1). Questo può essere spiegato pensando alla flocculazione che caratterizzava il campione (Figura 3.4). È ragionevole presumere che i flocculi non siano stati rilevati dalla sonda perché troppo grandi e che il pretrattamento li abbia rotti in particelle più piccole, rilevate nella misurazione dopo il primo pretrattamento. Infatti, l'intervallo di rilevamento della sonda era fino a 101,8 μm , dove le dimensioni dei flocculi sono normalmente di 1-2 mm, ma in alcuni casi occasionali anche superiori a 10 mm [42]. In supporto a questa teoria, è possibile osservare il numero totale di particelle rilevate dalla sonda in tutte e tre le misurazioni: questo è intorno a 1.324 per il campione non-pretrattato e aumenta a 2.201 e 3.032, rispettivamente, con il primo pretrattamento e con il secondo. Nel caso di 20% di ampiezza, osservando le curve di distribuzione in Figura 6.13 e i relativi valori medi in Tabella 6.2, è possibile notare che anche in questo caso la dimensione media delle particelle aumenta, ma in misura minore. Lo stesso vale per le curve cumulative in Figura 6.14 e i valori di D50 e D90 in Tabella 6.2. Questi risultati possono essere spiegati considerando che la sonda è il componente del sonicator che trasmette le onde ultrasonore al liquido sonicato ed è responsabile della creazione della cavitazione. L'ampiezza rappresenta l'estensione massima consentita rispetto alla massima estensione di cui è capace la sonda. Quindi, se l'amplitudine è piccola, la superficie vibrante della sonda sarà anch'essa piccola. Detto ciò, è ragionevole pensare che, a causa dell'ampiezza minore, con il 20% di amplitudine un numero inferiore di flocculi sia stato disgregato, portando solo a un leggero aumento della dimensione media, a differenza del caso di 50% di amplitudine. L'andamento del numero totale di particelle aumenta anche in questo caso da 1.324 per il campione non-pretrattato a 2.201 e 3.032 dopo i pretrattamenti.

Tabella II: *Clostridium acetobutylicum*:parametri delle curve di distribuzione
(media \pm deviazionestandard); D50 e D90; numero totale di particelle calcolato con il Sequip-software.

Ampiezza		media \pm deviazione standard	D50 (μm)	D90 (μm)	Nr. di particelle
50%	BT	4,71 \pm 1,31	4,07	5,86	1.324
	AT	6,21 \pm 1,00	5,46	8,21	22.418
	AST	6,07 \pm 0,98	5,35	8,03	19.013
20%	BT	4,71 \pm 1,31	4,07	5,86	1.324
	AT	4,93 \pm 1,32	4,24	5,92	2.201
	AST	5,13 \pm 1,40	5,56	6,15	3.032

- *Bacillus subtilis*. L'ultrasonificazione in continuo costituisce l'unico pre-trattamento testato e due diversi valori di ampiezza (50% e 30%) sono stati confrontati. Nel caso di 50% di ampiezza, per avere una prima idea dell'effetto del trattamento sulla distribuzione delle dimensioni delle particelle misurata dalla sonda, è possibile osservare gli istogrammi delle Figure 6.15 e 6.18. Da queste si può dedurre che la distribuzione delle dimensioni delle particelle si sposta in entrambi gli esperimenti a diametri maggiori dopo il pretrattamento. La stessa analisi può essere eseguita osservando le curve di distribuzione in Figura 6.10 e 6.13 e i relativi valori medi nella Tabella 6.3. In entrambi gli esperimenti la media delle particelle del campione pretrattato è 7 μm e diventa 8,5 μm con il pretrattamento. Lo stesso vale per le curve cumulative (Figure 6.17 e 6.20) e i valori di D50 e D90 (Tabella 6.3). In entrambi gli esperimenti, il D50 è 6 μm per il campione non-pretrattato e 7,5 μm per il pretrattato. Il D90 muta dacirca 8,5 μm a 11 μm con lo step di pretrattamento. Una spiegazione plausibile per i valori presentati è che anche i campioni della coltura di *B. subtilis* utilizzati per condurre questi esperimenti presentavano flocculazione, non osservata, a causa del colore giallognolo delle beute utilizzate per questo tipo di coltura, a differenza che per *C. acetobutylicum*. Anche in questo caso, a supporto di questa teoria, è possibile osservare il numero totale di particelle rilevate dalla sonda: 10.000 per il campione non pre-trattato e 40.000 per il pretrattato. Nel caso di 30% di ampiezza, gli istogrammi (figure 6.21 e 6.24) richiamano quelli visti in precedenza, ma le curve di distribuzione (figure 6.22 e 6.25) e i relativi valori medi (tabella 6.3) mostrano un comportamento diverso tra il primo e il secondo esperimento. La media è, rispettivamente, 6,20 μm (primo esperimento) e 7,74 μm (secondo esperimento) per il campione non-pretrattato e 5,58 μm (primo esperimento) e 8,45 μm (secondo esperimento) dopo lo step di pretrattamento. È possibile vedere che la media rimane quasi costante, tenendo conto della deviazione standard che è compresa tra 1 e 1,5. Lo stesso vale per la D50 (Tabella 6.3), mentre per entrambi gli esperimenti il D90 (Tabella 6.3) aumenta in entrambi gli esperimenti con il pretrattamento. Questi risultati possono essere spiegati ricorrendo di nuovo al valore di ampiezza. Ovvvero, è ragionevole pensare che, a causa dell'ampiezza minore, il pretrattamento abbia rotto i flocculi in modo meno grave rispetto al caso del 50%, creando particelle più grandi dopo il pretrattamento, che possono essere rilevate solo nel valore del D90.

Tabella III: *Bacillus subtilis*: parametri delle curve di distribuzione (media \pm deviazionestandard); D50 e D90; numero totale di particelle calcolato con il Sequip-software.

Ampiezza			media \pm deviazione standard	D50 (μm)	D90 (μm)	Nr. di particelle
50%	Primo esperimento	BT	7,10 \pm 0,87	6,40	9,02	13.041
		AT	8,45 \pm 1,22	7,59	11,12	39.206
	Secondo esperimento	BT	7,03 \pm 1,59	6,29	7,94	8.758
		AT	8,53 \pm 1,27	7,70	10,55	38.714
30%	Primo esperimento	BT	6,20 \pm 0,78	5,44	6,99	3.082
		AT	5,58 \pm 1,04	5,21	11,80	6.319
	Secondo esperimento	BT	7,74 \pm 1,69	7,68	19,54	9.313
		AT	8,42 \pm 2,54	9,04	32,14	23.154

- Substrato. Il mulino con sfere abrasive e il sonicatore a ultrasuoni sono stati testati. Nel primo caso, osservando i valori di D50 e D90 di entrambe le ripetizioni (tabella 6.7), questi sono sempre più piccoli dopo la fase di pretrattamento. Poiché il PF è un substrato e in esso non è presente alcuna fase biologica, lo scopo del pre-trattamento era di ridurre il più possibile la dimensione delle particelle per rendere il substrato più disponibile per i microrganismi. È possibile, quindi, concludere che lo scopo è stato raggiunto; osservando il D50, la dimensione delle particelle è stata ridotta dal pretrattamento del 32% nel primo esperimento e del 29% nel secondo, mentre, guardando al D90, la riduzione ha raggiunto il 58% nel primo esperimento e il 10% nella ripetizione. Nel caso del sonicatore a ultrasuoni, è possibile trarre conclusioni attraverso l'analisi delle curve cumulative mostrate nella Figura 6.32, estrapolando i valori di D50 e D90 (Tabella 6.8). Osservando il D50, questo è stato ridotto del 20% nel primo esperimento e del 40% nel secondo, mentre rispetto al D90, la riduzione è stata del 18% nel primo caso e del 69% nel secondo.

Tabella IV: Substrato: parametri delle curve di distribuzione (media±deviazione standard); D50 e D90; numero totale di particelle calcolato con il Sequip-software.

Pretrattamento			D50 (μm)	D90 (μm)
Mulino con sfere abrasive	Primo esperimento	BT	12,83	38,76
		AT	8,72	16,17
	Secondo esperimento	BT	31,31	92,43
		AT	22,13	82,71
Sonicatore a ultrasuoni	Primo esperimento	BT	152,40	791,64
		AT	121,66	646,16
	Secondo esperimento	BT	163,28	1270,28
		AT	98,48	399,15

- Brodo di fermentazione. L'ultrasonicazione in continuo è l'unico tipo di pretrattamento, che sia stato testato sul brodo di fermentazione. Inoltre, sono stati osservati due valori di ampiezza (50% e 20%) e per ciascuna ampiezza l'esperimento è stato ripetuto due volte. In entrambi i casi, il campione ha subito un primo pretrattamento di 2 minuti e poi un ulteriore di 1,5 minuti. Nel caso di 50% di ampiezza, i valori medi (Tabella 6.7) mostrano un aumento di 2-3 μm nel diametro delle particelle del campione con i due consecutive pretrattamenti in entrambi gli esperimenti. Il valore del D50 (Tabella 6.7) ha un comportamento simile; aumenta di circa 1 μm nel primo esperimento e rimane quasi costante nel secondo esperimento. D'altra parte, i valori del D90 (Tabella 6.7) mostrano una netta diminuzione del 15% e dell'11% del diametro delle particelle del campione (due volte) pretrattato (AST). Infine, guardando le curve di distribuzione (Figure 6.39 e 6.43), è possibile vedere chiaramente che le tre sono una curva unica fino all'85% (primo esperimento) e al 65% (secondo esperimento), dopo di che la curva relativa al campione non pretrattato si separa e va a giacere su diametri maggiori. Nel caso di questi due esperimenti, è possibile, quindi, affermare che il pretrattamento ha agito esclusivamente sul taglio D50-D100. Poiché il brodo di fermentazione contiene la biomassa insieme al substrato, e la prima di solito si trova nello slot D0-D50, un pretrattamento che

influenza solo il taglio D50-D100 corrisponde a un buon pretrattamento (che non influisce sui microrganismi responsabili della DA). Nel caso di 20% di ampiezza, osservando il D50 (Tabella 6.8), questo diminuisce del 6% (primo esperimento) e del 16% (secondo esperimento) dopo 2 minuti di pretrattamento, mentre la riduzione diventa del 14% (primo esperimento) e 23% (secondo esperimento) dopo 3,5 minuti. Il D90 (Tabella 6.7), invece, nel primo esperimento diminuisce del 10% con il primo step di pretrattamento (e rimane costante con il secondo step) e nel secondo esperimento rimane costante. Questi risultati possono essere spiegati in due modi. Un valore di ampiezza piccolo porta a non avere alcun effetto significativo sul campione o può essere visto come influenzante il taglio D0-D50, al contrario di una ampiezza più grande, che è stata osservata influenzare il taglio D50-D100. Secondo entrambe le filosofie, il pretrattamento con il 50% di ampiezza è più adatto al brodo di fermentazione, che quello con il 20% di ampiezza.

Tabella V: Brodo di fermentazione: parametri delle curve di distribuzione (media±deviazionestandard); D50 e D90; numero totale di particelle calcolato con il Sequip-software.

Aampiezza			media±deviazione standard	D50 (µm)	D90 (µm)
50%	Primo esperimento	BT	7,02±2,04	7,30	17,54
		AT	6,52±1,33	7,27	15,06
		AST	9,30±2,75	8,67	14,89
	Secondo esperimento	BT	6,12±1,63	8,73	16,67
		AT	7,94±2,51	7,99	14,95
		AST	9,37±4,14	8,45	14,78
20%	Primo esperimento	BT		8,52	19,40
		AT		8,47	17,54
		AST		7,36	17,54
	Secondo esperimento	BT		9,52	16,78
		AT		8,02	17,54
		AST		7,36	17,54

A ulteriore completamento, un'analisi energetica è stata effettuata, per

- confrontare le diverse tecnologie di pretrattamento;
- effettuare un bilancio energetico.

L'energia richiesta per produrre un cambio Δx di 1 µm nella dimensione delle particelle è stata calcolata. Il calcolo è stato effettuato con la formula 1.11. I risultati sono riportati in Tabella 6.9. Confrontando i valori di energia specifica richiesti per una diminuzione Δx di 1 µm nel D90, il pretrattamento di sonicazione in continuo è il più dispendioso in termini energetici, seguito dal mulino a sfere abrasive e, infine, dal sonicator a ultrasuoni. I valori sono di circa 13.000 J/µm per la ultrasonicazione in continuo, circa 7.000 J/µm per il mulino a sfere abrasive e circa 100 J/µm per la sonicazione.

Tabella VII: Energia richiesta per produrre una diminuzione Δx nella dimensione delle particelle.

Campione	Pretrattamento	gvs		J/ μm (D50)	J/ μm (D90)
Substrato	Mulino a sfere abrasive	3,1	Primo esperimento	21.885	3.984
			Secondo esperimento	9.805	9.258
	Sonicazione a ultrasuoni (batch)	0,2	Primo esperimento	781	165
			Secondo esperimento	370	27
Brodo di fermentazione	Sonicazione in continuo	1,2	Primo esperimento		10.398
			Secondo esperimento		14.923

L'energia richiesta per pretrattare 1 gvs di substrato e brodo di fermentazione è stata calcolata e rapportata all'LHV della materia prima per determinare se il pretrattamento è energeticamente sostenibile. Il calcolo è stato effettuato sfruttando anche alcuni dati dalla letteratura, riportati in Tabella 6.10. La formula utilizzata per il calcolo dell'energia specifica è la 1.12 per il pretrattamento con il mulino a sfere abrasive e il sonicatore a ultrasuoni, mentre l'equazione 1.13 è stata sfruttata per il sonicatore in continuo. Nel primo caso, il consumo specifico di energia (J/gvs) è risultato essere pari a 0,47 (kWh/kgBS per un diametro delle particelle di circa 0,3 mm [45]. Infine, la percentuale di LHV è stata ottenuta utilizzando un valore di quest'ultimo pari a 14,5 KJ/g, pari a quello della paglia [46]. I risultati sono riportati in Tabella 6.11. Il più grande consumo specifico di energia è attribuibile al sonicatore in continuo, seguito dal mulino a sfere abrasive e, infine, dal sonicatore a ultrasuoni. I risultati sono coerenti con il paragone tra tecnologie ed è possibile osservare che alcun pretrattamento investigato in questo lavoro è energeticamente sostenibile, in quanto, se così fosse, il pretrattamento richiederebbe una spesa non superiore al 5% dell'LHV della biomassa.

Tabella VIII: Energia richiesta per trattare 1 gvs di substrato e brodo di fermentazione e la spesa in termini di %LHV necessaria per effettuare il pretrattamento.

Campione	Pretrattamento	E (J/gVS)	% LHV
Substrato	Mulino a sfere abrasive	1692	12
	Sonicazione	1400	10
Brodo di fermentazione	Sonicazione in continuo	2914	20

Conclusioni

I pretrattamenti meccanici sono ampiamente utilizzati per una serie di processi industriali. Nel campo della biotecnologia, in particolare nel processo di digestione anaerobica, i pretrattamenti svolgono un ruolo chiave. L'influenza dei pretrattamenti può essere suddivisa nell'effetto prodotto sulla fase biologica e quello prodotto sulla fase abiotica organica (cioè il substrato). Tuttavia, la maggior parte delle applicazioni industriali richiede fasi di pretrattamento che mirano a ridurre la dimensione delle particelle del substrato, senza compromettere la vitalità delle cellule microbiche altrettanto presenti nel sistema. In questo lavoro di ricerca, è stato osservato l'effetto dei pretrattamenti su substrato, biomassa e sistemi combinati separatamente. Inoltre, la distribuzione della dimensione delle particelle è stata studiata attraverso diverse tecniche per quantificare l'influenza di ciascun pretrattamento.

Prima di tutto, le colture pure di *Clostridium acetobutylicum* e *Bacillus subtilis*, pretrattate con sonicazione a ultrasuoni, non risultano danneggiate, come dimostrato dal conteggio delle cellule eseguito con il plating o dalla tecnica di *in-situ* retro-riflessione laser. Inoltre, a piccole inferiori (cioè tra il 20 e il 30%), le cellule sono meno danneggiate e in maniera irregolare, mentre ad un'ampiezza di sonicazione più elevata (cioè 50%) l'effetto del pretrattamento è più marcato. Tuttavia, il conteggio delle cellule non fornisce una misura dello stato metabolico di quest'ultime, che potrebbe anche essere compromesso a causa dell'applicazione dei pretrattamenti. Sono necessari ulteriori studi per quantificare l'effetto dei pretrattamenti sulla fase biologica nella sua totalità.

Successivamente, un substrato eterogeneo costituito da una miscela di fibre di erba, piccoli residui di cespugli e terreno in parti uguali, diluito con acqua deionizzata al 20% (*m/m*) di biomassa secca (materie prime preparate) è stato pretrattato (separatamente) con il mulino a sfere abrasive e il sonicatore a ultrasuoni. In entrambi i casi è stata osservata una riduzione della dimensione delle particelle attraverso la tecnica di *in-situ* retro-riflessione laser e, poiché si tratta di un substrato privo di fase biologica, lo scopo del pretrattamento di rendere più solubile il substrato è stato raggiunto. La spesa energetica ha ammontato al 10% dell'LHV della biomassa per il sonicatore e al 12% per il mulino a sfere abrasive.

Infine, un brodo di coltura complesso pretrattato con la sonicazione ha comportato uno spostamento della distribuzione granulometrica a diametri minori, particolarmente marcato nel taglio D50-D100 nel caso di ampiezza del 50%, mentre nello slot D0-D50 per un'ampiezza inferiore (20%), sempre secondo la tecnica di *in-situ* retro-riflessione laser. In questo caso, invece, sfruttando il sonicatore in continuo, la spesa energetica ha ammontato al 20% dell'LHV della biomassa.

Tuttavia, è opportuno considerare che la dimensione media delle particelle varia anche da campione a campione della stessa coltura pura, substrato o brodo di fermentazione e, pertanto, un lavoro sperimentale più approfondito si rende necessario per valutare il comportamento di sistemi particolari.

TABLE OF CONTENTS

1. Introduction to Anaerobic Digestion.....	1
1.1 The microbiology of Anaerobic Digestion.....	3
1.1.1 Hydrolysis	5
1.1.2 Acidogenesis	5
1.1.3 Acetogenesis.....	6
1.1.4 Methanogenesis.....	6
1.1.4.1 Bacteria and reactions involved	6
1.1.5 Energetic rationale.....	7
1.2 Microbial consortia	7
1.2.1 Clostridia	7
1.2.2 Bacilli	9
1.3 Feedstock flexibility.....	10
1.4 Pre-treatment	11
1.4.1 Mechanical pre-treatment methods	11
1.4.1.1 Shearing.....	11
1.4.1.2 Ball milling.....	12
1.4.1.3 High-pressure homogenization	13
1.4.1.4 Rotor-stator degradation.....	13
1.4.1.5 Ultrasonification.....	14
1.4.2 Thermal	15
1.4.3 Chemical pre-treatment methods	16
1.4.3.1 Alkali pre-treatment	16
1.4.3.2 Acid pre-treatment.....	16
1.4.4 Biological pre-treatment methods	17
1.4.4.1 TSAD	17
1.4.4.2 Enzymatic pre-treatment method	17
1.4.5 Shear stress induced on bacteria.....	17
1.5 In situ laser back-reflection	19
1.6 Probability distribution.....	20
2. Purpose of the thesis.....	21
3. Materials and Feedstocks	23
3.1 Bacilli	23
3.1.1 LB Agar plates	24

3.2 Clostridia	25
3.3 Fermentation broth (FB).....	27
3.4 Prepared Feedstock (PF)	28
4. Mechanical Treatments	29
4.1 Bead mill	29
4.2 Ultrasonification.....	30
4.3 Rotor-stator degradation.....	31
4.4 Continuous flow-ultrasonification.....	32
5. Data Analysis	35
5.1 Cells counting using an Image Analysis Software.....	35
5.2 In situ laser back-reflection	36
6. Results	39
6.1 Cells counting.....	39
6.1.1 Effects on cell viability of Bead Milling.....	39
6.1.2 Ultrasonification.....	40
6.1.3 Rotor-stator degradation.....	42
6.1.4 Continuous flow-ultrasonification.....	43
6.2 In situ laser back-reflection	44
6.2.1 <i>Clostridium acetobutylicum</i>	44
6.2.1.1 Continuous ultra-sonification at 50% of amplitude on <i>C. Acetobutylicum</i> ...	45
6.2.1.2 Continuous ultra-sonification at 20% of Amplitude on <i>C. acetobutylicum</i> ..	47
6.2.2 <i>Bacillus subtilis</i>	48
6.2.2.1 Continuous ultra-sonification at 50% of Amplitude on <i>B. subtilis</i>	49
6.2.2.2 Continuous ultra-sonification at 30% of Amplitude on <i>B. Subtilis</i>	51
6.2.3 Prepared Feedstock	54
6.2.3.1 Bead mill pre-treatment on PF	55
6.2.3.2 Ultrasonification pre-treatment on PF.....	57
6.2.4 Fermentation Broth	59
6.2.4.1 Continuous ultra-sonification at 50% of Amplitude on FB	59
6.2.4.2 Continuous ultra-sonification at 20% of Amplitude on FB	62
6.3 Energetical analysis.....	65
6.3.1 Comparison between technologies.....	65
6.3.2 Energetical balance	66
7. Conclusions	69
8. Acknowledgment	71

9. References	73
---------------------	----

1. Introduction to Anaerobic Digestion

Fossil fuels, as the name suggests, are very old. Due to this fact and also to the limited amount available of these resources, a future supply is uncertain. Furthermore, the exploitation of these resources has undesirable effects on the environment, regarding climate issues, greenhouse gases emissions and acidic rain formation, in addition to the negative effects on human health. Therefore, it is suitable to reduce the dependence on oil and secure future supply of energy. Along these lines, biofuels intervene as an alternative to fossil fuels; they are mainly grouped in *four generations* [1]:

- First Generation biofuels are biodiesel from vegetable oils and ethanol from fermentation of simple sugars contained in sugar crops or starch crops and biogas;
- Second generation biofuels are made from lignocellulosic biomass, agricultural residues or waste plant material i.e. sustainable feedstock that is not destined to human consumption;
- Third generation biofuels involve algae cultivation, that do not use arable-land and fix CO₂;
- Fourth generation biofuels, unlike third-generation biofuels, do not require the destruction of biomass and include electro fuels and photobiological solar fuels.

Biogas is a biofuel of Second Generation produced through the process of Anaerobic Digestion (AD) starting from different organic materials, such as sewage sludge, zootechnical waste, agricultural biomass and other wastes (Table 1.1).

Biogas consists of methane (50-70%), carbon dioxide (30-50%) and some impurities, such as ammonia, hydrogen sulphide, siloxane and halides. The calorific value of biogas is dependent only on the methane content; biogas containing 55% CH₄ has a calorific value of 21,5 MJ/Nm³ while pure methane has a calorific value of 35,8 MJ/Nm³ [2]. For this reason, CO₂ should be removed and earmarked for other aims (Figure 1.1).

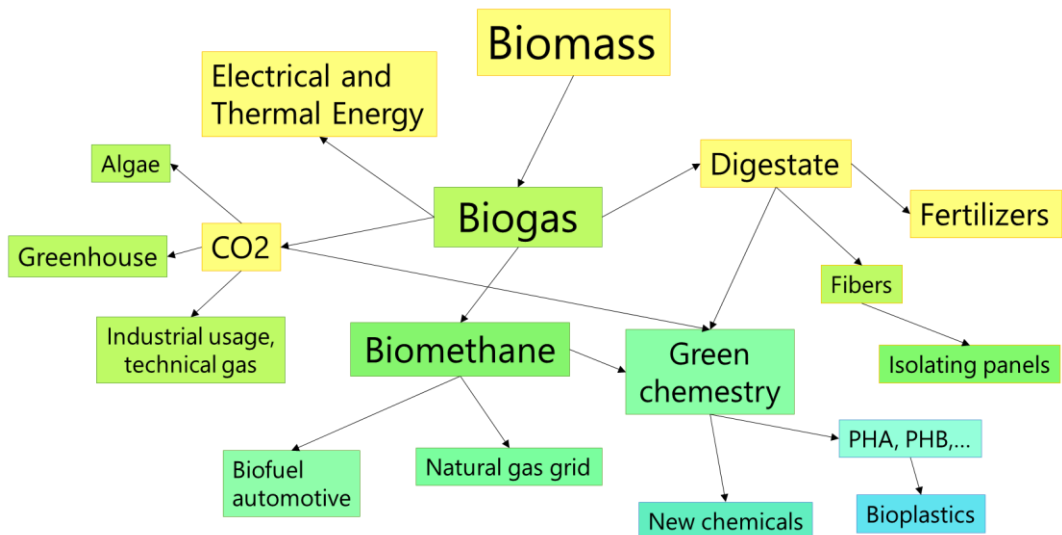


Figure 1.1: Development of biogas production chain [3].

Table 1.1: Industrial Wastes Amenable to AD [4].

Substrate	Example of substrate	Yield in biogas (m³/tonne of VS)	CH₄ in biogas (%)
Sewage		300-550	60-65
	Bovine	300-450	60-65
	Pork	450-550	60-65
Manures		200-550	60-65
	Bovine	200-300	60-65
	Pork	450-550	60-65
	Ovine	240-500	60-65
Dedicated crops		300-650	50-60
	Maize silage	350-550	53-55
	Beetroot	450-550	55-60
	Grass	300-500	53-55
	Clover	300-500	50-55
Agro-industrial byproducts		300-600	50-60
	From juices processing	500-600	55-60
	Brewers grains	300-400	50-55
	Molasses	300-450	50-55
	Straw	450-550	53-55
	From cereals distillation	400-500	50-55
Wastes		300-850	50-70
	Organic fraction of municipal solid waste	300-450	50-60
	From food services	650-800	50-60

The number of biogas plants in Europa practically tripled in only 6 years, reaching the value of 17,376 biogas plants in 2015. With 1,550 biogas plants, Italy is second after Germany which has 10,846 (Figure 1.2).

In Germany, for the year 2011 about 18 billion kWh of electricity were generated from biogas, which means supplying around five million houses with electricity [5]. When biogas is converted into electricity in cogeneration units, heat is also produced: with around 18 billion kWh, heat is provided to over 530,000 houses [5]. Moreover, once upgraded to biomethane, biogas is a motor fuel similar to natural gas. Hence, biomethane can be used as fuel in natural gas-powered vehicles without technical modifications. Nearly 200 of about 900 natural gas-filling stations sold fuel containing 5-100% bio-methane [5].

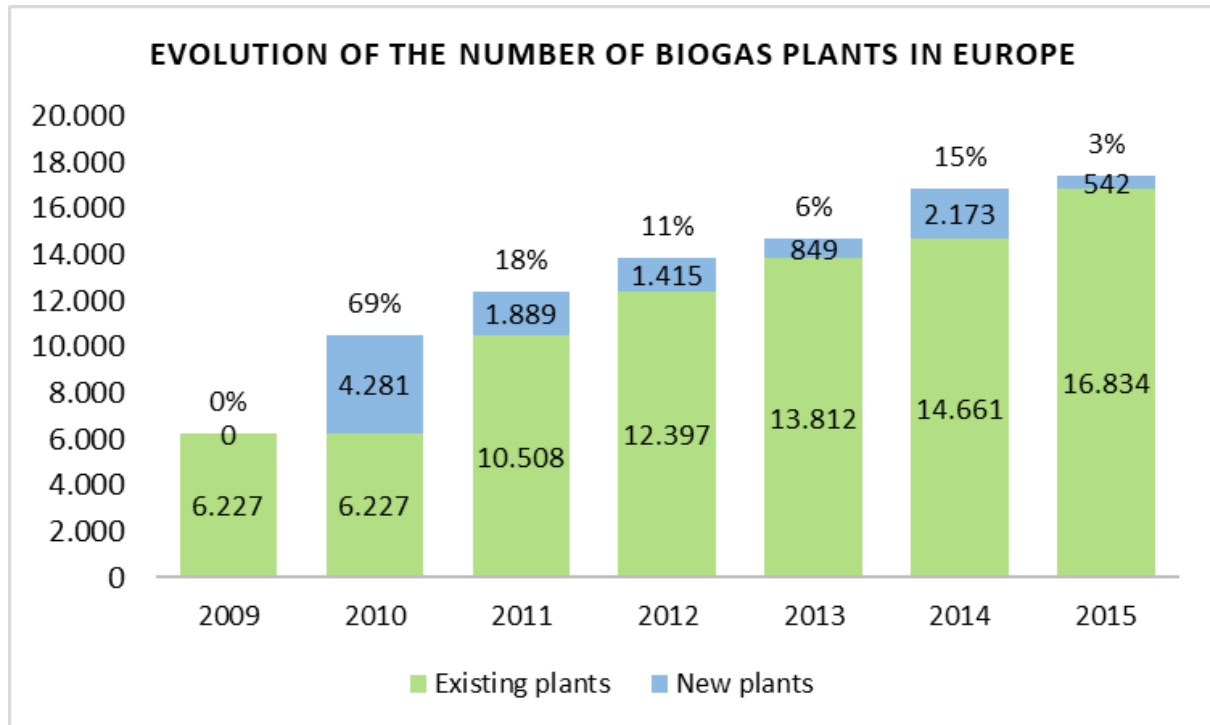


Figure 1.2: Biogas plants [6].

1.1 The microbiology of Anaerobic Digestion

Anaerobic digestion represents a catabolic process, in which bacteria degrade substrate using enzymes. They have a protein nature and can catalyse biochemical reactions thanks to active sites. Furthermore, they can be broadly classified as endo- or exoenzymes; both are produced in the cell, but the second ones are released outside the cell (Figure 1.3). A large and diverse community of bacteria is required to ensure that the proper exoenzymes and endoenzymes for degradation of the substrates are present, since no bacterium produces all of them by its own (Table 1.2).

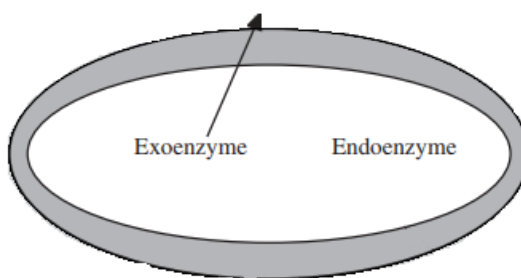


Figure 1.3: Enzymes used by bacteria to degrade substrate [7].

The bacterial activity in AD can be strictly/facultative anaerobic (sludge digestion) or strictly aerobic (sludge stabilization). Aerobes derive biosynthetic energy and produce metabolites only in presence of free molecular oxygen, as they produce ATP through aerobic respiration. Strict

anaerobes, on the other end, are inactive in the presence of free molecular oxygen. They lack certain enzymes that are essential for bacteria to survive in presence of oxygen, as they remove reactive oxygen species. These result from the reduction of molecular oxygen and cause intracellular damages. While the facultative anaerobic term establishes an ideal growth condition for the absence of oxygen, but, if the oxygen partial pressure rises in the medium, it is non-toxic to these microorganisms and can continue to grow. Certain species, called microaerophiles, instead, grow best in the presence of low amounts of oxygen.

Table 1.2: Exoenzymes and substrates [7].

Substrate	Example	Exoenzyme	Bacterium	Product	Yield ($m^3 CH_4/k$ g) [4]
Polysaccharides	Saccharolytic	Cellulase	<i>Cellulomonas</i>	Simple sugars	0,40
Proteins	Proteolytic	Protease	<i>Bacillus</i>	Amino acids	0,50
Lipids	Lipolytic	Lipase	<i>Mycobacterium</i>	Fatty acids	0,85

The AD process is composed by different steps (Figure 1.4), as it is briefly hereinafter discussed. Prior to AD the feedstock is prepared by removing contaminants such as grits, metals, and other particles depending on the specific source of the substrate.

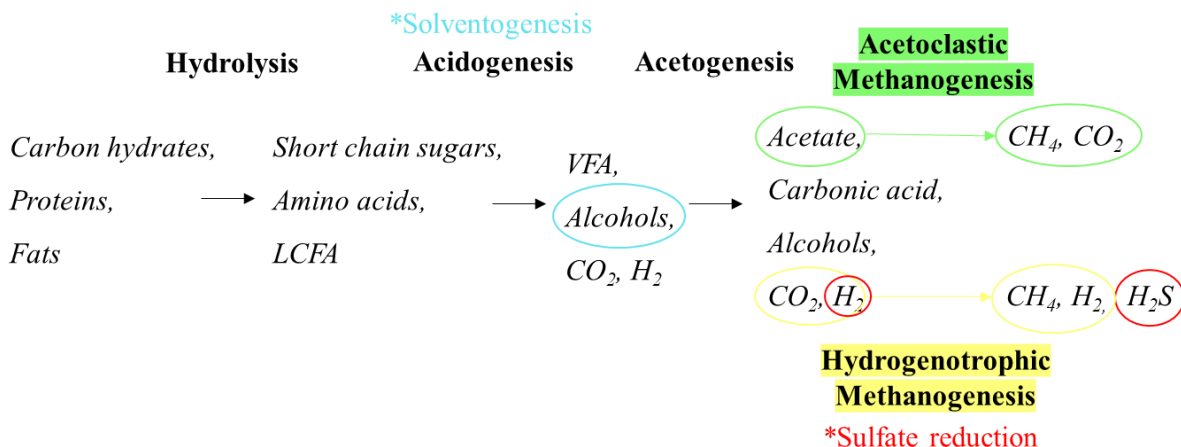


Figure 1.4: Biochemistry of AD.

In each phase one metabolic group of microorganisms is more active than the others: the microorganisms that play the key role in the first three stages of AD (hydrolytic-fermentative bacteria, acidogenic bacteria) are part of the domain *Bacteria*, on the other hand in the last step, aceticlastic methanogens and hydrogenotrophic methanogens are members of the *Archaea* domain (Figure 1.5).

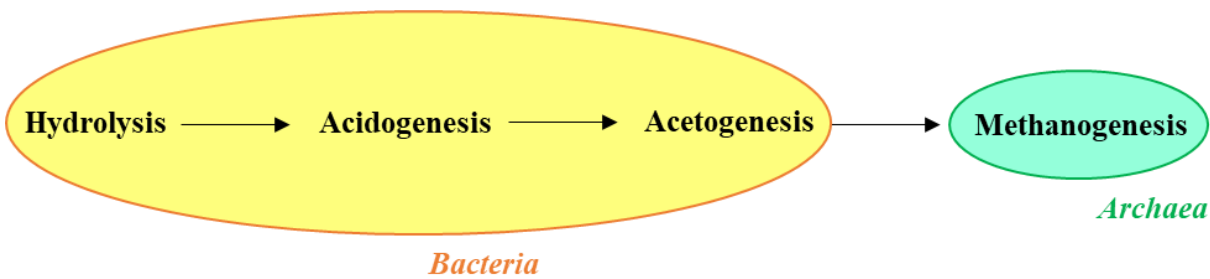


Figure 1.5: Domain of microorganisms in AD steps.

1.1.1 Hydrolysis

The first step of the process, *hydrolysis*, involves the feedstock disintegration operated by facultative and obligatory anaerobic bacteria through the production of exoenzymes (hydrolyses). Carbohydrates (such as cellulose) are broken down into simple sugars; proteins become individual amino acids; while fats, esters of the alcohol, glycerol and three fatty acid chains, have the latter parts removed from the head group. When the substrate is complex, this step is the rate-determining step.

1.1.2 Acidogenesis

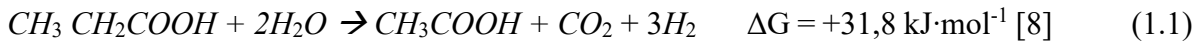
During the second step, *acidogenesis*, monomers formed in the hydrolysis step are converted into short-chain (C1-C5) organic acids (butyric acid, propionic acid, acetic acid), alcohols, a few organic-nitrogen and organic-sulphur compounds, together with hydrogen and carbon dioxide. It is also commonly known as the first fermentative step. A pH value lower than 5,5 induce solvents productions (such as alcohols and acetone); the cells enter the second phase, known as *solventogenesis*.

- Pathways of degradation of sugars:
 - formation of propionic acid via the succinate pathway and the acrylic pathway (degradation of pyruvate);
 - formation of butyric acid via the butyric acid pathway;
- Pathways of degradation of fatty acids: β -oxidation (stepwise, in each step one acetate is set free).
- The pathway of degradation of amino acids is the Stickland reaction (two amino acids per time are split: one act as hydrogen donor, the other as acceptor). During splitting of cysteine, hydrogen sulphide is released.

With the development of fixed-film bacterial growth in anaerobic digesters, many soluble organic wastes can be digested quickly and efficiently [7].

1.1.3 Acetogenesis

The third step, *acetogenesis*, or the second fermentation, involves the conversion of the volatile acids (VFA) (1.1) [8] and alcohols to acetic acid and hydrogen gas.



The acetogenic bacteria are obligatory H₂ producers, inhibited by an excessive amount of the product (hydrogen). Then, a syntrophic relationship must exist between the acetogens and hydrogenotrophic methanogens [9]. Syntropy is the phenomenon for which one species lives off the products of another species [9]. Indeed, the second ones constantly remove the products of metabolism of the first ones from the substrate, keeping the hydrogen partial pressure at a low level, suitable for the acetogenic bacteria. Problems can occur when the acetogens create a syntrophic relationship instead with a methanogenic species with other organisms, that compete with methanogens for H₂. In waste water technology, some facultative anaerobes reduce sulphate (SO₄²⁻) to hydrogen sulphide (Figure 1.6). In this case, the hydrogenotrophic methanogens form less methane (receive less feed) and are also toxically affected by hydrogen sulphide. Furthermore, many of the monomers (e.g. sugars) can be catabolized by homoacetogenic bacteria to acetate, which then serves as substrate for acetoclastic methanogens converting it to CH₄ and CO₂.

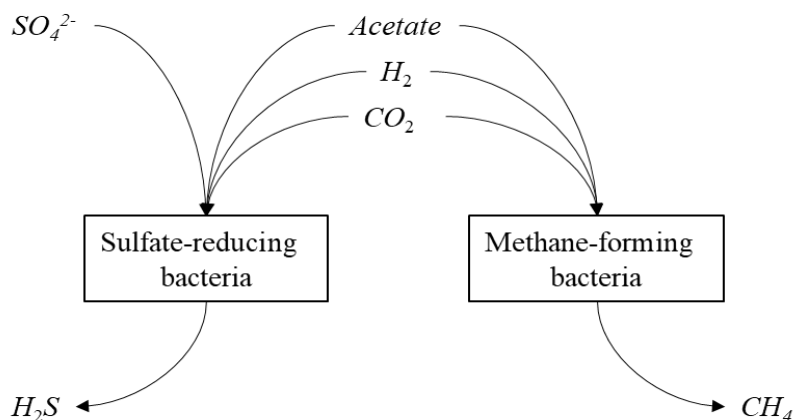


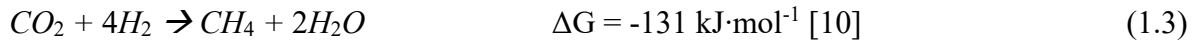
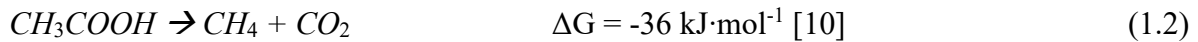
Figure 1.6: Competition between sulphate-reducing bacteria and methane-forming bacteria [7].

1.1.4 Methanogenesis

1.1.4.1 Bacteria and reactions involved

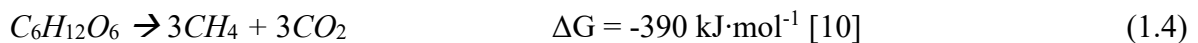
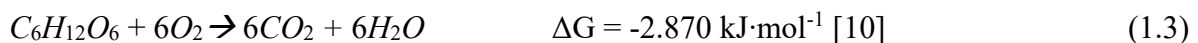
Methane-forming bacteria, grouped in the domain *Archaea* (Figure 1.3), that gathers a wide spectrum of microorganisms living in extreme environments, that are prohibitive for all other organisms (methane-forming bacteria, extremely halophilic, thermoacidophile, extremely thermophilic). Because of the long reproduction time, a long retention period is required in the digester (at least 12 days). Methane-forming bacteria grow as microbial consortia, are obligate anaerobes and grow on a limited number of simple substrates. They obtain energy and building blocks for the biosynthesis from hydrogen, 1-C compounds (formate, methanol, carbon dioxide, carbon monoxide and methylamine) and acetate (2-C). Mainly two groups can be distinguished: hydrogenotrophic methanogens and acetoclastic methanogens, converting hydrogen and carbon

dioxide, or acetic acid, respectively, to methane. Methane production occurs, therefore, from the degradation of acetate (1.1) and the reduction of carbon dioxide by hydrogen gas (1.2) [7]. The second pathways are believed to account for about 27-30% of CH₄ production in AD reactors.



1.1.5 Energetic rationale

If only glucose is considered as substrate of AD (most fermentable substance), the combustion reaction (1.4) would release about 2870 kJ, while the reaction of conversion of glucose to methane through AD (1.3) releases only 390 kJ.



Microorganisms take advantage of the energy present in the carbon-carbon bonds, causing a change in the oxidation state of carbon-atoms from 0 in the glucose to -4 in the methane. In the new oxidation state lies energy, which is stored in this way in the product (methane) and is not released; as shown clearly by the Gibbs free energy of 1.4, lower than the one of 1.3. This stored energy can be exploited afterwards, for example by combustion. If this is the case, methane LHV is about 800 kJ/mol and since 3 mol of methane are gained, the amount of energy theoretically obtained is about 2400 kJ/mol, closed to the Gibbs free energy of the reaction 1.3. Though the |ΔG| is higher in the combustion reaction, the biomass can hold a great amount of water that should be vaporized, but AD process occurs in presence of water. Moreover, the process is driven at low-temperature ranges, under stable continuous operating-mode and without the need of light (ensuring a 24h-production).

1.2 Microbial consortia

The phyla of Bacteria responsible for AD are Firmicutes and Archaea. Firmicutes are the syntrophic-fermenters bacteria responsible for the digestion of VFAs (see chapter 1.1.3). Due to the great availability of VFAs, Firmicutes are quantitatively dominant in the digester. The phylum Firmicutes is majorly composed of two classes: Clostridia (13%) and Bacilli (76%) [11].

1.2.1 Clostridia

Clostridia are a class of Gram-positive, rod-shaped, endospore-forming (see chapter 1.2.2) bacteria. The endospores are the “dormant state” to which the bacteria can reduce themselves

under stressful environmental conditions, also for very long periods. Furthermore, Clostridia are anaerobic or aerotolerant and can be viewed as the evolutionary predecessors of Bacilli.

This class of microorganisms includes saprotrophic (decomposing) organisms, living in anaerobic habitats containing organic matter, including soils, aquatic sediments, and anaerobic tissues (such as intestinal tracts of animals). As such, they got a strictly fermentative-type of metabolism by which they convert many simple and complex carbohydrates (e.g. cellulose), as well as CO₂/H₂ or CO, (Table 1.3) but also amino acids, proteins and other organic molecules.

Table 1.3: Substrates clostridia can utilize [12]. BW stays for Biomass Wastes (e.g. agricultural) and OW for Other Wastes (e.g. sludge).

Feedstock	Substrate	Monomeric subunit	Clostridia group
<i>Crops</i>	Molasses	Glucose, Fructose	Solventogenic
<i>Crops</i>	Starch	Glucose	Solventogenic, some Cellulolytic
<i>Crops, BW</i>	Cellulose	Glucose	Cellulolytic, some Solventogenic
<i>Crops, BW</i>	Hemicellulose	Glucose, Xylose, Mannose, Galactose, Rhamnose, Arabinose	Cellulolytic, Solventogenic
<i>Crops, BW</i>	Pectin	Galacturonic acid, Rhamnose	Cellulolytic, Solventogenic
<i>OW</i>	Glycerol		Solventogenic
<i>OW</i>	Cheese way	Lactose	Solventogenic
<i>OW</i>	Short chain fatty acids (acetic, butyric, lactic)		Solventogenic
<i>OW</i>	Unknown		Cellulolytic, Acetogen
<i>Crops, BW, OW</i>	CO ₂ /H ₂ , CO		Acetogen

The products may be gas (such as CO₂ and H₂), alcohols, carboxylic acids, ketones of C2 to more than C8 (Table 1.4). During growth, first the acidogenic phase occurs, then, as the pH decreases due to the accumulation of acids, the culture enters the stationary phase, shifting to solventogenic phase (see Figure 1.2). Indeed, a pH value lower than 5,5 induce solvents productions, such as alcohols and acetone (i.e. *solventogenesis*). In this phase, strains such as *Clostridium acetobutylicum*, *Clostridium beijerinckii*, *Clostridium butyricum*, *Clostridium saccharobutylicum* and *Clostridium saccharoperbutylacetonicum* produce butanol in high concentration with acetone (or isopropanol) and ethanol. This process is called Acetone–butanol–ethanol (ABE) fermentation [13].

Costridia encompass as well many acetogens that fix CO₂ (using e.g. H₂) or CO (alone) and use one-carbon compounds (e.g. formate or methanol), some of them are *Clostridium ljungdahlii*, *Clostridium thermoaceticum*, *Clostridium carboxidivorans*.

Cellulolytic clostridia digest cellulose, such as *Clostridium thermocellum*, *Clostridium cellulolyticum* and *Clostridium phytofermentans*.

Finally, when clostridia grow on amino acids or fatty acids, malodours compounds are produced.

Table 1.4: Products of clostridia [12].

	Products	Organisms
gas	H ₂ , CO ₂	Acetogens, Solventogenic,
2-C	Ethanol, Acetic acid	Cellulolytic
3-C	Propanone, Propionic acid, Propanol, 1,3-propanediol, Lactate, Acrylate	Solventogenic, Propionic, others
4-C	Butyric acid, Butanol, Acetoin, Succinate, 2,3-butanediol	Acetogens, Solventogenic, others
5-C	Pentanoic acid (Valeric a.)	<i>C. scatologenes</i> , <i>C. kluyveri</i> , others
6-C	Hexanoic acid (Caproic a.), Hexanol, 2-hydroxy-4-methylpentanoate	<i>C. scatologenes</i> , <i>C. kluyveri</i> , <i>C. butyricum</i>
8-C	Octanoic acid (Caprylic a.)	<i>C. kluyveri</i>

1.2.2 Bacilli

Bacilli is a class of Gram-positive, rod-shaped, endospore-forming bacteria. Bacilli are obligate aerobes or facultative anaerobe and can be viewed as the evolutionary successors of the anaerobic Firmicutes Clostridia.

During H₂ production by anaerobic (Clostridia) and facultative bacterial population (Bacilli) in fermentation, various metabolic pathways can be simultaneously present during H₂ production. Figure 1.7 shows some of the alternative metabolic pathways.

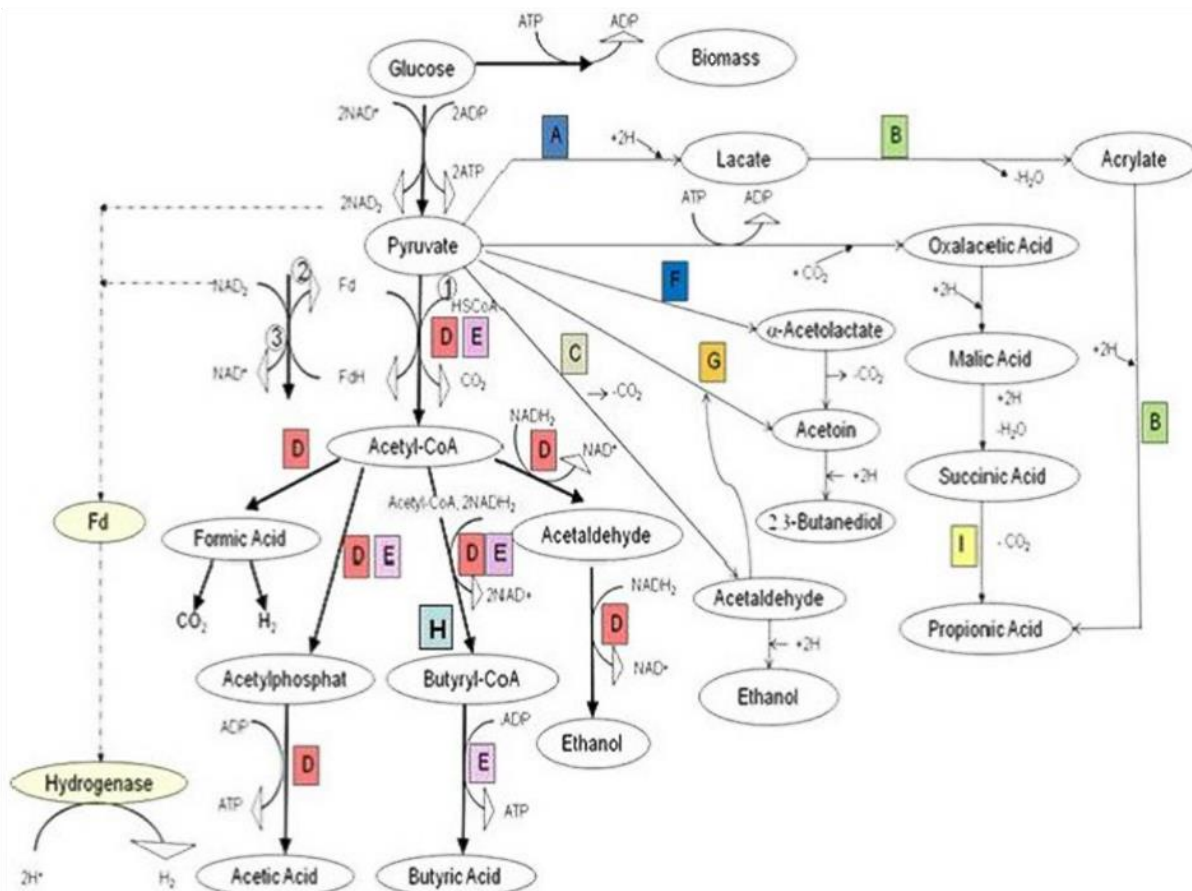


Figure 1.7: Metabolic pathway of glucose by hydrogen-producing bacteria in AD [14]. Letters indicate the organisms that conduct the reaction: **A**, Lactic acid bacteria (*Streptococcus*, *Lactobacillus*); **B**, *Clostridium propionicum*; **C**, Yeast, Acetobacter, Zymomonas, *S. ventriculi*, *E. amylovora*; **D** Enterobacteriaceae (coli-aerogens); **E**, *Clostridia*; **F**, Aerobacter; **G**, Yeast; **H**, *Clostridia* (butyric, butylic organisms); **I**, Propionic acid bacteria.

1.3 Feedstock flexibility

In absence of essential nutrients, the microorganism's growth stops. Therefore, it is often needed to feed possibly essential nutrients together with the substrate. The essential nutrients can be divided into macronutrients (carbon source and nitrogen source) and micronutrients (trace minerals). As carbon source, for example, the sugar is consumed very fast, unlike lignocellulose, that, indeed, is made up of three types of polymers (i.e. cellulose, hemicellulose and lignin) strongly interlinked by covalent bonds and non-covalent forces. Moreover, intermediate products of the metabolism can also have a limiting or even inhibiting effect.

In general, every biomass can be used as substrate if it contains carbohydrates, proteins, fats, cellulose, and hemicellulose as main components. Different wastes have been already utilized; the form ranges from solid, semi-solid and liquid, such as manure or by-products of industry, agricultural farms, disposal plants, etc. The use of more than one substrate (co-digestion) for biogas production has some advantages including: faster degradation rate, cost-effectiveness in terms of product formation, optimization of moisture and nutrient contents and concentration reduction of inhibitory compounds [14]. For example, nowadays in most agricultural biogas

plants liquid manure is fermented quite often combined with different co-substrates, such as energy crops [14]. The addition of solid-organic waste to liquid manure can increase the yield of biogas (per digester volume); this thanks to the higher content of readily-degradable organic substances. The same approach is valid for sewage sludges, where co-substrates consist in this case of floated materials, such as fat remains from pig slaughter.

1.4 Pre-treatment

Since the anaerobic biological process is so slow, its economic viability becomes questionable and hence institutions hesitate to invest in any form of this potentially sustainable process [16]. Generally, hydrolysis has been identified to be the key step in determining the rate of the digestion process, due to the presence of hardly degradable matrices in the substrates. Based on this, different pre-treatment methods aimed at improving the hydrolysis have been carried out [17]. The problem lies in lignocellulose materials and its specificity regards the behaviour of the lignin as a barrier preventing the biodegradation. Pre-treating the substrate before it enters the anaerobic reactor means breaking lignin and hemicellulose and reducing the crystalline structure of cellulose. In this way, the available surface area exposed to the attack of microorganisms is higher and a faster digestion is promoted. The pre-treatments currently applicable are classified according to different categories:

- mechanical (grinding, ultrasound, etc.)
- thermal
- chemical (through use of alcohols, acids, ozone, etc.)
- biological (by specific microorganisms or by specific enzymes)

The classification is hereinafter more extensively illustrated.

1.4.1 Mechanical pre-treatment methods

The mechanical pre-treatment leads to smaller particles or to squeezed substrate pieces. Indeed, particle size can affect the rate of anaerobic digestion as it affects the availability of a substrate (i.e. the surface area) to hydrolysing enzymes. This is particularly true with plant fibres; AD of pre-treated and not pre-treated sisal fibre waste was carried out and the methane yield increased by 23% (from $0,18 \text{ m}^3 \text{ CH}_4/\text{kgvs}$ to $0,22 \text{ m}^3 \text{ CH}_4/\text{kgvs}$) when the fibre size was reduced to 2 mm (from 100 mm) with a shearing pre-treatment. [18]. Also, the viscosity in the digester decreases consequently to a reduction of the particle size, making mixing easier, as the system results to be more homogeneous.

1.4.1.1 Shearing

Knife mills or shredders can be used to, respectively, cut or shred the substrate. Knife mills are usually used for wet feedstock, that is continuously cut until it is small enough to pass through a sizing screen [19]. Shredders are limited to biomass with a moisture content of under 15% [20], but many industrial shredders use substrates with much higher moisture contents.

1.4.1.2 Ball milling

In this pre-treatment, glass beads (grinding media) are thrown against the cells.

The acceleration of the beads is obtained:

- by shaking the entire container (Figure 1.8 and 1.9);

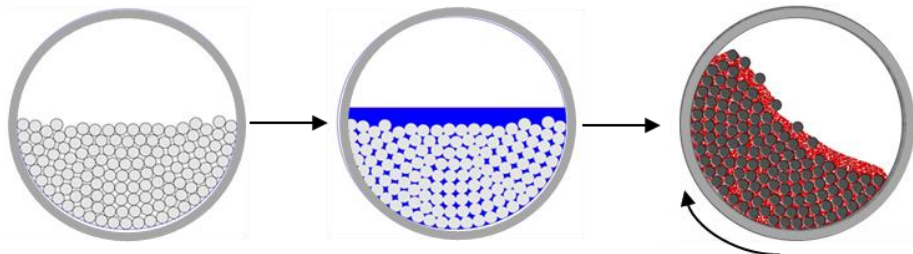


Figure 1.8: Bead milling in which the entire container is shaken [21].



Figure 1.9: Example of bead milling machine with 2 containers [22].

- by a spinning agitator within the container (Figure 1.10).

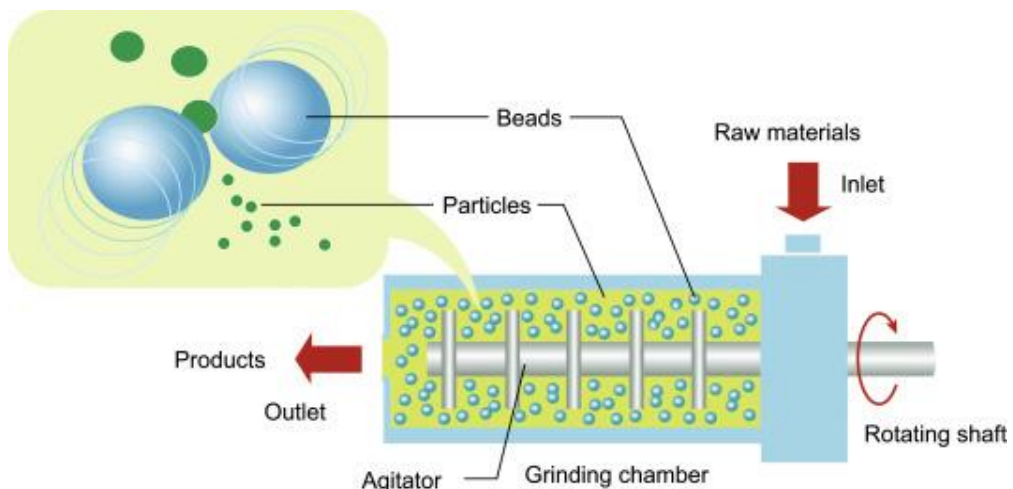


Figure 1.10: Bead milling in which a spinning agitator accelerates the beads [23].

1.4.1.3 High-pressure homogenization

The pressure is increased up to several hundred bars and then the suspension is homogenized under strong depressurization. The French press is an example of high pressure homogenizer. It works applying first a pressure of 83 MPa on the sludge and then releasing it quickly by opening a needle valve. The decrease of the pressure creates a very high shear force on the particles, making them explode.

1.4.1.4 Rotor-stator degradation

The rotor-stator homogenizer is composed of a rotating metal shaft (*rotor*) inside a stationary open-ended tube (*stator*), this is shaped with slots in the end (Figure 1.11).



Figure 1.11: Rotor and stator [24].

The rotation of the rotor creates a suction effect which draws the sample into the space between the rotor and stator, here the sample is subject to high shear forces due to the small space and the homogenization occurs (Figure 1.12).



Figure 1.12: Rotor-stator shear by spinning shaft, inside view [25].

1.4.1.5 Ultrasonification

Ultrasound can be applied either *indirectly* through a bath or *directly* by a probe. Direct sonication, as the probe is in direct contact with the sample, guarantees more efficient operation. Indeed, the treatment is based on the utilization of acoustic waves, which are propagated by the probe into the liquid in contact with it. In particular, acoustic waves are compression-rarefaction waves, that, when propagated into a liquid at high intensities, generate alternative high- and low-pressure cycles. During the low-pressure cycle, the liquid reaches the vapour pressure, creating small bubbles. During the high-pressure phase the bubbles can no longer keep the balance between the pressure and the viscosity forces and implode violently. The violent implosion of these might disrupt the nearby substrate's particles' walls, that could release intercellular matter that can be then more easily degraded by microorganisms during AD. Cavitation is therefore the phenomenon behind the ultrasonification and it is always accompanied by intense local heating, that in some case can reach up to 5000 K (Figure 1.13).

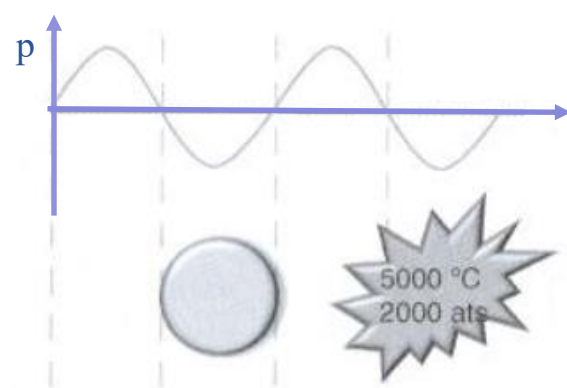


Figure 1.13: Cavitation phenomenon [26].

The ultrasonic equipment is composed by four components: generator, converter (or transducer), booster and probe (or horn or sonotrode) (Figure 1.14).



Figure 1.14: Ultrasonic equipment [27].

The generator transforms AC line power in high frequency electrical energy (20 - 100 kHz), which is received from the converter and further transformed into vibration (electrical energy is converted into mechanical energy), thanks to the piezoelectric material of which the converter is made. The booster increases the amplitude of the waves and the probe finally propagates the acoustic waves into the medium. Several studies have shown that the rate of bacterial degradation can accelerate up to 4 times compared to conventional treatment [28].

Continuous sonication of an input stream is also possible (Figure 1.15). The liquid sample is pumped into the sonicator's chamber through the inlet at the bottom of the unit. While passing, the sample undergoes sonification. The processed liquid exits the unit from an outlet port. The sonication settings and the flow rate can be adjusted. Because sonication generates heat, a water jacket is available to protect the sample from overheating. The water jacket surrounds the chamber and cold water is recirculated inside it; so, the chamber is cooled down from the external surface.

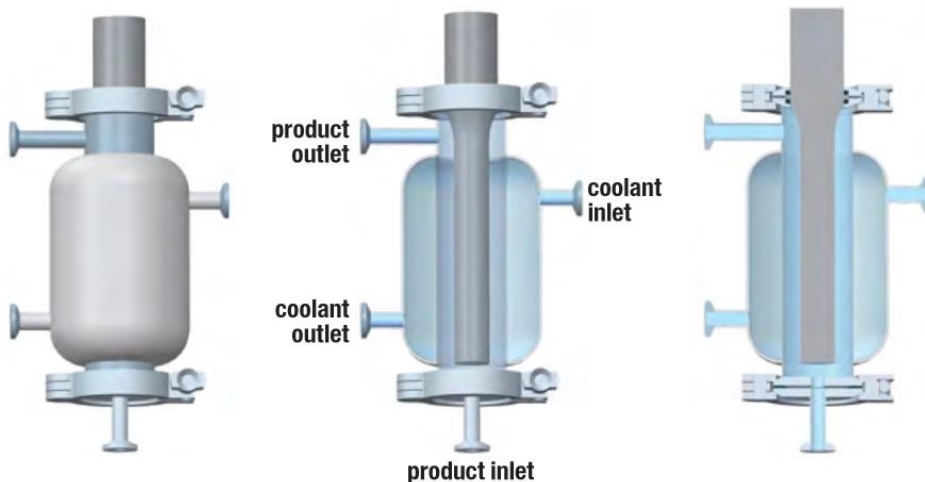


Figure 1.15: Continuous sonication [29].

1.4.2 Thermal

This is one of the most applied at industrial scale for AD of various substrates. The temperature range goes from 50-250 °C, as sludge solubilisation was seen at temperatures as low as 50°C [30]. The retention time clearly increases with the decreasing of the temperature, as the kinetic of the any reaction is favoured by the temperature. Reported retention time varies from 0 minutes to 72 hours [31]. Thermal pre-treatment removes pathogen, improves dewatering and reduces viscosity of the digestate, but inhibitory compounds can be formed, especially for long thermal treatment times. Regarding this, one of the most known phenomena is the Maillard reaction between carbohydrates and amino acids. It occurs at temperature values higher than 150°C or at lower temperatures (<100°C) for a longer time and results in the formation of complex substrates difficult to biodegrade [30]. The effect of the treatment depends anyway on the substrate type and temperature range [30]. Finally, even though the thermal pre-treatment requires a great amount of energy, the energy requirements during the pre-treatment step can be covered by the extra methane production with a positive net-back [32].

1.4.3 Chemical pre-treatment methods

Chemical pre-treatments consist in the addition of chemical substances, like alkalis, strong acids or oxidants to achieve the destruction of the organic compounds, improve the hydrolysis rate and enhance the biogas production. AD generally requires an adjustment of the pH towards a greater alkalinity, thus alkali pre-treatment is the preferred chemical method [33].

Chemical pre-treatments are not suitable for easily biodegradable substrates, due to their accelerated degradation and subsequent accumulation of VFA [34]. On the opposite, the effect is clearly positive on substrates rich in lignin [35].

1.4.3.1 Alkali pre-treatment

The alkali treatment causes high pH values in the substrate. It is important to underline that high salts concentration can cause bacterial cells to dehydrate due to osmotic pressure [36]. Moreover, light metal ions (i.e. sodium) are required for microbial growth and, consequently, affect specific growth rate. While moderate concentrations stimulate microbial growth, excessive amounts slow down the growth, and even higher concentrations can cause severe inhibition or toxicity [36]. This pre-treatment may be useful for acidic and lignin-rich substrates that could otherwise not be anaerobically digested [20]. About 55% of the dry matter can be decomposed, especially when using NaOH to saponify [37]. Other chemicals can be used, such as lime or ammonia, but the high costs of alkalis in general make this technology economically unattractive (Table 1.5).

Table 1.5: GER of some Alkalies (SimaPro Database).

Chemical	GER (MJ/Kg)
Soda, powder	5,99
Ammonia, liquid	43,6
Ammonia, partial oxidation, liquid	49,5
Ammonia, steam reforming, liquid	41,8

1.4.3.2 Acid pre-treatment

Acid treatment is the most widely used conventional pre-treatment method for lignocellulosic feedstocks on industrial scale [38], even if the corrosive and toxic nature of most acids requires a suitable material for building the reactor [39]. Acid pre-treatment can be used in combination with heat, but at high temperatures from 60°C to 160°C (temperatures higher than 160°C in combination with acids show a drop in methane production) [20], that make the process not anymore energetically sustainable.

1.4.3.3 Oxidative pre-treatment

Oxidative pre-treatment is based on the use of radicals. The radicals are formed during the oxidation reaction, that is the reduction of the oxidizing agent, such as oxygen, ozone (O_3) and hydrogen peroxide (H_2O_2). By using ozone, the substrate can become permeable and water-insoluble macromolecules can decompose themselves into smaller-water soluble molecules.

The disadvantages include the formation of toxic substances for the methanogens (e.g. formaldehyde) and the increased amount of free carbon, that cannot be degraded during AD.

Table 1.6: GER of some oxidizers (SimaPro Database).

Chemical	GER (MJ/Kg)
Ozone, liquid	174
Hydrogen peroxide, 50% in H ₂ O	23,8

1.4.4 Biological pre-treatment methods

1.4.4.1 TSAD

Also called pre-acidification, two-stage digestion or dark fermentation coupled to methanogenic reactor, it consists of separating the first two steps of the process (*hydrolysis* and *acidogenesis*) from the second two (*acetogenesis* and *methanogenesis*). The pH value in the first digester lies between 4 and 6, inhibiting methane production (that occurs at pH values higher than 6,5) and causing a volatile fatty acids accumulation, but the enzymes responsible for the degradation of cellulose, hemicellulose and starch work very well under these conditions. CO₂ is also formed in the first digester and at low pH it is released in the gas produced in the pre-acidification step. Therefore, in the following stage the methane concentration is higher.

1.4.4.2 Enzymatic pre-treatment method

A mixture of enzymes, different from the ones already present (produced by the microorganisms of AD), is added. The addition can occur in the digester in which AD takes place, in the first step of a two-step AD process (see chapter 1.3.4.) or in a dedicated vessel for the enzymatic pre-treatment. There is some evidence to suggest that enzymes added directly to the biogas reactor are degraded quickly after addition [20]. Several batch AD studies have indicated that the addition of enzymes to the first stage of a two-stage AD process leads to slightly higher substrate solubilisation and to higher biogas yields [20]. The mixture of enzymes may include different types that are able to specifically degrade: cellulose, hemicellulose, pectin and starch.

1.4.5 Shear stress induced on bacteria

Pre-treatments can impact not only the substrate, but the microorganisms of AD as well in case of wet AD processes, where fresh feedstock is slurried with the addition of water. In this case, dewatering is the first stage of postdigestion processing; the dewatered solid fraction is destined to be fertilizer and the water is recycled to supply the plant. In this case, microorganisms of AD are treated together with the substrate. Clearly, the wanted effect for the substrate (its breakage) is not desirable for the microorganisms as well; which should not be damaged in order to be able to drive the different phases of the AD process. The domain (see Figure 1.3) and the evolution underwent by the specific type of microorganism determine how easy AD microorganisms can be broken.

The Gram-positive bacterial cell is contained in a cell membrane, that is still surrounded by the cell wall. The membrane's function is not to protect the cell from osmotic shock, but it is rather elastic, interactive and semi-permeable, as it is mostly formed of phospholipids and proteins. Here, concentration gradients are actively maintained through transport systems, such as electron transport chain to produce ATP. Between the cell membrane and the cell wall a periplasmic space is located. The cell wall is thin and rigid; it is made up of peptidoglycan, that gives a structure to the cell envelope. It gains its strength from its chemically bonded nature. The peptidoglycan layer is composed of N-acetyl-glucosamine and N-acetyl-muramic acid residues stucked by β -(1-4)-glycosidic bonds. The chains are crossed-linked by a tetrapeptide through the NAM residue. The peptides are further cross-linked, and the result is a rigid strict structure, that provides shape, tensile strength and protection from osmotic shock. Gram-positive bacteria, such as *Bacillus*, possess a thick cell wall composed of 50-80% peptidoglycan together with teichoic acid. On the other hand, Gram-negative bacteria have a relatively thin cell wall consisting of a few layers of peptidoglycan (even though this is the major responsible for cell resistance) but surrounded by a second lipid-protein bilayer membrane, that comprises proteins, lipopolysaccharides and phospholipids. The Firmicutes, such as *Clostridia* and *Bacilli* (see Chapter 1.2), and Actinobacteria are classified as Gram-positive bacteria.

Methane-forming bacteria, classified in the domain Archaea (see Figure 1.3, Chapter 1), present a different cell wall. The cell wall lacks muramic acid, and the cell membrane does not contain an ester lipid as its major constituent [7] (Figure 1.16).

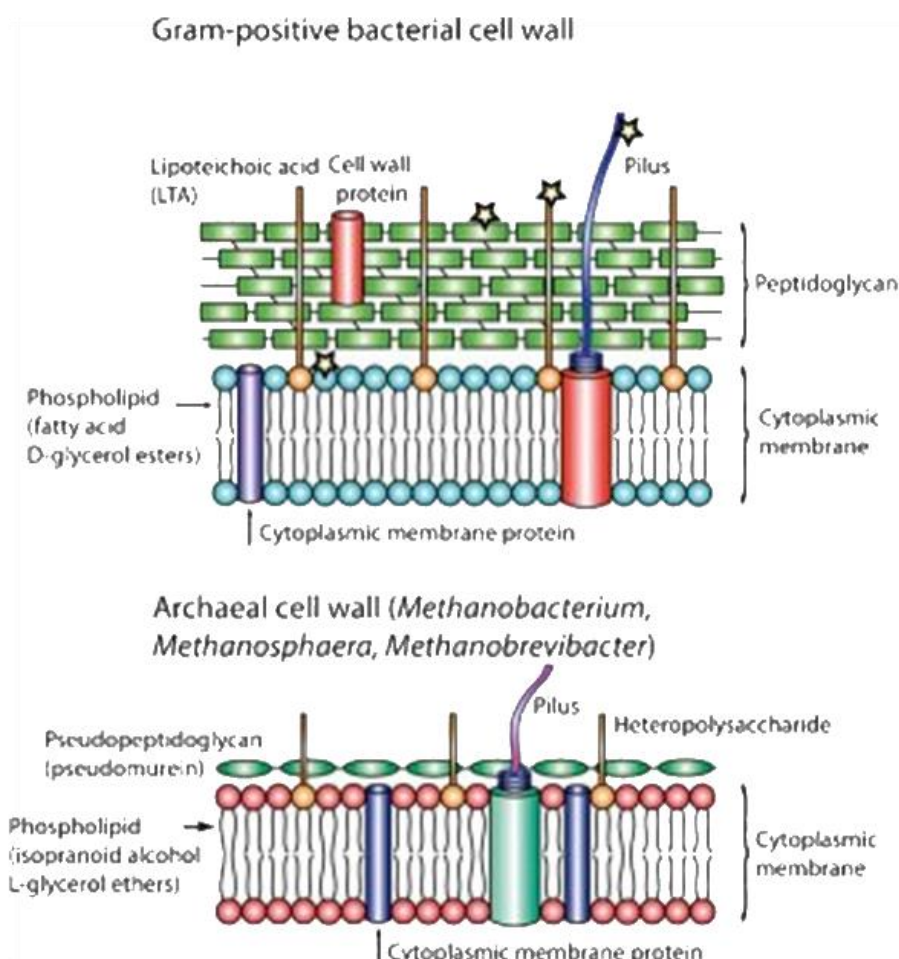


Figure 1.16: Comparison between cell wall of bacteria and cell wall of methanogens [40].

It is possible to conclude that methanogens will be more affected by shear stresses, due to the constitution of both cell membrane and cell wall, that lack of certain components responsible for strength and resistance, that, on the opposite, are found in the composition of membrane and wall of Gram-positive bacterial cells.

1.5 In situ laser back-reflection

The optical-based method FBRM (focused beam reflectance method) is based on the detection of backscattered laser light and the time of flight (TOF) of the beam. However, only elongated-shape particles can be efficiently analysed and not spherical-shaped particles (bacteria).

It is desirable now to focus on a three-dimensional optical reflectance method (3D-ORM) probe of Sequip S+E GmbH. It is equipped with an excitation beam that can be moved in three dimensions, opening the doors to the analysis of spherical bacteria. Furthermore, the probe is heat-sterilisable (internal electronic parts can be removed for this purpose) and can be used for *in situ* measurement. Additionally, information about the cell size distribution are returned. The components of the probe are briefly hereinafter discussed (Figure 1.17).

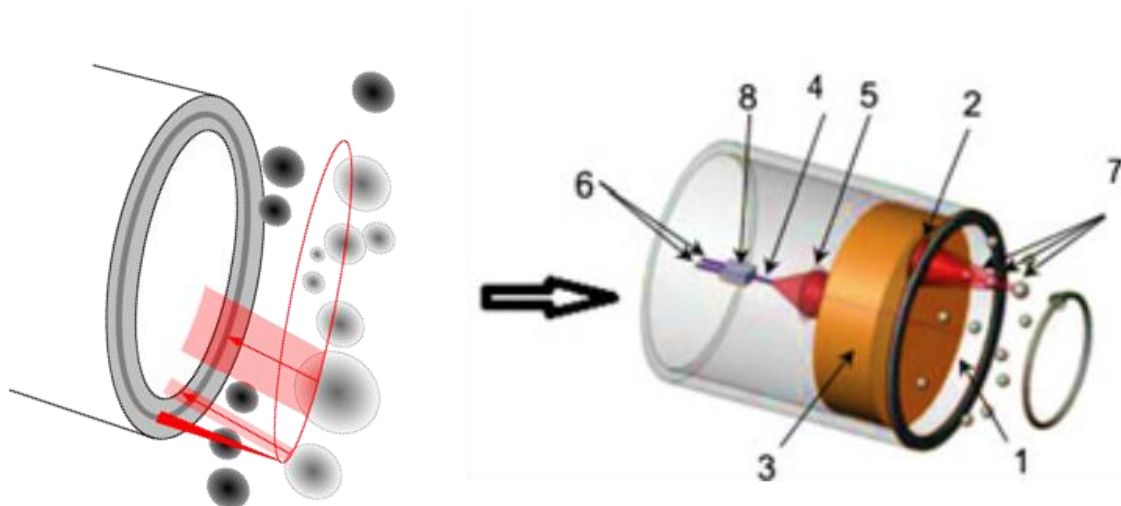


Figure 1.17: Schematic representation of the Sequip-probe [41]. A highly efficient focusing length (2) allows to scan precisely microbial cells, that enter the multiple focal planes surrounding the probe. The laser beam has an intensity inferior to 5 mW. The inlet of the laser beam into the probe is accomplished by a 12,8 µm single-mode fibre (6). The separation of incoming and outgoing signals is realized with a fibre optic coupler (8). Thanks to the rotating optical system (3) and the dynamic focus (7), the imaging of a spiral path with the diameter of 8.5 mm takes place. The coupling out of the reflected signals from the probe is realized with the incoming single-mode fibre (6). The small cross section of such fibre (4) ensures that only particles directly or close to the focal point are detected.

1.6 Probability distribution

A probability distribution is a mathematical model which connects the values of a variable to the probability that such values can be observed. Probability distributions are used for modelling the behaviour of a phenomenon of interest in relation to the total amount of cases in which the experimenter observes a stated sample. The variable of interest is seen as one random variable whose probability law expresses the degree of uncertainty with which his value can be observed. Furthermore, in continuous distributions the variable is expressed on a continuous scale.

Probability distributions are expressed by a mathematical law called probability density functions (PDF). The probability density functions of interest for this work are the following ones.

- The normal distribution, where the *mean* **a** and the *variance* **b**² (or standard deviation **b**) of a random variable (*x*) are the parameters of major interest as they express respectively the central tendency and the variability of the random variable.

$$y = \frac{1}{\sqrt{2\pi}b} e^{-\frac{(x-a)^2}{2b^2}} \quad (1.5)$$

- The Cauchy distribution

$$y = \frac{1}{\pi b \left(1 + \left(\frac{x-a}{b}\right)^2\right)} \quad (1.6)$$

- The Gamma distribution

$$y = \frac{1}{b^a \Gamma(a)} x^{a-1} e^{-\frac{x}{b}} \quad (1.7)$$

- The logistic distribution

$$y = \frac{1}{b} \left(e^{\frac{x-a}{2b}} + e^{-\frac{x-a}{2b}} \right)^{-2} \quad (1.8)$$

- The log-normal distribution is the probability distribution of a random variable whose logarithm has a normal distribution.

$$y = \frac{1}{x\sqrt{2\pi}b} e^{-\frac{(\ln x - a)^2}{2b^2}} \quad (1.9)$$

- The log-logistic distribution is the probability distribution of a random variable whose logarithm has a logistic distribution.

$$y = \frac{\frac{b}{a} \left(\frac{x}{a}\right)^{b-1}}{\left(1 + \left(\frac{x}{a}\right)^b\right)^2} \quad (1.10)$$

2. Purpose of the thesis

This thesis project was conducted at the Technische Universität Berlin in the Bioprocess Engineering laboratory in the Scale up/down & PAT Group under the supervision of Dr. S. Junne, where “biogas processes” is one of the research lines currently under study.

Biogas production from biomass is a representative example of the modern challenges faced in large scale bioprocesses.

Today, the most successful policy in biogas operation is “don’t touch don’t breathe”. In the future, beyond a high flexibility on methane production to respond to the energy demand, efficient biogas production should be robust to different substrates to take advantage of any kinds of biomass available. The identification of the optimal conditions is a bottleneck, since results of the laboratory-scale are not often up-scalable, and evaluation implemented directly on a large-scale takes time, especially when operating in continuous mode. On the other hand, energetic expenditure evaluation on laboratory-scale can be very useful.

Mechanical pre-treatments evaluation and particle-size distribution monitoring in liquid phase is the object of study of this work. To assess the pre-treatment effect in connection with the aim, the particle-size distribution was analysed before and after each pre-treatment. Optimal performance of the pre-treatment step leads to a shift in the feedstock’s particle-size distribution to smaller diameters without damaging considerably the biomass. The biomass is present when fresh feedstock needs to be slurried with the addition of water. Dewatering is the first stage of postdigestion processing and the water took back in this stage is recycled to supply the plant (see chapter 1.3.6). The result is a feedstock containing microorganisms. Biomass, feedstock and fermentation broth (feedstock containing biomass) were separately investigated.

3. Materials and Feedstocks

3.1 Bacilli

The Bacilli species utilized in this work is:

Table 3.1: Scientific classification.

Domain	Bacteria
Phylum	Firmicutes
Class	Bacilli
Order	Bacillales
Family	Bacillaceae
Genus	<i>Bacillus</i>
Species	<i>B. subtilis</i>
Strain	DSM 21393 genetically modified with inhibited capacity of forming spores

First, a glycerol stock of this strain was produced. As dealing with a bacterial culture, Lysogeny broth (LB) was used as medium (Table 3.2) for the inoculation, after autoclaving, cooling down to room temperature and neutralizing ($\text{pH} = 7,0$) the solution, by adding NaOH. One Ultra Yield Flask was filled with a volume of 50 mL of LB, inoculated with 50 μL of inoculum and placed in the shaker at 200 rpm and 30 °C. The following morning, as bacterial growth was appreciated, the preparation of the glycerol stock took place. A volume of 500 μL of the overnight culture has been added to the same volume of a 50% v/v-glycerol solution in a 2 mL Eppendorf tube for 16 times (obtaining 16 replicates), gently mix afterwards and stored at a temperature of -80 °C.

Table 3.2: LB Medium composition.

Tryptone	10,0	g/L
Yeast extract	5,0	g/L
Sodium chlorate	5,0	g/L

The desired concentration for the pure culture of this microorganism used to run the experiments was around 5 g/L (i.e. which corresponds to an optical density measured at 600 nm of 15), in order to simulate AD feedstock, such as industrial sludge. Such a high OD₆₀₀ value could not be reached using LB as medium; in several attempts obtained values were in

general $OD_{600} < 4$), therefore it was resorted to another medium (Table 3.3), able to increase the biomass-growth.

In the preparation of the medium, thiamine and biotin solutions were sterilized by using a $0.22\ \mu m$ filter, instead of entering the autoclave. The culture was prepared in Ultra yield flasks either of 500 mL or of 2500 mL (according to needs of the experiment), by filling them with a volume of respectively 50 mL or 250 mL.

Table 3.3: Composition of the second medium used for *B. subtilis*.

Tryptone	10,00	g/L
Yeast extract	7,50	g/L
Sodium chlorate	5,00	g/L
Glucose	2,50	g/L
Thiamine	0,05	g/L
Biotin	0,05	g/L
Sigma 204 antifoam	1,00	mL

3.1.1 LB Agar plates

Solids supports were essential to grow microorganisms and assess the cell viability before and after the pre-treatment was applied. The selected solid support is Agar plates, due to the convenience for the planned tests.

The plates prepared for this work were LB agar plates, this means that they are made up of LB medium (see Table 3.2), kept semi-solid/gel-like by agar. The role of this medium is, as for liquid cultures, to provide nutrients and carbon source for microbial growth. The specific composition and ingredients to prepare LB-agar are reported in Table 3.4.

Table 3.4: LB-agar composition.

Tryptone	10,00	g/L
Yeast extract	5,00	g/L
Sodium chlorate	5,00	g/L
Agar	14,00	g/L

The prepared solution was vigorously shaken by hand in a closed cylinder of 10 L, then poured in a glass flask, closed with a cork top and tin foil, and lastly autoclaved. Once autoclaved, the glass flask was brought to the laminar bench, where Petri dishes of 5 cm-diameter were already opened and labelled. At this point the plates were filled up with the right amount of LB-agar (i.e. approximately half of the plate), only after sterilizing with fire the border of the flask. The plates were allowed to cool down and, afterwards, they were closed and stored in the fridge.

3.2 Clostridia

The Clostridia species utilized in this work is:

Table 3.5: Scientific classification of *C. acetobutylicum*.

Domain	Bacteria
Phylum	Firmicutes
Class	Clostridia
Order	Clostridiale
Family	Clostridiaceae
Genus	<i>Clostridium</i>
Species	<i>C. acetobutylicum</i>
Strain	ATCC824

The first step was inoculation of the culture. Initially 1 L of the medium Clostridia Growth Medium (CGM) (Table 3.6) was prepared, autoclaved and checked for the pH value, that should be around 5. It is noteworthy that, during the preparation of the medium, the salts MnSO₄, FeSO₄ and MgSO₄ were sterilized by filtration, as well as p-aminobenzoic acid, but separately from the other compounds.

Table 3.6: CGM Medium composition.

KH ₂ PO ₄	0,0750	% w/w H ₂ O
K ₂ HPO ₄ 3H ₂ O	0,0982	% w/w H ₂ O
NaCl	0,1100	% w/w H ₂ O
MnSO ₄ H ₂ O	0,0010	% w/w H ₂ O
p-Aminobenzoic-acid	0,0004	% w/w H ₂ O
MgSO ₄	0,0348	% w/w H ₂ O
FeSO ₄ 7H ₂ O	0,0010	% w/w H ₂ O
Asparagine	0,2000	% w/w H ₂ O
Yeast extract	0,5000	% w/w H ₂ O
(NH ₄) ₂ SO ₄	0,2000	% w/w H ₂ O
Glucose	8,0000	% w/w H ₂ O
Sigma 204 antifoam	1,0000	mL

Successively, a 500 mL glass bottle was sealed with two-screw connections glass-cup, each linked to a gas-filter through a tube (Figure 3.1); the bottles were then sterilized and filled up with the medium. The system was flushed with nitrogen (N_2) at 1,5 bars for around 3 minutes through the filters to remove the oxygen and ensure anaerobic conditions. At this point the medium was transferred to five previously sterilized 10 mL screw glass tubes for a volume of 5 mL each (Figure 3.2). Four of them were inoculated with 100 μ L (0,02 % v/v) of inoculum and one with 500 μ L (0,10 % v/v). The glass tubes were closed in the anaerobic jar (Figures 3.1 and 3.2) with sachets to capture the remaining oxygen (wet to start the reaction) and finally placed in the incubator at 37 °C. The anaerobic jars used in the experiments are airtight boxes; closures equipped with stoppers made in butyl-rubber prevents air. They are always coupled with *sachets*, filled with an oxygen-binding reagent mixture that oxidizes small iron particles and releases CO.

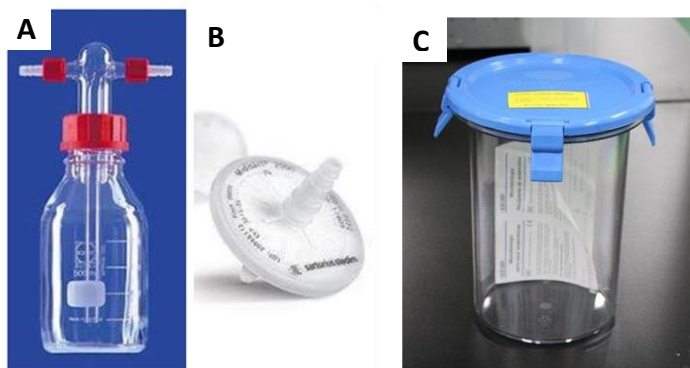


Figure 3.1: A: Gas-bottle with screw connections; B: Gas-filter; C: Anaerobic jar.

After two days, other three glass screw cap tubes were each one filled with 5 mL, subjected to a thermal treatment (70 °C for 10 minutes) and inoculated with 1 mL of the previous culture.

One week later, the plating phase took place. It was performed distributing on LB Agar plates a volume of 10 μ L collected from a sample obtained diluting the culture by a factor 1:1000. This dilution was reached through the following steps:

- i) 2 mL of a 1 M NaCl solution were transferred in an Eppendorf tube and 2 μ L of the culture were added.
- ii) 2 mL of a 1MNaCl solution were transferred in an Eppendorf tube and 2 μ L of the previous sample were added (4 times in total).

Then, the plates were afterwards collocated into the anaerobic chamber, after flushing with nitrogen, and incubated.

After five weeks, an aliquot of 450 mL of medium was inoculated in a 500 mL glass bottle. This step was performed only after the oxygen was removed from the medium by using the glass bottle with screw connections linked to gas-filters and nitrogen, as described above (see Chapter 3.2).

The cultivation was stopped when flocculation was observed (see Figure 3.3).

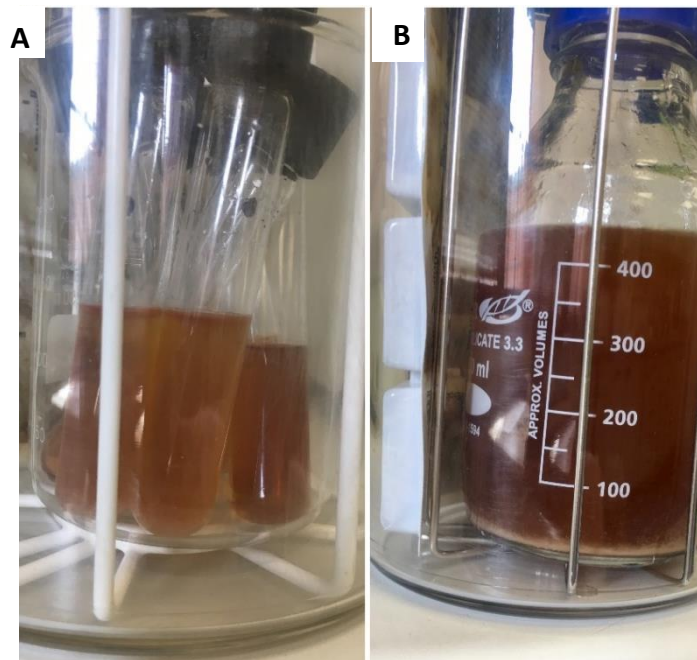


Figure 3.2: *C. acetobutylicum* cultures grown in: A) glass screw glass tubes and B) glass bottle, placed in the anaerobic jar with sachets.



Figure 3.3: Flocculation of *C. acetobutylicum* culture.

3.3 Fermentation broth (FB)

In general, the fermentation broth is a complex media in which the following phases coexist:

- raw substrates;
- microorganisms and their components (i.e. biological phase);
- chemical additives;
- fermentation products;

- gases such as oxygen and other metabolic gases.

It should be noted that the nature of FB is given by the coexistence of solid, liquid and gas phases combined and, at the same time, in different ways, interacting among them. The composition of the fermentation broth is fundamental to understand the phenomena that interact in such systems, but it is difficult to be monitored in real time.

The fermentation broth sample used in this work is the result of the fermentation conditions in Table 3.7.

Table 3.7: Characterization of the FB used in this work.

Feed	Semi-continuous
Working volume	16 – 17 L
Temperature	38 °C (mesophilic)
Substrate	Co-digestion of Maize silage/ grass silage in a proportion 90/10 of VS
Organic loading rate	3,0 – 3,5 gvs d ⁻¹ L ⁻¹
pH (fermentation broth)	7,5 – 7,8
Biogas yield	0,6 – 0,7 L gvs ⁻¹
Methane content	50 – 55% (v/v)
Carbon dioxide content	43 – 48% (v/v)

3.4 Prepared Feedstock (PF)

Within the context of the present work, “*prepared feedstock*” refers to a mixture of grass fibres, small residues from bushes and soil in equal parts, diluted with deionised water resulting in approximately 20% (w/w) of dry biomass (Figure 3.4). The mentioned biomass is commercially available, already prepared, and it was necessary only to carry out the dilution with water.



Figure 3.4: PF.

4. Mechanical Treatments

Different experiments were carried out depending on the sample analysed. The following table (4.1) has the purpose to ease the understanding about which pre-treatment each kind of sample underwent.

Table 4.1: Summary of the experiments.

	Bead Mill	Ultrasonification	Rotor-Stator degradation	Continuous flow-ultrasonification
<i>C. acetobutylicum</i>				×
<i>B. subtilis</i>	×	×	×	×
Culture Broth				×
PF	×	×		

4.1 Bead mill

Initially, a volume of 4 mL of the diameter of 0,5 mm was rinsed with a 70% v/v-ethanol solution by using a 125 µm – nylon filter (Roth, Germany), to sterilize them. To make the ethanol evaporate, the glass beads were placed in the oven at 50 °C until it was evident that all the ethanol was evaporated. The inner parts of the steel container were rinsed with 70% v/v-ethanol solution. The container was then filled with 4 mL of glass beads and the desired amount of sample and then closed tightly. It was closed by screwing one part of the container on the other one; since the container was afterwards vigorously shaken, it was necessary to take care that no glass beads were in the engraved lines on the borders that consent to screw, to avoid the release of the cell suspension during the experiment. The container was clamped to the shaking-arms of the machine and the machine switched on. The settings, that include time and the frequency were modified to the desired conditions (variable among experiments) and a constant frequency of 30 Hz. After the imposed time was elapsed, the containers were removed from the machine, opened and turned fast up site down, spilling the contents in a sterile Falcon tube through a 125 µm – nylon filter placed on a plastic funnel. The filter was used to separate the glass beads from the sample. Since the machine includes 2 containers, and each time both were filled with the same volume of sample, experiments were always performed in duplicates.

The ball milling treatment was performed on PF (16 mL for 10 min) and on *B. Subtilis* suspension (see Table 4.2). For the experiments conducted using a cell suspension of *B. Subtilis*, the following the procedure described hereinafter was followed. The Falcon tube was closed and transported under the laminar bench. Here, 2 µL of the sample were added to 2 mL of NaCl solution in an Eppendorf tube (diluting by a factor of 1:1000) and 20 µL of this solution was added to other 2 mL of NaCl solution in another Eppendorf tube, using the same dilution

criteria. This sample obtained with the second dilution was used for the plating phase ($10 \mu\text{L}$ per one agar plate) (see following Chapter). The plates were afterwards incubated at 30°C .

Table 4.2: Protocols of experiments *B. Subtilis* suspension – Bead Mill.

First set of experiments				Second set of experiments			
Volume		Time		Volume		Time	
8	ml	5	min	8	ml	5	min
8	ml	10	min	8	ml	10	min
8	ml	15	min	8	ml	20	min
2	ml	10	min				
16	ml	10	min				

For the operating principle, see Chapter 1.3.2.2.

4.2 Ultrasonification

Prior to the experiment, the *sonotrode* was sterilized with a 70% v/v-ethanol solution. The machine was set according to the amplitude and cycles values desired for each experiment, where:

- *cycle time* is the period of application of the ultrasound in percentage of 1 second;
- *amplitude* is the distance between the state of the horn fully extended and the state of the horn fully contracted (Figure 4.1). If an amplitude of 50% is set up, then the extension of the horn doesn't exceed the 50% of the total one.

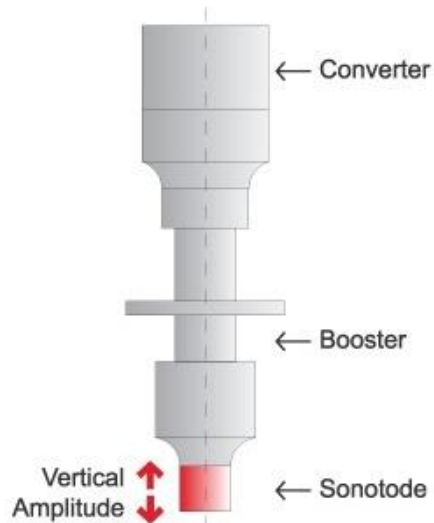


Figure 4.1: Sonotrode and its amplitude.

The *sonotrode* was then immerse in the sample by using an adjustable support, on which the sample was located.

The ultrasonification-treatment was performed on PF (50% amplitude; 0,7 cycle; 6x20 sec) and on *B. Subtilis* suspension (Table 4.3). When the experiments were carried out on a cell suspension of *B. Subtilis*, a sterile 1,5 mL-Eppendorftube was filled up with a volume of 1 mL of this. The sample was kept on ice for the entire duration of the experiment and break intervals of 10 seconds were performed, to protect the samples from overheating. After the first trial, in the second set of experiments it was decided to elongate the time of application of the treatment and the experiments were performed in duplicates. Furthermore, in the second set *B. Subtilis* suspension was plated before the treatment as well, to compare the growth on agar plates before it and after the application of the treatment.

Table 4.3: Protocol of experiments *B. Subtilis* suspension - Ultrasonification.

	Cycle	Amplitude		Time	
<i>First set of experiments</i>	0,7	50	%	3x10	sec
	0,7	50	%	3x20	sec
	0,7	50	%	3x40	sec
	0,7	25	%	3x20	sec
<i>Second set of experiments</i>	0,7	50	%	6x20	sec
	0,7	25	%	6x20	sec

For the operating principle, see Chapter 1.3.2.5.

4.3 Rotor-stator degradation

For the operating principle, see Chapter 1.3.2.4.

The experiments were carried out on a cell suspension of *B. Subtilis* (around 10 mL volume), contained in a 50 ml-Falcon tube. Prior to the experiment, the stator was sterilized with 70%-ethanol. The single setting that the machine requires is the frequency value, that can be chosen between 4 different ones. The highest frequency (20500 min^{-1}) was the desired one, but only one set of experiments could be performed this way. The first trial was conducted without keeping the sample on ice and two samples out of three were overheated (due to the largest application times). The second trial was performed always cooling the samples with ice. Afterwards, the machine had technical problems to achieve the highest frequency. Therefore, another set of experiments was then performed using the lowest frequency value (800 min^{-1}). However, due to technical difficulties, this pre-treatment was no longer tested. The protocol of the experiments is reported in Table 4.4.

Table 4.4: Protocol of experiments *B. Subtilis* suspension – Rotor-stator degradation.

	Frequency		Time	
<i>First set of experiments</i>	20500	min^{-1}	5	min
	20500	min^{-1}	10	min
	20500	min^{-1}	15	min
<i>Second set of experiments</i>	800	min^{-1}	5	min
	800	min^{-1}	10	min
	800	min^{-1}	15	min

For the operating principle, see Chapter 1.3.2.4.

4.4 Continuous flow-ultrasonification

First, it was necessary to build up the setup, to proceed with the experiments (Figure 4.2). Silicone tubes of an adequate diameter (~3 mm) were cut sufficiently long to connect the ultrasonicator's chamber and were tightened using zip ties. Four tubes were required with the following functions:

- I. connect the sink tube and the reactor (cooling water in);
- II. connect the reactor and the sink (cooling water out);
- III. connect the fresh sample-container and the reactor through the pump (sample in);
- IV. connect the reactor and the treated sample-container (sample out). This tube was equipped with a tap to close or open, tightened to the tube with a zip tie.

A pump that enabled to run the experiments in the desired residence time range (i.e. in the range 20 rpm) was selected. The method consisted in using water and a chronometer; this was started as the first drop of water was entering the chamber and stopped when the first drop of water was leaving the chamber. Three pumps that could fit the diameter of the tubes were tested in the laboratory, presenting different pumping capacities: 10, 20 and 50 rpm. The 50 rpm-pump resulted in very short permanence times and the 10 rpm-pump resulted in long permanence times at any rpm, therefore the most appropriate for the experiments was the 20 rpm-pump.

Once built the continuous-flow ultrasonicator configuration inclusive pump, it was necessary to determine the experimental link between the setting of the pump and the exact permanence-time in the experimental protocol. As the viscosity is an intrinsic characteristic of the substrate, for each combination of type of substrate and desired permanence time the pump setting was set by pumping the substrate in the reactor in non-operating mode and timing the permanence of the sample in the ultrasonicator's chamber.

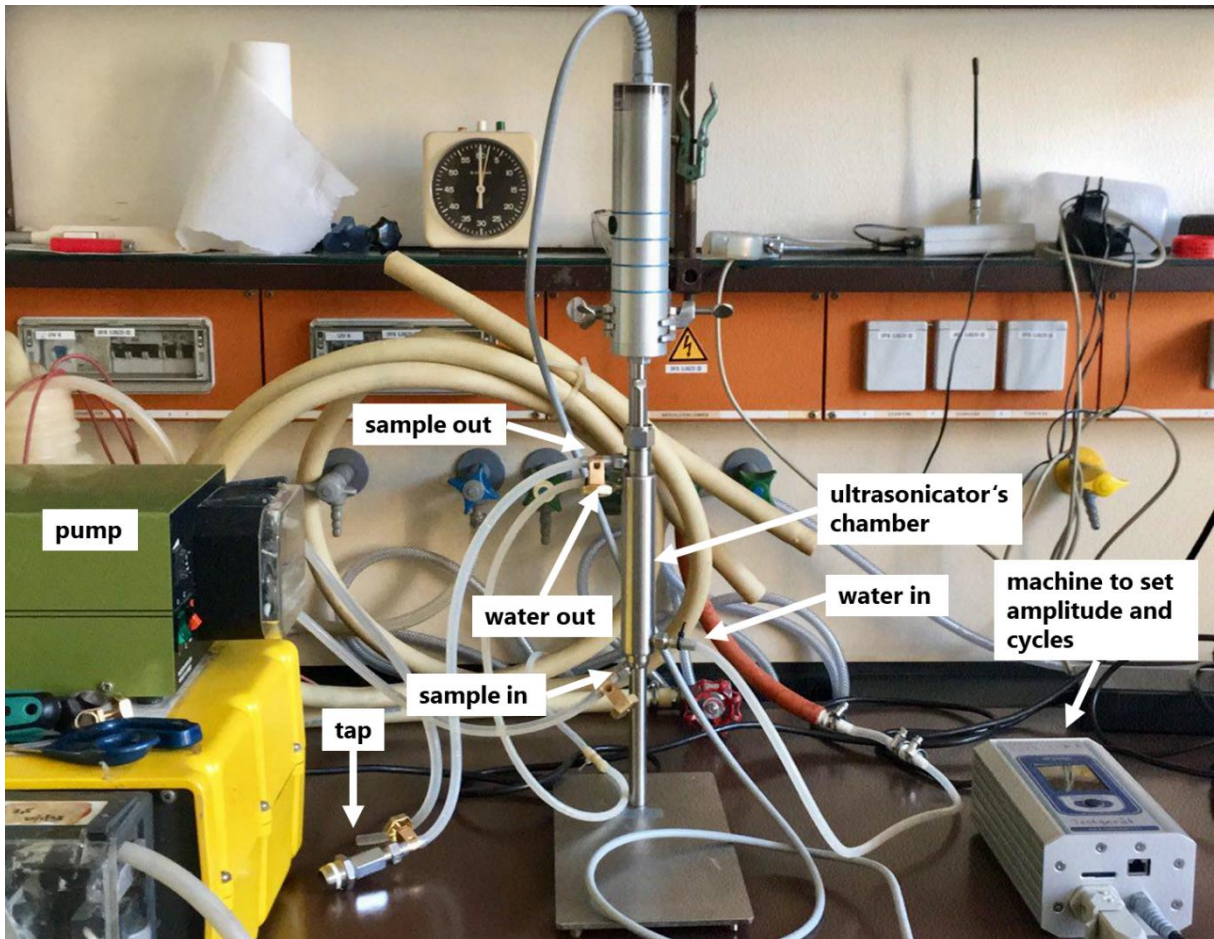


Figure 4.2: Picture of the experimental setup of the continuous flow-ultrasonicator.

Finally, to perform the experiments it was necessary to follow the following steps:

1. set amplitude and cycles in the machine;
2. open the sink;
3. immerse the “sample-in tube” in the fresh sample-container;
4. switch on the pump;
5. start the sonification with the machine.

Experiments were performed on the following substrates:

- *B. Subtilis* culture;
- *C. acetobutylicum* culture;
- Fermentation broth;
- Prepared Feedstock.

The set of experiments reported in Table 4.5 was performed with *B. Subtilis* suspension in duplicates, plating afterwards as described in chapter 4.1, also before the treatment. The desired amplitude values were the ones already used in the case of ultrasound (not continuous), but the machine could be set only with amplitude values that are a multiple of 10. Because of this, it was chosen to use either 30 and 20 or one of these two values.

Table 4.5: Set of experiments performed with *B. Subtilis* suspension followed by plating.

Amplitude		Cycle	Time	
50	%	0,7	2	min
30	%	0,7	2	min
20	%	0,7	2	min

Some experiments were performed one more time (in duplicates) (Table 4.6), using laser-back reflection as cell counting–method (method illustrated in the following chapter).

Table 4.6: Set of experiments performed with *B. Subtilis* suspension.

Amplitude		Cycle	Time	
50	%	0,7	2	min
30	%	0,7	2	min

The experiments performed on *C. acetobutylicum* are the following ones (table 4.7).

Table 4.7: Set of experiments performed with *C. acetobutylicum* culture.

Amplitude		Cycle	Time	
50	%	0,7	2,0	min
			3,5	min
20	%	0,7	2,0	min
			3,5	min

The protocol of experiments performed on FB is shown in table 4.8.

Table 4.8: Set of experiments performed with a fermentation broth.

Amplitude		Cycle	Time	
50	%	0,7	2	min
20	%	0,7	2	min

For the operating principle, see Chapter 1.3.2.5.

5. Data Analysis

5.1 Cells counting using an Image Analysis Software

Every time that the plating phase took place (only in some experiments with *B. Subtilis* suspension), the plates were photographed after incubation and the pictures were analysed by using the software *Fiji* (version 1.4). This is an image processing software, distributed by *ImageJ*, that groups a lot of plugins which facilitate scientific image analysis.

First of all, the scale was set, namely correspondence between 1 pixel and 1 cm. The picture of the plate was cut till have a square, the sides of which were tangent to the circle of the plate (Figure 5.1 A). The diameter of the plate was fixed (i.e. 5,2 cm) as well as the pixels of the picture (variable from picture to picture). These were divided for the diameter and the correspondence between 1 pixel and 1 cm found. In case of a non-perfect square (a rectangular), the average was used as value for the side of the correspondent square. The channels of the picture where then split to blue, green and red. Only one of the three resulting pictures was chosen, and the threshold applied to it. Afterwards the part containing the cells was selected, cropping the rest of the picture. The command *binary* consented to transform the picture in a black and white 8-bit format one. The colours were inverted to obtain the cells in black and the background in white (Figure 5.1, B).

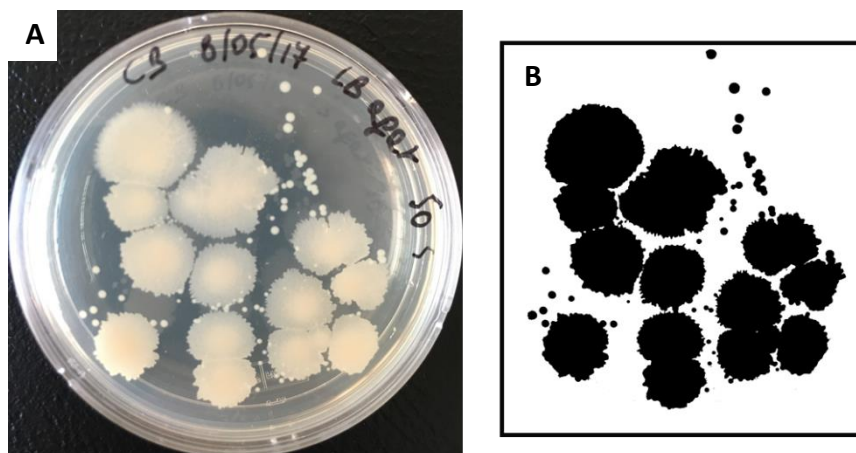


Figure 5.1: Photograph of a cultivating plate (A) and binary contrast image of the area occupied by the cells on the same plate (B).

Finally, the calculation of the area (%) of the picture (red square) occupied by the cells (Figure 5.2, B) was done with the software. By means of the scale set at the initial phase, the software was able to provide the area (cm^2) of the picture (red square) self as well. Considering what previously stated, the area (%) was transformed in area (cm^2) of the picture occupied by the cells. Knowing also the area of the plate through its diameter (i.e. $(\pi d^2)/4$) (Figure 5.2, A), the area (%) of the plate occupied by the cells was obtained from the mathematical ratio.

The number of cells on the plate was calculated as well with the software, but the calculated value included a lot of small points (result of the sloppy accuracy of the method) and therefore the number of cells was resulting overestimated.

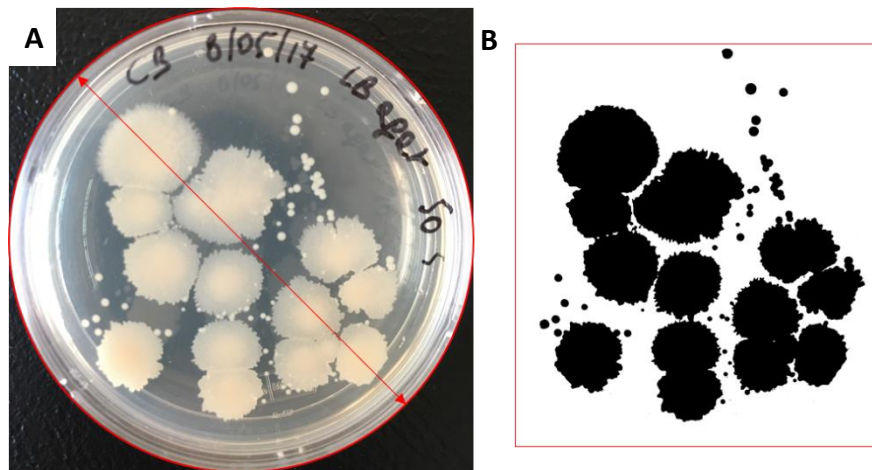


Figure 5.2: A: area of the plate, calculated as area of a circle through its diameter (i.e. $(\pi d^2)/4$); B: area (%) of the red square occupied by the cells (%) was calculated with the program, the area (cm) of the red square was known, so the area (cm) of the red square occupied by the cells was automatically known.

5.2 *In situ* laser back-reflection

In situ laser back-reflection was used as alternative method to plating for *B. Subtilis* suspension and, in general, as a method to analyse particle size distribution before and after treatment for all substrates. The analysis with the probe were conducted as it is shown in Figure 5.3. The sample was always transferred to a specific glass jar, as it was the only container available in the laboratory that consented to work with a probe inclination of about 45° . The glass tin was equipped with a little magnet as well, to be able to use the stirrer. Only in such a configuration (tilted probe and agitated suspension), it was possible to do the required measurements.



Figure 5.3: Picture of the experimental set-up for *in-situ* laser back-reflection measurements.

The Sequip-probe was then connected to a computer, where the Sequip-software to use in combination with it was installed. Here it was possible to see histograms and cumulative curves in real-time and export excel files of the data collected during the measurement (Figure 5.4).

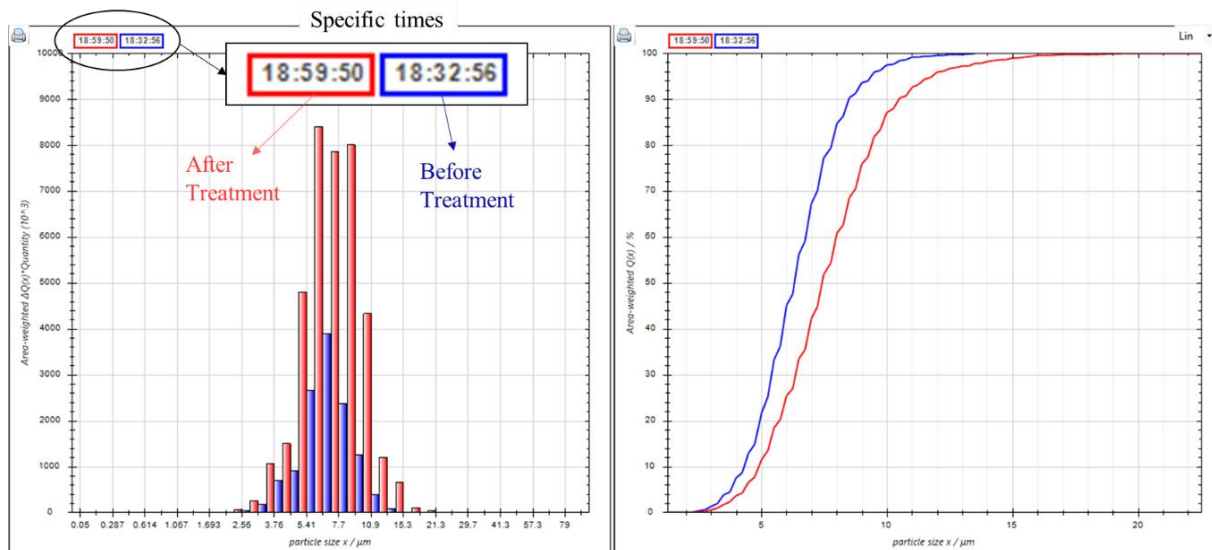


Figure 5.4: Interface of the Sequip-software.

6. Results

6.1 Cells counting

6.1.1 Effects on cell viability of Bead Milling

The first set of exploratory experiments were conducted in order to screen the optimum pre-treatment conditions, such as time and volume. The initial tested time for growth, under *in vitro* conditions, corresponded to 24 h, which resulted in overgrowth of the biomass within the petri dishes. As it can be noted in Figure 6.1, these experiments did not allow the proper quantification of colonies/granules and therefore the analysis with the Software *Fiji* was not performed. However, the simple visual analysis of the plates indicated that biomass was not severely affected due to the pre-treatment step since the inoculated plates exhibited good microbial growth.

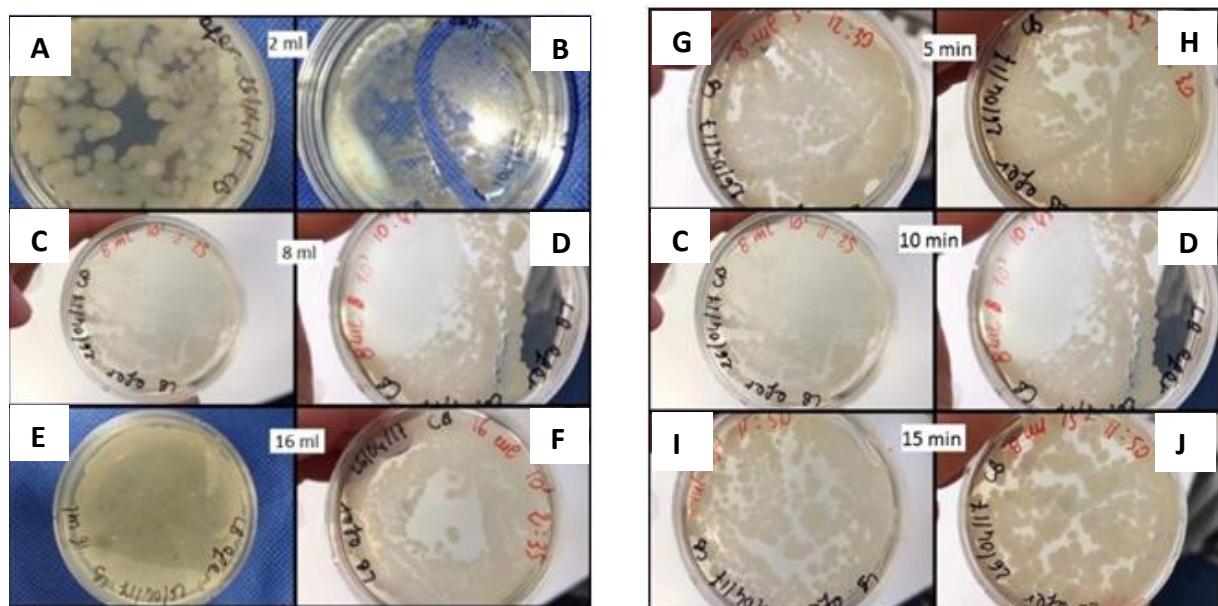


Figure 6.1: Pictures of the plates resulting from the first set of experiments (on the left grouped according to the Volume, on the right according to the Time of the treatment).

As described in chapter 4.1, the shaker was filled with 4 mL of glass beads and a variable amount of cell suspension. After the treatment, the content of the shaker was spilled in a filter to separate the glass beads from the cell suspension, collected afterwards into a sterile Falcon tube. Because of the above-mentioned filtration step, it was found to be difficult to work with a cell suspension-volume of 2 mL. Indeed, this is inferior to the beads volume (4 mL) and, hence hardly separable. In the next experiments, because of the problem found with 2 mL-volume and to maintain only one variable (the time), the volume was taken constant and equal to 8 mL.

Moreover, it was chosen to consider a longer time of application of the pre-treatment (20 min) to investigate if biomass would have been severely affected; the results of the second set of experiments are shown in Figure 6.2.

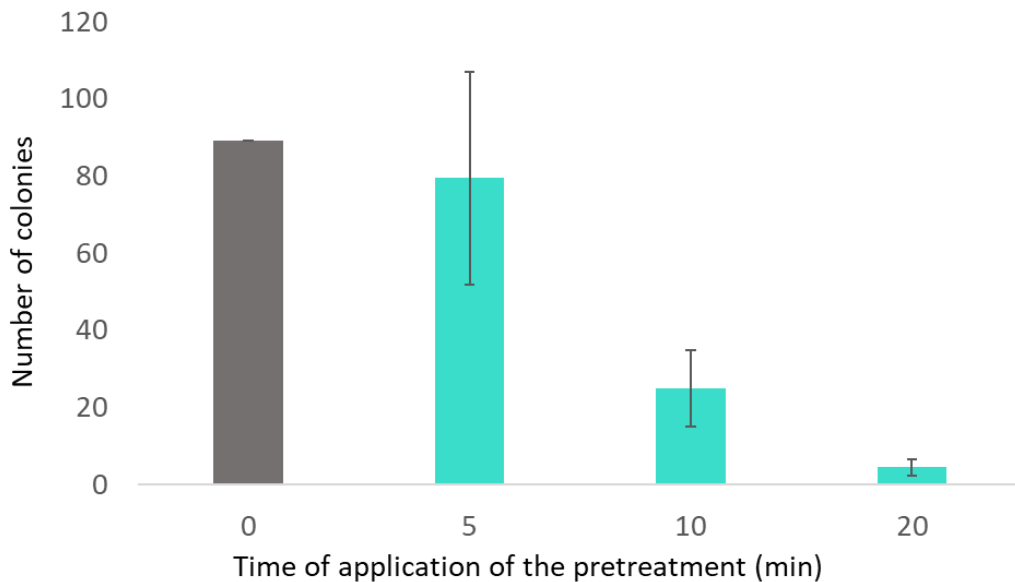


Figure 6.2: Result of cell counting before ($t=0$) and after bead milling treatment was applied, at different times.

The times of application of the treatment are:

- 0 min (before the cell suspension was subjected to the treatment),
- 5 min,
- 10 min,
- 20 min.

From the observation of the histogram, it is possible to conclude that, unlike for 5 min, where the number of colonies diminished by 10%, for 10 min and 15 min of pre-treatment biomass resulted severely affected with significant reductions of, respectively, 70% and 85%.

The presented standard deviation also represents the degree of uniformity that can be achieved with the pre-treatment. For shorter times (i.e. 5 min), the cells are damaged unevenly while at longer exposition times to the pre-treatment the effect of the pre-treatment is more marked on the whole population.

6.1.2 Ultrasonification

The first set of exploratory experiments were conducted in order to screen the optimum pre-treatment time and amplitude; the results are reported in Figure 6.3. Observing the diagram, it is evident that, going from an application time of 30 s (3 times 10 s) to one of 2 min (3 times 40 s), the biomass was not damaged. Indeed, for a longer treatment time and for the same amplitude value (50 %), the area occupied by the colonies on the plate slightly increases of about 20 % from 3x10s to 3x40s and it remains almost constant from 3x20s to 3x40s. The same

goes for the number of colonies that increases by 200% from 3x10s to 3x40s (at 50% of amplitude).

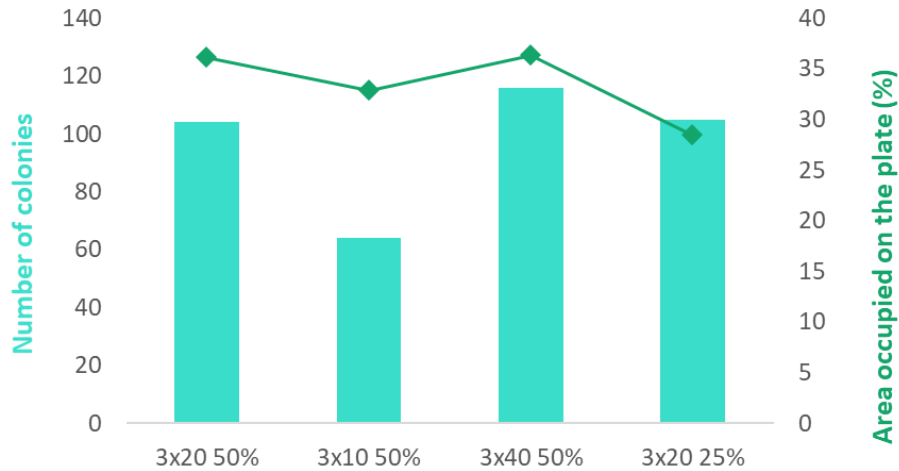


Figure 6.3: Result of cell counting for ultrasonification.

It was decided, so, to maintain only the longest time of application of the pre-treatment (constant variable now, 2 min) and to perform the experiment at two different amplitude values (50% and 25%).

In Figure 6.4 the results of the second set of experiments are illustrated. Both experiments (with 50% amplitude and with 25% amplitude) was repeated 2 times from the same starting sample of cell suspension (i.e. without treatment). Compared to the no-treatment sample, the cells occupy a lower area after treatment, which was the expected trend. On the other hand, the number of cells increases after the treatment.

Analysing the results of such experiments, it should be considered that many factors can influence the outcomes, such as: the initial cell number, environmental conditions (nutrients, pH, temperature, competitors, inhibitory compounds), among others. However, having regard to the above (end of chapter 6.1.1) it is possible to sum up that at lower amplitudes (i.e. 25%), the cells are damaged unevenly while at higher sonification amplitude (i.e. 50%) the effect of the pre-treatment is more marked on the whole population.

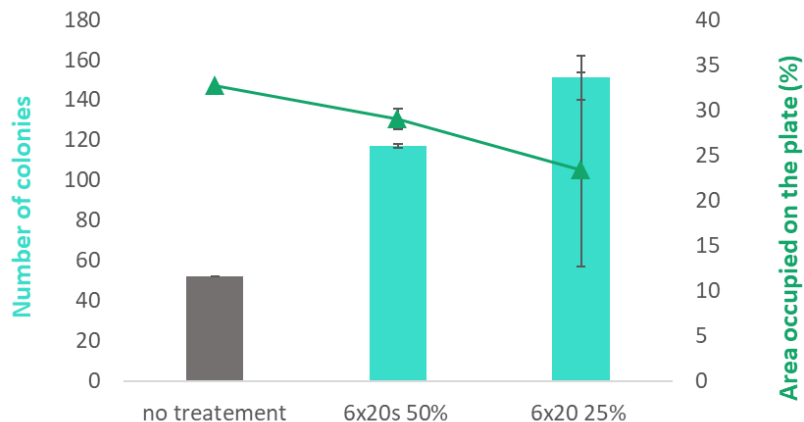


Figure 6.4: Result of cell counting for ultrasonification.

6.1.3 Rotor-stator degradation

Figure 6.5 shows the results obtained, performing experiments by using the rotor-stator degradator. The green line refers to the biggest frequency (20500 min^{-1}) and the blue line to the lowest one (800 min^{-1}). In the first case, the pre-treatment step resulted in a linear decline of the area occupied from the colonies on the plate (in percentage of the total area of the plate) with the rise of the treatment time. Unlike, at low frequency, biomass was not severely affected from the pre-treatment.

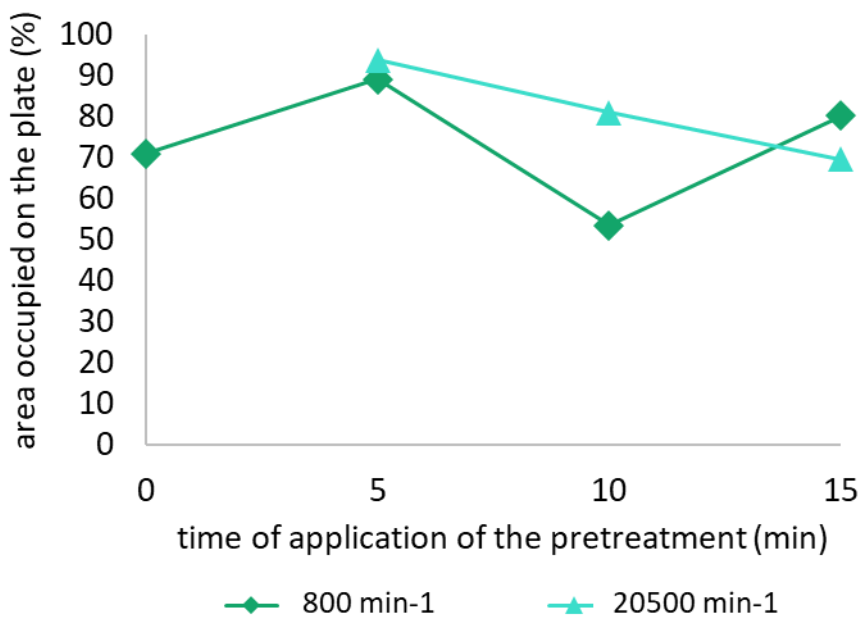


Figure 6.5: Result of cell counting for rotor-stator degradation.

In Figure 6.6 it is possible to see that the inoculated plates do not exhibited microbial growth, when the pre-treatment step is performed (for a time of 10 min and a time of 15 min) without keeping the sample in ice, probably due to the high temperature reached in the sample during the treatment.

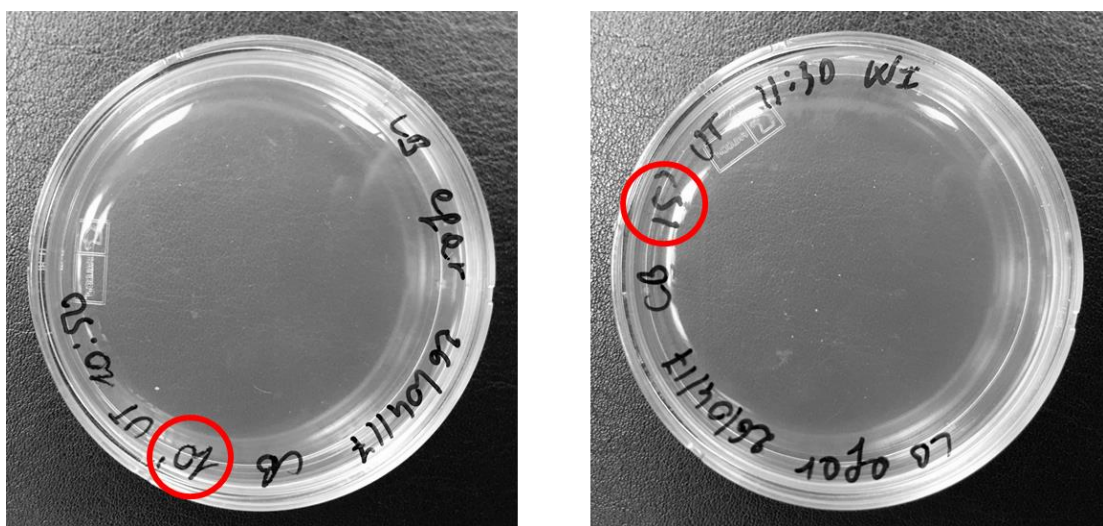


Figure 6.6: Photographs of two plates, that show how severely *B. subtilis* cultivation was affected by a rotor-stator treatment of 10 min (A) and 15 min (B) without keeping the sample in ice.

Regarding the number of cells, the incubation time was the initial tested time corresponded to 24 h, so a proper quantification of colonies could not be performed. However, the simple visual analysis of the plates (Figure 6.7) indicated that the number of colonies decreases with the rise of the time of application of the pre-treatment, similar to the trend obtained for the area.

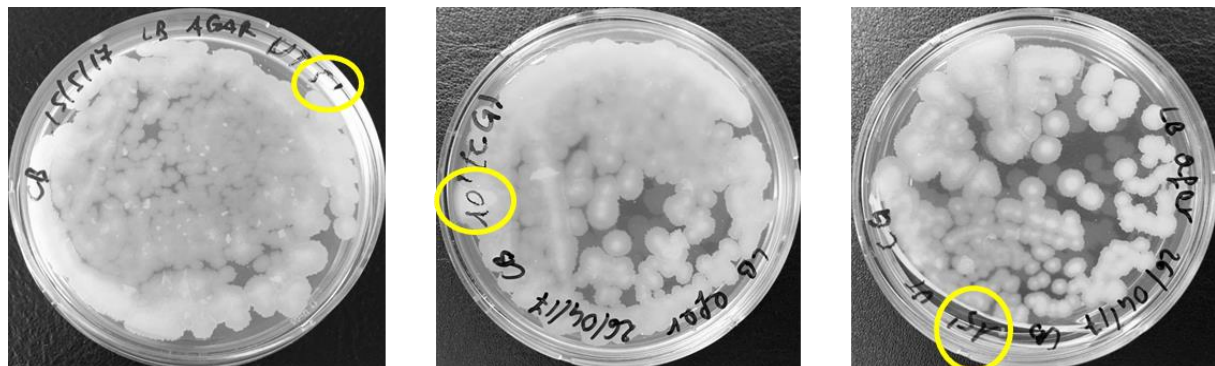


Figure 6.7: Photograph of the three plates related to the ultrasonification treatment performed with 25000 min^{-1} of frequency.

6.1.4 Continuous flow-ultrasonification

As already mentioned, the desired amplitude values were 50% and 25% as for the previous experiments related to ultrasonification (chapter 6.1.2), but the continuous flow-ultrasonicator used in the laboratory worked only with values multiples of 10. For this reason, the amplitude values used are: 50%, 30% and 20%. The results are reported in Figure 6.8. Each experiment was repeated 2 times using the same starting sample of cell suspension.

It is possible to see that in every case biomass was not severely affected from the pre-treatment step. In particular, in every case, compared to the no-treatment sample, the number of colonies on the plate decreases after the pre-treatment step (around 50%), whereas the area occupied from the colonies on the plate (in percentage of the total area of the plate) generally increases, except for 20%-amplitude in which it remains almost constant (slight decrease of 5%). Compared to the effect generally obtained, by using batch ultrasonification (i.e. not continuous, see chapter 6.1.2), the result is in this case the opposite, as it was previously found that the cells occupied a lower area after the pre-treatment step, while the number of cells increased (after the pre-treatment step).

The same reasoning for the standard deviation can be made as for ultrasonification (chapter 6.1.2); the presented standard deviation represents also the degree of uniformity that can be achieved with the pre-treatment. For bigger amplitudes (i.e. 20%), the cells are damaged unevenly while at lower sonification amplitude the effect of the pre-treatment is more marked on the whole population.

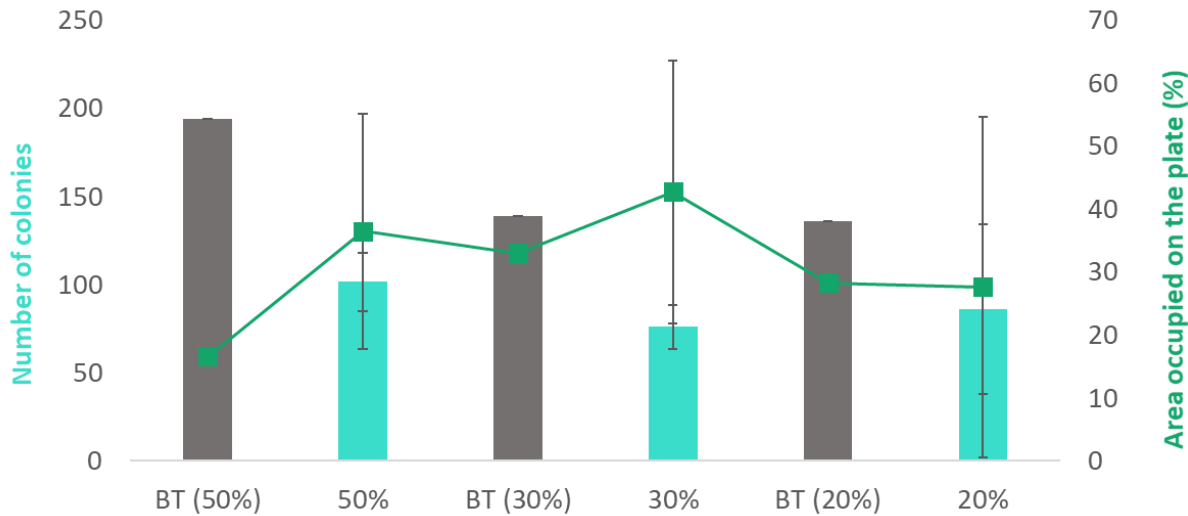


Figure 6.8: Result of cell counting for continuous flow-sonification. BT means ‘Before Treatment’, so “BT (50%)” represents the analysis of the sample used to perform the experiment with 50% of amplitude before the treatment and “50%” the analysis of the same sample after the treatment. The same goes for the other amplitude values.

6.2 *In situ* laser back-reflection

The elaboration of the data coming from *in situ* laser back-reflection methodology was leading for every experiment to one:

- Histogram;
- Diagram showing the cumulative curves;
- Diagram showing the distribution curves: only when it was possible to model the data with a probability density function (for further details about probability distributions see chapter 1.4)

The Histogram reports the quantity of particles ($q_0(x)$, on the y-axis) intercepted by the probe with a certain diameter-range (*particle size x*, on the x-axis).

The cumulative curve shows the frequency of occurrence of values of a diameter-range less than a reference diameter-value. From such curves it is possible to extract the D50 and D90, that are diameter values greater or equal to the diameter owned by 50% and 90% of particles in the sample.

The distribution curve is the result of the transformation of the discrete distribution shown in histograms to a continuous distribution. In addition, the mean value and its standard deviation were calculated.

6.2.1 *Clostridium acetobutylicum*

Continuous flow-ultrasonification is the only pre-treatment step that was tested on *C. Acetobutylicum*. Experiments were conducted at two different amplitude values: 50% and 20%.

In both cases the sample of *C. acetobutylicum* culture underwent a first treatment of 2 min and then an additional one of 1,5 min under the same conditions and it was analysed with the probe before and after treatment.

6.2.1.1 Continuous ultra-sonification at 50% of amplitude on *C. Acetobutylicum*

For a qualitative understanding of the particle-size distribution measured with the probe, it is possible to observe the histogram in Figure 6.9. According to it, the particle-size distribution shifts to larger diameters after the first treatment to come back to smaller ones after the second treatment. In both case the before-treatment distribution results to cover smaller diameter values. The same analysis can be done looking at the distribution curves in Figure 6.10 and the related mean values in Table 6.1. The mean is 4,71 μm before treatment, it becomes 6,21 μm after the first treatment and it comes back to a value (6,07 μm) smaller than the last one, but bigger than the first one. The same behaviour can be observed in the cumulative curves (Figure 6.11) and the resulting D50 and D90 values (Table 6.1). This can be explained thinking about the flocculation that was characterizing the *C. acetobutylicum* culture sample used to conduct the experiments (Figure 3.4). It is reasonable to assume that very large floccules were not detected by the probe in the measurement before the treatment and that the treatment broke them into smaller particle, which were detected in the measurement after the first treatment. Indeed, the range of detection of the probe was until 101,8 μm , where floccules' dimensions are normally of 1-2 mm, but in some occasional cases even more than 10 mm [42]. Moreover, these were further damaged by the second treatment. In further support of this theory, it is possible to observe the total number of particles detected by the probe in all the three measurements: this is around 1.324 before treatment, it increases to 2.201 with the first treatment and it increases further (3.032) with the second.

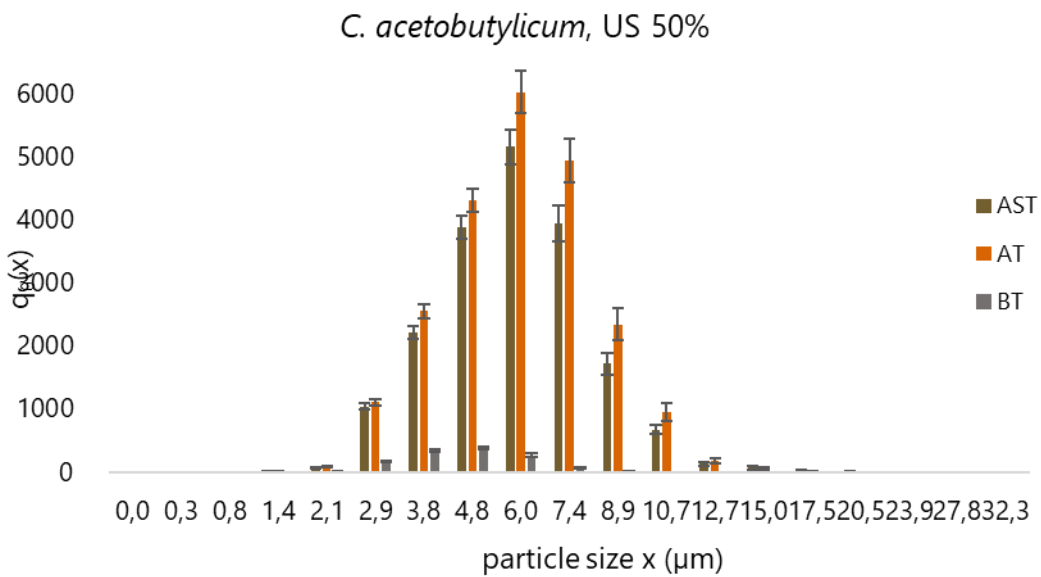


Figure 6.9: Quantity of particles $q_0(x)$ intercepted by the probe with a certain diameter-range before (BT) and after (AT) continuous flow-ultrasonification step on *C. acetobutylicum* culture (at 50% amplitude for 2min).

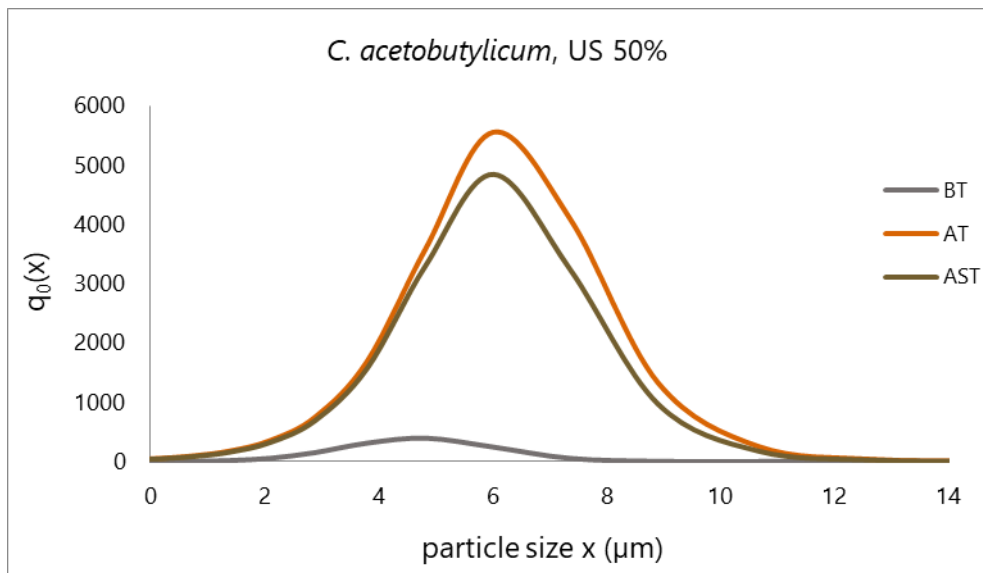


Figure 6.10: Diagram showing the distribution curves before (BT) and after (AT) continuous-flow ultrasonification pre-treatment step on *C. acetobutylicum* culture (at 50% amplitude for 2min).

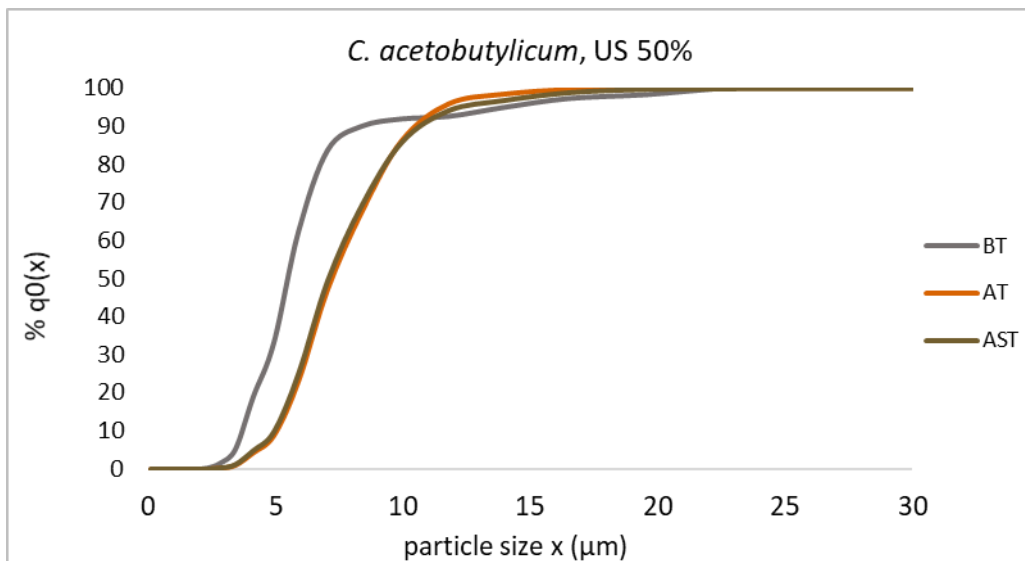


Figure 6.11: Diagram showing the cumulative curves before (BT) and after (AT) continuous-flow ultrasonification pre-treatment step on *C. acetobutylicum* culture (at 50% amplitude for 2min).

Table 6.1: Continuous ultrasonification on *C. acetobutylicum* culture (at 50% A for 2 min): parameters of the distribution curves (mean \pm standard deviation); D50 and D90 extracted from the cumulative curves; total number of particles calculated with the Sequip-software.

	mean \pm st. deviation	D50 (μm)	D90 (μm)	Nr. of particles
BT	4,71 \pm 1,31	4,07	5,86	1.324
AT	6,21 \pm 1,00	5,46	8,21	22.418
AST	6,07 \pm 0,98	5,35	8,03	19.013

6.2.1.2 Continuous ultra-sonification at 20% of Amplitude on *C. acetobutylicum*

Observing the distribution curves in Figure 6.13 and the related mean values in Table 6.2, it is possible to notice that the mean is 4,71 μm before treatment, it increases to 4,93 μm with the first treatment and it further increases (5,13 μm) with the second one. The same goes for the cumulative curves in Figure 6.14 and the resulting D₅₀ and D₉₀ values in Table 6.2. The D₅₀ is 4,07 μm before the treatment, 4,24 μm after the first treatment and 5,56 μm after the second one. The D₉₀ is 5,86 μm before the treatment, 5,92 μm after the first treatment and 6,12 μm after the second one. These results can be explained considering that the set amplitude of this experiment was 20%, unlike the previous one (50%). The horn is the component that transmits ultrasonic vibrations to the liquid being sonicated and is responsible for creating cavitation (see Chapter 4.2). The amplitude represents the maximum allowed extension of the horn compare to the maximum extension of which it is capable. This means that if the amplitude is smaller, the horn's vibrating surface is smaller. So, it is reasonable to think that, due to the smaller amplitude, the first treatment was not sufficient to disrupt the floccules and that the process of disruption of these continued during the second treatment. The total number of particles detected by the probe comes in support also this time, being smaller (1.324) before the treatment, greater (2.201) after the first treatment and still larger (3.032) after the second one.

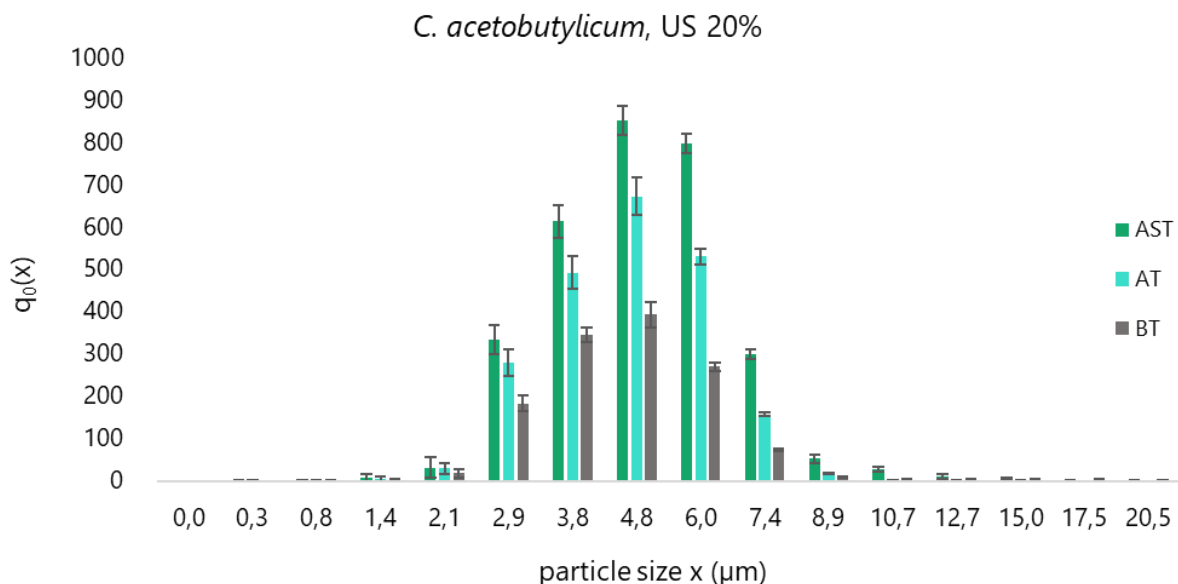


Figure 6.12: Quantity of particles $q_0(x)$ intercepted by the probe with a certain diameter-range before (BT) and after (AT) continuous flow-ultrasonification step on *C. acetobutylicum* culture (at 20% amplitude for 2min).

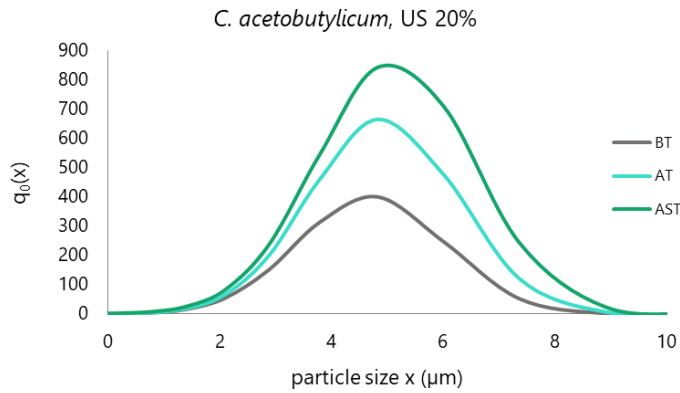


Figure 6.13: Diagram showing the distribution curves before (BT) and after (AT) continuous-flow ultrasonification pre-treatment step on *C. acetobutylicum* culture (at 20% amplitude for 2min).

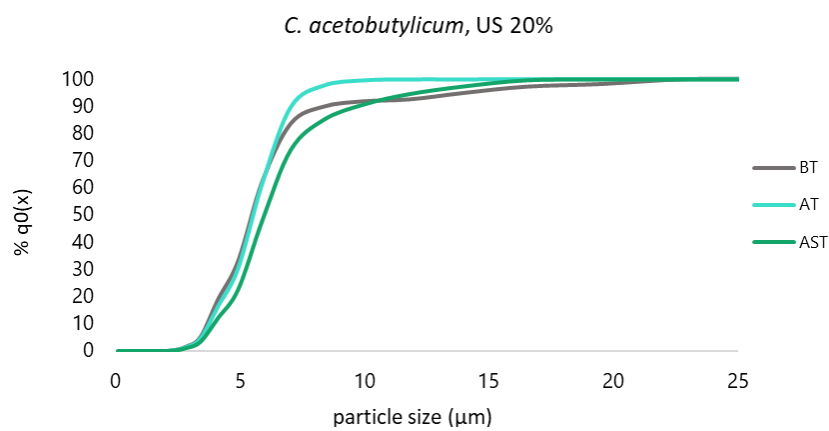


Figure 6.14: Diagram showing the cumulative curves before (BT) and after (AT) continuous-flow ultrasonification pre-treatment step on *C. acetobutylicum* culture (at 20% amplitude for 2min).

Table 6.2: Continuous ultrasonification on *C. acetobutylicum* culture (at 20% A for 2 min): parameters of the distribution curves (mean \pm standard deviation); D50 and D90 extracted from the cumulative curves; total number of particles calculated with the Sequip-software.

	mean\pm st. deviation	D50 (μm)	D90 (μm)	Nr. of particles
BT	4,71 \pm 1,31	4,07	5,86	1.324
AT	4,93 \pm 1,32	4,24	5,92	2.201
AST	5,13 \pm 1,40	5,56	6,15	3.032

6.2.2 *Bacillus subtilis*

Continuous flow-ultrasonification is the only pre-treatment step tested on *B. subtilis* together with the use of the probe. Two amplitude values were used (50% and 30%) and for each amplitude the experiment was repeated two times.

6.2.2.1 Continuous ultra-sonification at 50% of Amplitude on *B. subtilis*

To get a first idea of the effect of the treatment on the particle-size distribution measured by the probe, it is possible to observe the histograms in Figures 6.15 and 6.18. These show that the particle-size distribution shifts in both experiments to larger diameters after the treatment and, so, that the experiments are coherent between them. The same analysis can be done observing the distribution curves in Figures 6.10 and 6.13 and the related mean values in Table 6.3. For both experiments, the mean is 7 µm before the treatment and reaches 8,5 µm after the treatment. The same goes for the cumulative curves (Figures 6.17 and 6.20) and the resulting D50 and D90 values (Table 6.3). For both experiments, the D50 is 6 µm before the treatment and 7,5 µm after the treatment. The D90 is 9 µm (first experiment) and 8 µm (second experiment) before the treatment to increase until 11 µm in both cases after the treatment.

The cause of such results can be that also the samples of *B. subtilis* culture used to conduct these experiments presented flocculation, not seen, because the Ultra Yield Flasks used were not in transparent glass as for *C. acetobutylicum*. So, as already mentioned in Chapter 6.2.1.1, it is possible to assume that the floccules were not detected by the probe in the measurement before treatment and that the treatment broke them into smaller particles, that the probe was able to detect in the measurement after the treatment. Also in this case, in support of this theory, it is possible to observe the total number of particles detected by the probe: 10.000 before treatment and 40.000 after the ultra-sonification treatment.

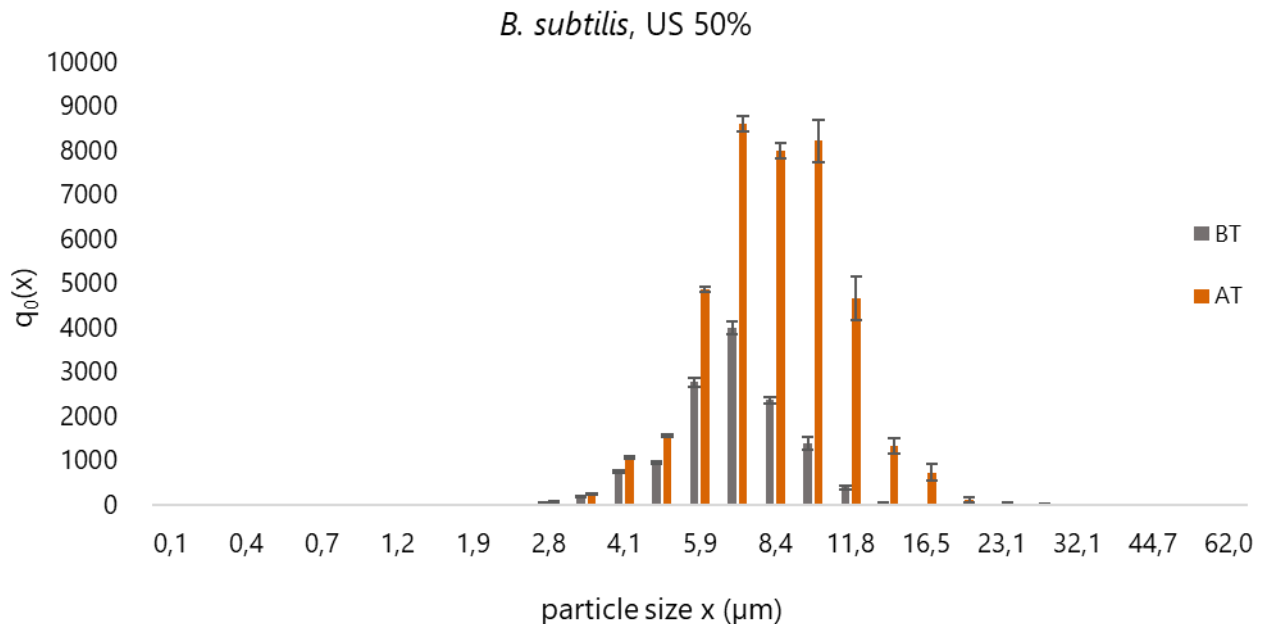


Figure 6.15: Quantity of particles $q_0(x)$ intercepted by the probe with a certain diameter-range before (BT) and after (AT) continuous flow-ultrasonification step on *B. subtilis* culture (at 50% amplitude for 2min).

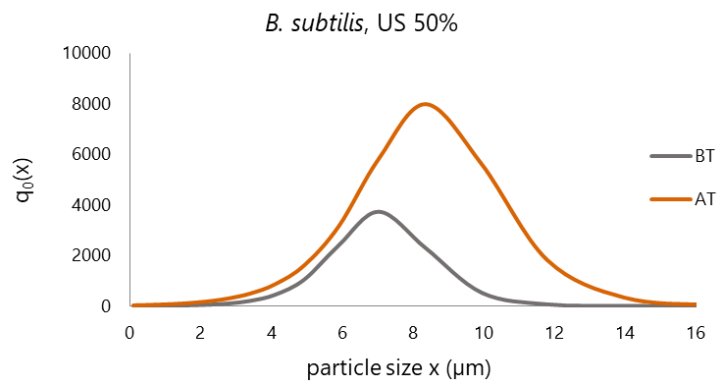


Figure 6.16: Diagram showing the distribution curves before (BT) and after (AT) continuous-flow ultrasonification pre-treatment step on *B. subtilis* culture (at 50% amplitude for 2min).

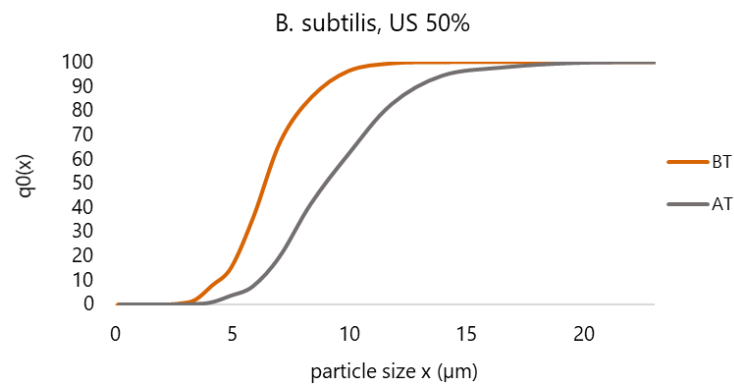


Figure 6.17: Diagram showing the cumulative curves before (BT) and after (AT) continuous-flow ultrasonification pre-treatment step on *B. subtilis* culture (at 50% amplitude for 2min).

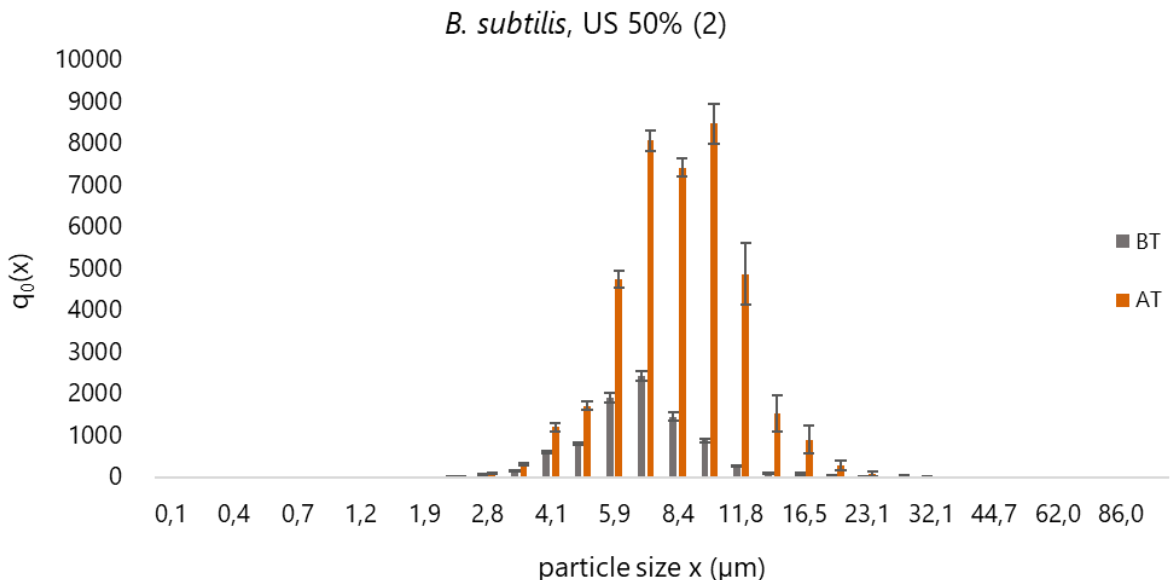


Figure 6.18: Quantity of particles $q_0(x)$ intercepted by the probe with a certain diameter-range before (BT) and after (AT) continuous flow-ultrasonification step on *B. subtilis* culture (at 50% amplitude for 2min), second experiment.

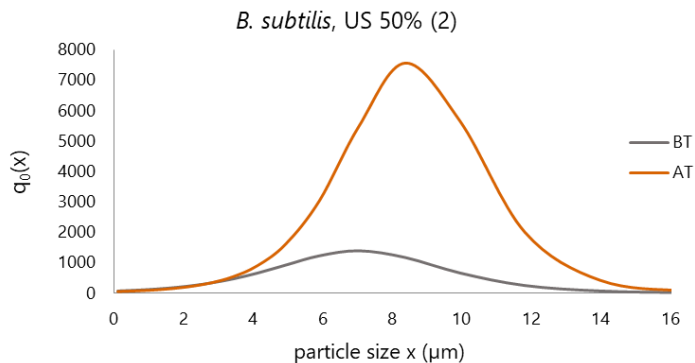


Figure 6.19: Diagram showing the distribution curves before (BT) and after (AT) continuous-flow ultrasonification pre-treatment step on *B. subtilis* culture (at 50% amplitude for 2min), second experiment.

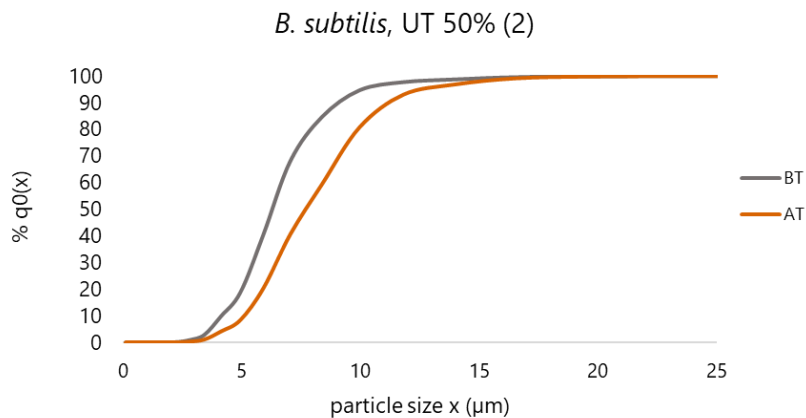


Figure 6.20: Diagram showing the cumulative curves before (BT) and after (AT) continuous-flow ultrasonification pre-treatment step on *B. subtilis* culture (at 50% amplitude for 2min), second experiment.

Table 6.3: Continuous ultrasonification on *B. subtilis* culture (at 50% A for 2 min): parameters of the distribution curves (mean \pm standard deviation); D50 and D90 extracted from the cumulative curves; total number of particles calculated with the Sequip-software.

		mean\pmst. deviation	D50 (μm)	D90 (μm)	Nr. of particles
First experiment	BT	7,10 \pm 0,87	6,40	9,02	13.041
	AT	8,45 \pm 1,22	7,59	11,12	39.206
Second experiment	BT	7,03 \pm 1,59	6,29	7,94	8.758
	AT	8,53 \pm 1,27	7,70	10,55	38.714

6.2.2.2 Continuous ultra-sonification at 30% of Amplitude on *B. Subtilis*

In this case, the histograms (Figures 6.21 and 6.24) recall the ones for 50% amplitude, but a deeper analysis can be made observing the distribution curves (Figures 6.22 and 6.25) and the related mean values (Table 6.3), as the behaviour is different from the first to the second experiment. The mean is, respectively, 6,20 μm (first experiment) and 7,74 μm (second

experiment) before treatment and 5,58 μm (first experiment) and 8,42 μm (second experiment) after treatment. It is possible to see that in the first experiment, the mean decreases with the treatment, while in the second one increases.

The same goes for the D50 (Table 6.3): it is, respectively, 5,44 μm and 7,68 μm before treatment and 5,21 μm and 9,04 μm after treatment.

But for both experiments, the D90 (Table 6.3) is bigger after treatment: it is around 7 μm (first experiment) and 19,5 μm (second experiment) before treatment to increase until 12 μm (first experiment) and 32 μm (second experiment) after treatment.

These results can be explained, as in Chapter 6.2.1.2, thinking that the amplitude value in this experiment was 30%, unlike the previous one (50%). So, it is reasonable to think that, due to the smaller amplitude, the treatment disrupted the floccules less severely than in the 50%-amplitude case, creating bigger particles after the treatment, that can be noticed only in the D90 value. The total number of particles detected by the probe comes in support also this time. In the first experiment, it is around 3.000 before treatment, which becomes the double after it, while in the second experiment it is 9.000 before treatment to reach 20.000 with the treatment.

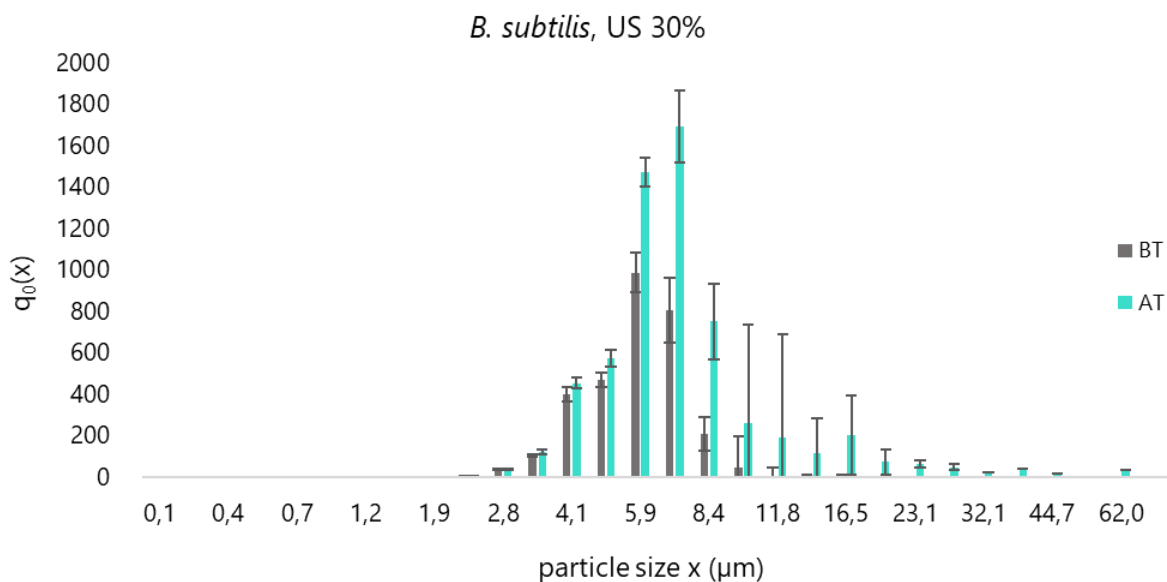


Figure 6.21: Quantity of particles $q_0(x)$ intercepted by the probe with a certain diameter-range before (BT) and after (AT) continuous flow-ultrasonification step on *B. subtilis*culture (at 30% amplitude for 2min).

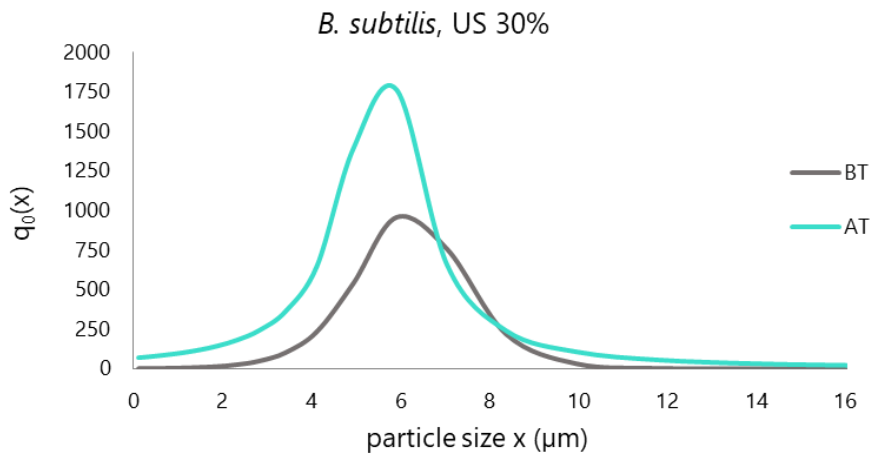


Figure 6.22: Diagram showing the distribution curves before (BT) and after (AT) continuous-flow ultrasonification pre-treatment step on *B. subtilis* culture (at 30% amplitude for 2min).

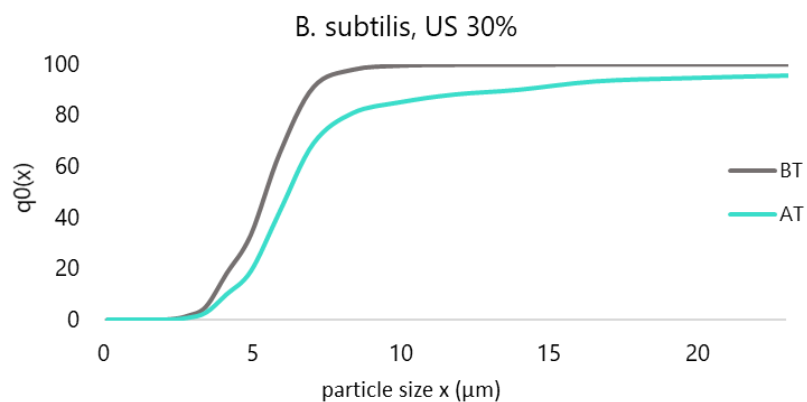


Figure 6.23: Diagram showing the cumulative curves before (BT) and after (AT) continuous-flow ultrasonification pre-treatment step on *B. subtilis* culture (at 30% amplitude for 2min).

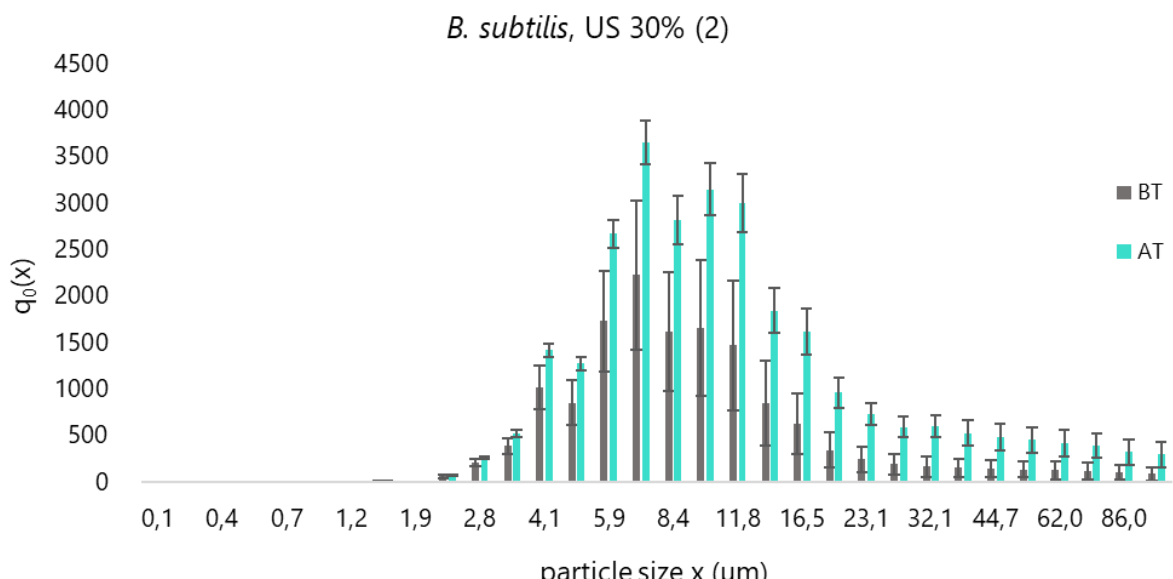


Figure 6.24: Quantity of particles $q_0(x)$ intercepted by the probe with a certain diameter-range before (BT) and after (AT) continuous flow-ultrasonification step on *B. subtilis* culture (at 30% amplitude for 2min), second experiment.

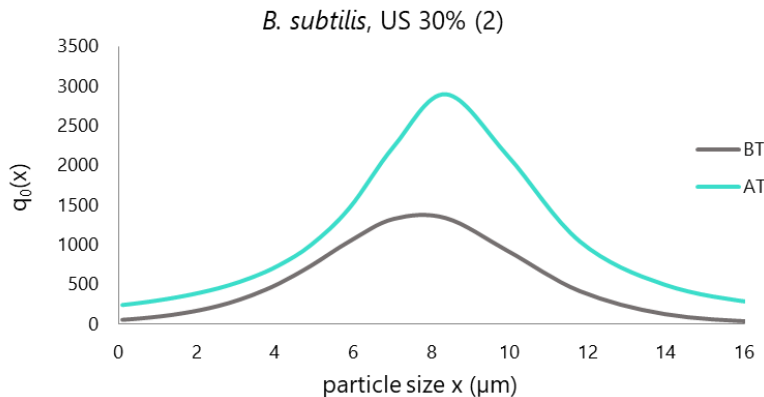


Figure 6.25: Diagram showing the distribution curves before (BT) and after (AT) continuous-flow ultrasonification pre-treatment step on *B. subtilis* culture (at 30% amplitude for 2min), second experiment.

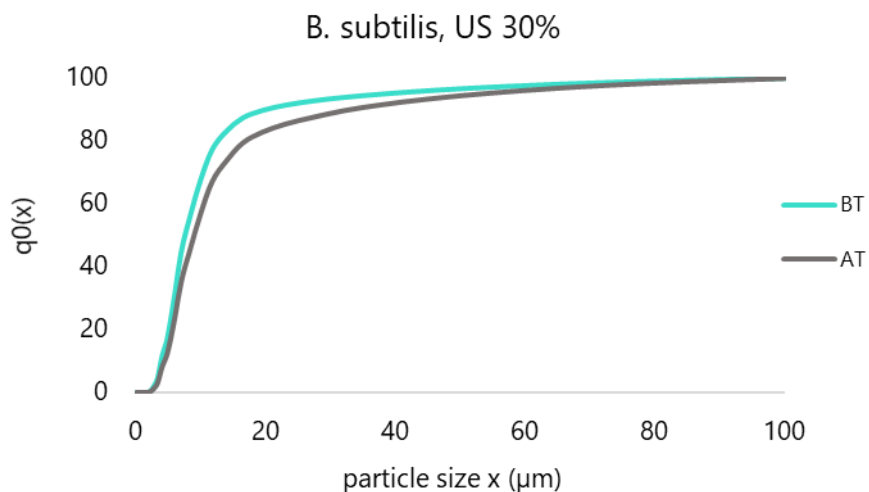


Figure 6.26: Diagram showing the cumulative curves before (BT) and after (AT) continuous-flow ultrasonification pre-treatment step on *B. subtilis* culture (at 30% amplitude for 2min), second experiment.

Table 6.4: Continuous ultrasonification on *B. subtilis* culture (at 30% A for 2 min): parameters of the distribution curves (mean \pm standard deviation); D50 and D90 extracted from the cumulative curves; total number of particles calculated with the Sequip-software.

		mean \pm st. deviation	D50 (µm)	D90 (µm)	Nr. of particles
<i>First experiment</i>	BT	6,20 \pm 0,78	5,44	6,99	3.082
	AT	5,58 \pm 1,04	5,21	11,80	6.319
<i>Second experiment</i>	BT	7,74 \pm 1,69	7,68	19,54	9.313
	AT	8,42 \pm 2,54	9,04	32,14	23.154

6.2.3 Prepared Feedstock

Two pre-treatment steps were tested on PF: bead mill and sonification.

6.2.3.1 Bead mill pre-treatment on PF

The experiment was repeated two times under the same conditions. Observing the D50 and D90 values of both repetitions (table 6.7), these are also always smaller after the pre-treatment step. As PF is a substrate and no biological phase is present in it, the aim of the pre-treatment was to reduce as much as possible the particle-size to make the substrate more available for the microorganisms. The purpose was good reached with the ball-milling treatment; looking at D50, the particle size was reduced by ball-milling of the 32% in the first experiment and 29% in the second one, while regarding the D90, the reduction reached the 58% in the first experiment and 10% in the repetition.

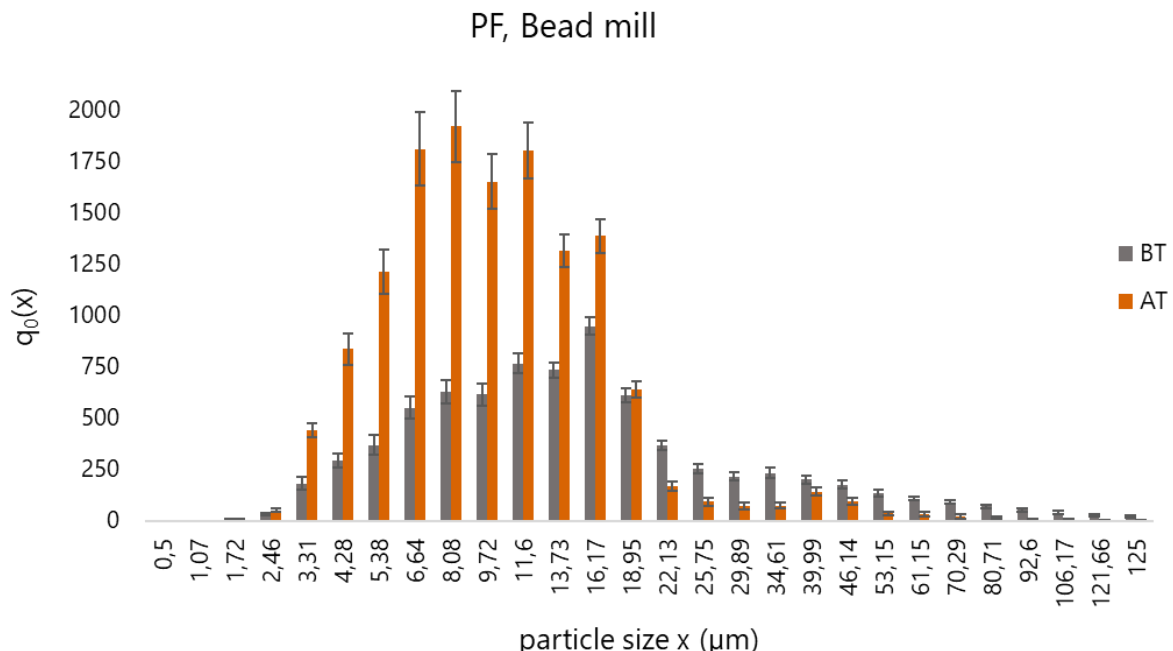


Figure 6.27: Quantity of particles $q_0(x)$ intercepted by the probe with a certain diameter-range before (BT) and after (AT) continuous flow-ultrasonification step on PF (for 10min with 16mL volume).

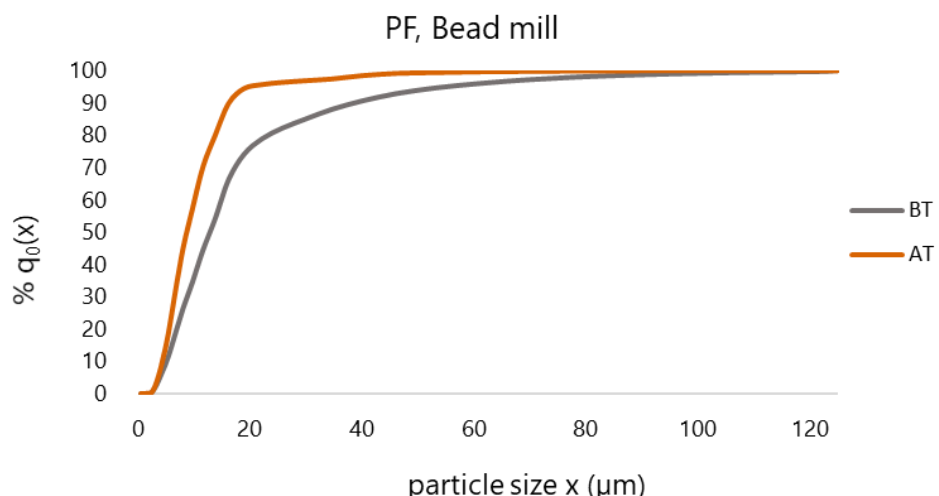


Figure 6.28: Diagram showing the cumulative curves before (BT) and after (AT) continuous-flow ultrasonification pre-treatment step on PF (for 10min with 16mL volume).

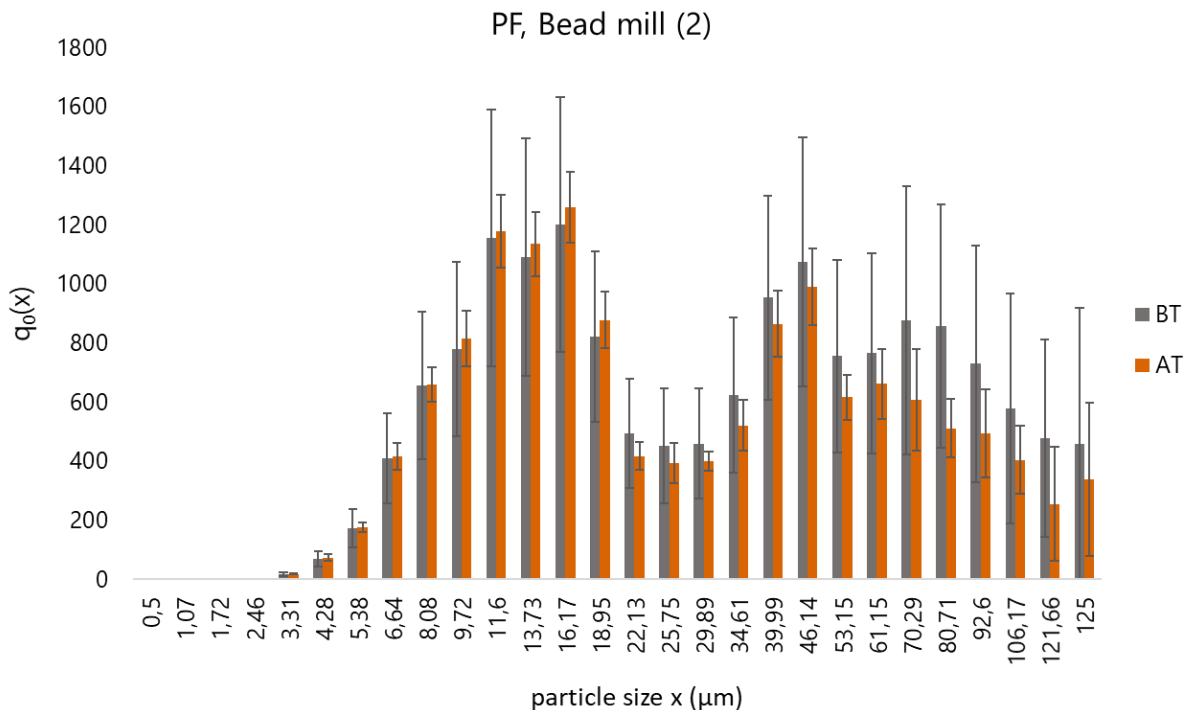


Figure 6.29: Quantity of particles $q_0(x)$ intercepted by the probe with a certain diameter-range before (BT) and after (AT) continuous flow-ultrasonification step on PF (for 10min with 16mL volume), second experiment.

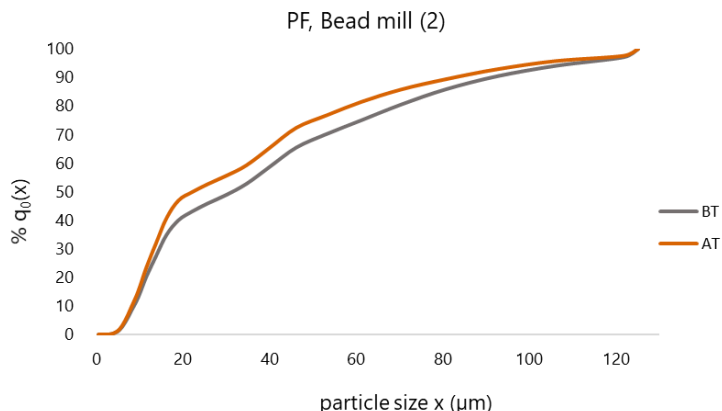


Figure 6.30: Diagram showing the cumulative curves before (BT) and after (AT) continuous-flow ultrasonification pre-treatment step on PF (for 10min with 16mL volume), second experiment.

Table 6.5: Continuous ultrasonification on PF (for 10min with 16mL volume): parameters of the distribution curves (mean \pm standard deviation); D50 and D90 extracted from the cumulative curves; total number of particles calculated with the Sequip-software.

		D50 (μm)	D90 (μm)
<i>First experiment</i>	BT	12,83	38,76
	AT	8,72	16,17
<i>Second experiment</i>	BT	31,31	92,43
	AT	22,13	82,71

6.2.3.2 Ultrasonification pre-treatment on PF

The second pre-treatment step tested on PF is ultrasonification. The experiment was repeated two times, but in both cases the data could not be model with a probability density function. The reason could be the large heterogeneity that characterizes this type of substrate. It is, however, possible to draw conclusions through the analysis of the cumulative curves shown in Figure 6.32, extracting the D₅₀ and D₉₀ values (table 6.8). Looking at D₅₀, this has been reduced by 20% by sonicating in the first experiment and 40% in the second one, while regarding the D₉₀, the reduction was of 18% in the first case and 69% in the second one.

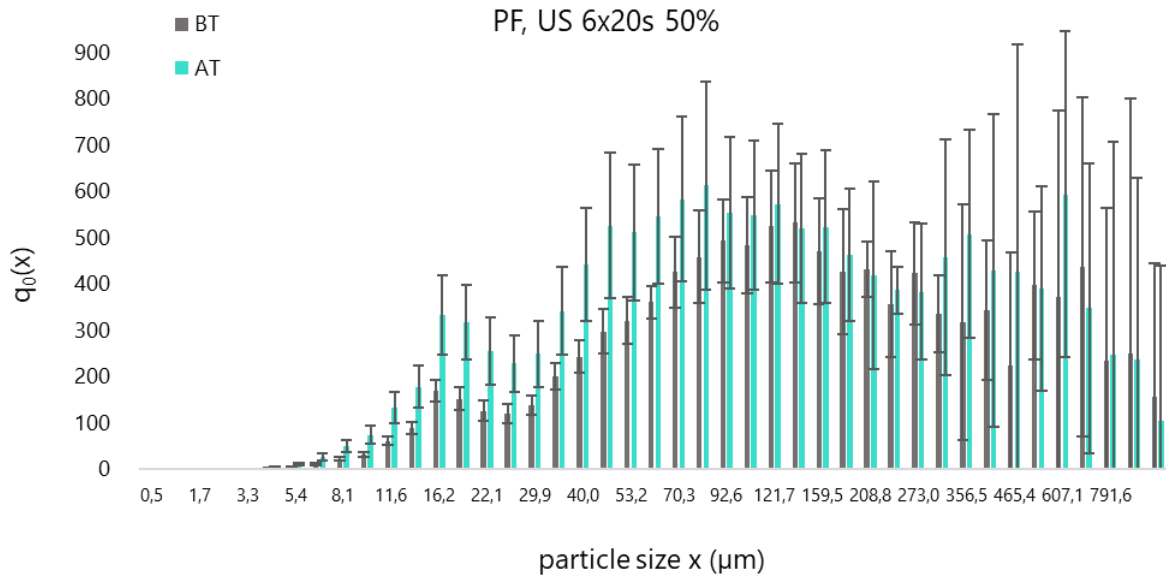


Figure 6.31: Quantity of particles $q_0(x)$ intercepted by the probe with a certain diameter-range before (BT) and after (AT) continuous flow-ultrasonification step on PF (at 50% amplitude, 6x20s).

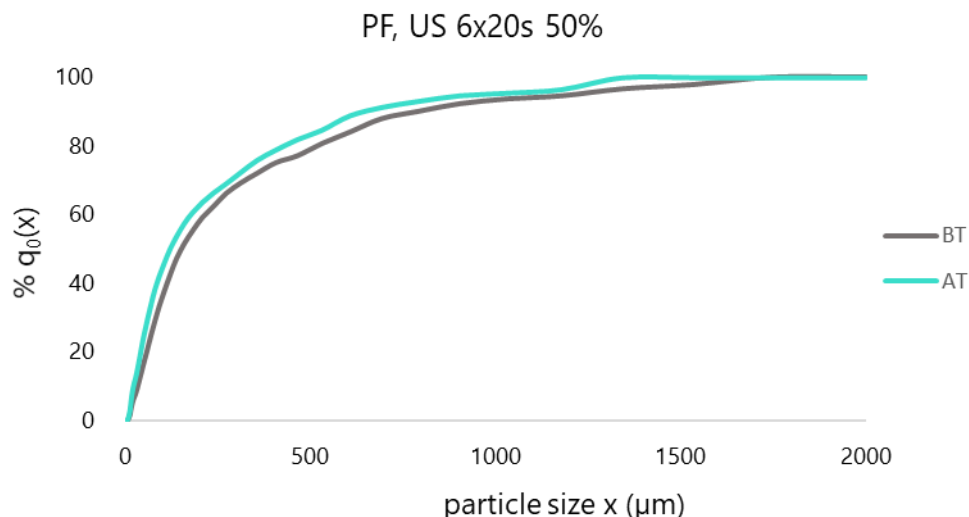


Figure 6.32: Diagram showing the cumulative curves before (BT) and after (AT) continuous-flow ultrasonification pre-treatment on PF (at 50% amplitude, 6x20s).

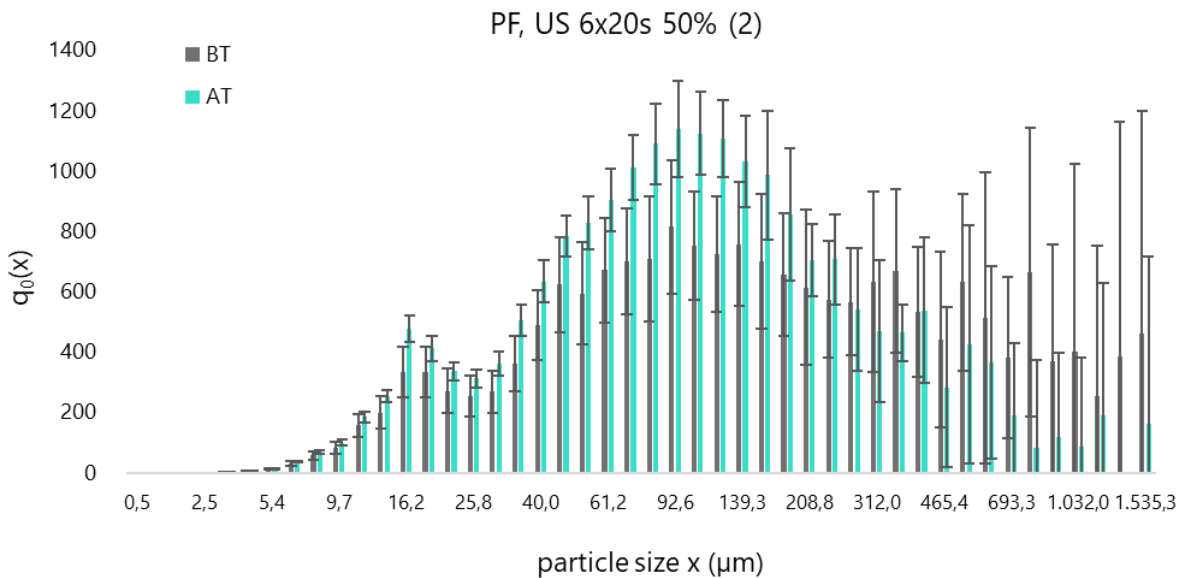


Figure 6.33: Quantity of particles $q_0(x)$ intercepted by the probe with a certain diameter-range before (BT) and after (AT) continuous flow-ultrasonification step on PF (at 50% amplitude, 6x20s), second experiment.

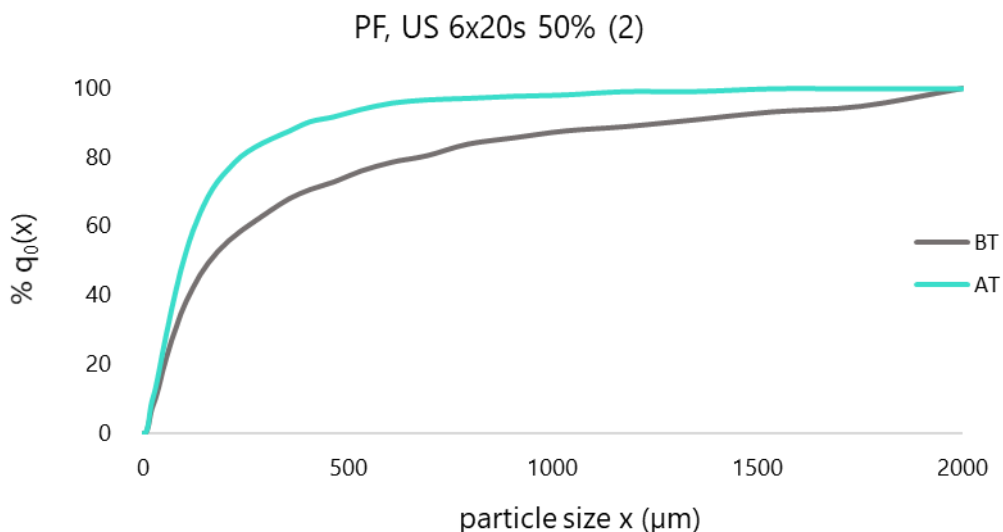


Figure 6.34: Diagram showing the cumulative curves before (BT) and after (AT) continuous-flow ultrasonification pre-treatment step on PF (at 50% amplitude, 6x20s), second experiment.

Table 6.6: Continuous ultrasonification on PF (at 50% amplitude, 6x20s): parameters of the distribution curves (mean \pm standard deviation); D50 and D90 extracted from the cumulative curves; total number of particles calculated with the Sequip-software.

		D50 (μm)	D90 (μm)
<i>First experiment</i>	BT	152,40	791,64
	AT	121,66	646,16
<i>Second experiment</i>	BT	163,28	1270,28
	AT	98,48	399,15

6.2.4 Fermentation Broth

Continuous flow-ultrasonification is the only pre-treatment step tested on FB. Two amplitude values were used (50% and 20%) and for each amplitude the experiment was repeated two times. In both cases the sample of FB underwent a first treatment of 2 min and then an additional one of 1,5 min under the same conditions. Moreover, the sample was analysed with the Sequip-probe before and after each treatment.

6.2.4.1 Continuous ultra-sonification at 50% of Amplitude on FB

From the analysis of the histograms (Figures 6.36 and 6.40) and of the distribution curves (Figures 6.38 and 6.42) it is possible to conclude that pre-treatment did not affect the particle size distribution of FB. The mean values (Table 6.7) also display an increase of 2-3 μm in the particles' diameter of the (two times) pre-treated sample (AST) in both experiments.

The D50 value (Table 6.7) has a similar behaviour, but it increases of around 1 μm in the first experiment after the second pre-treatment and it remains almost constant in the second experiment (8,73 μm before pre-treatment and 8,45 μm after the second pre-treatment). On the other hand, the D90 values (Table 6.7) show a clear decrease of 15% and 11% in the particles' diameter of the (two times) pre-treated sample (AST). Finally, looking at the distribution curves (Figures 6.39 and 6.43), it is possible to see clearly that the three curves are one curve until 85% (first experiment) and 65% (second experiment), after whereupon the before-treatment curve detach itself lying on bigger diameter values.

In the case of these two experiments, it is possible to affirm that the pre-treatment affected the D50-D100 cut. Since FB contains biomass and substrate and the first usually lies in the D0-D50 slot, a pre-treatment that influences the D50-D100 cut can be seen as a good pre-treatment that does not affect the microorganisms (responsible for AD).

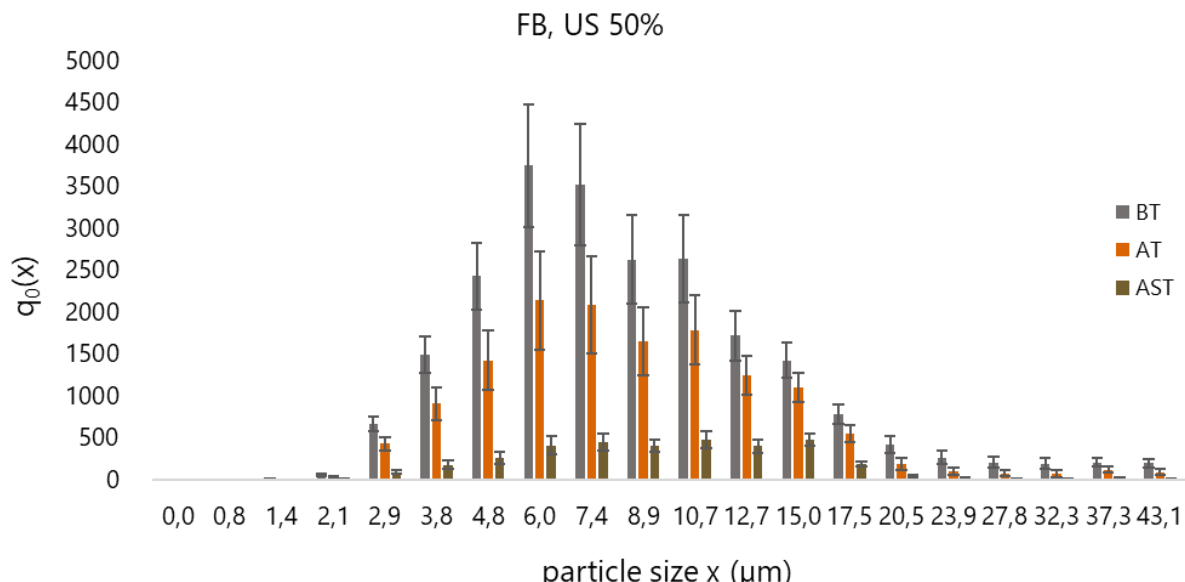


Figure 6.35: Quantity of particles $q_0(x)$ intercepted by the probe with a certain diameter-range before (BT) and after (AT) continuous flow-ultrasonification step on PF (at 50% amplitude, for 2 min).

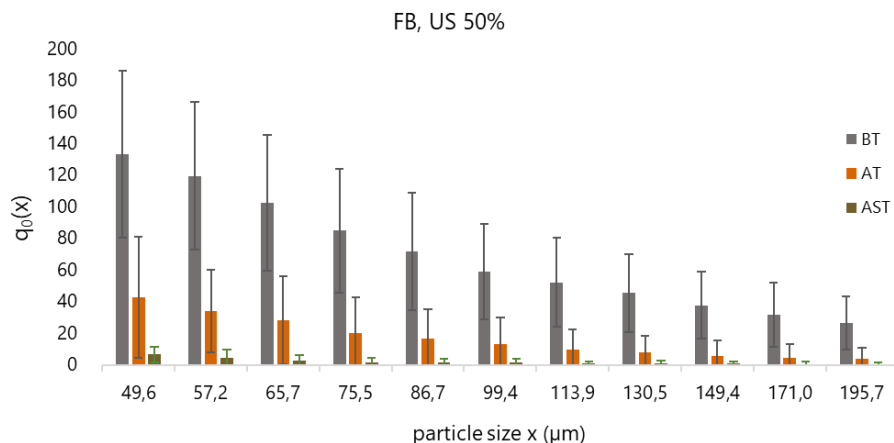


Figure 6.36: Zoom on diameters bigger than 49,6 μm .

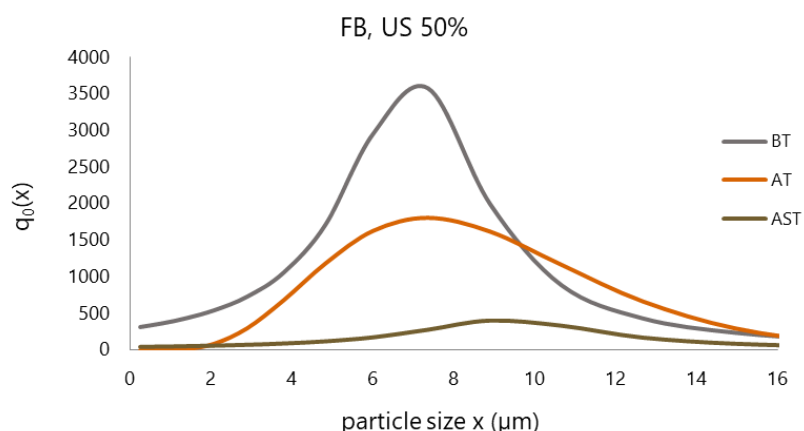


Figure 6.37: Diagram showing the distribution curves before (BT) and after (AT) continuous-flow ultrasonification pre-treatment step on PF (at 50% amplitude, for 2 min).

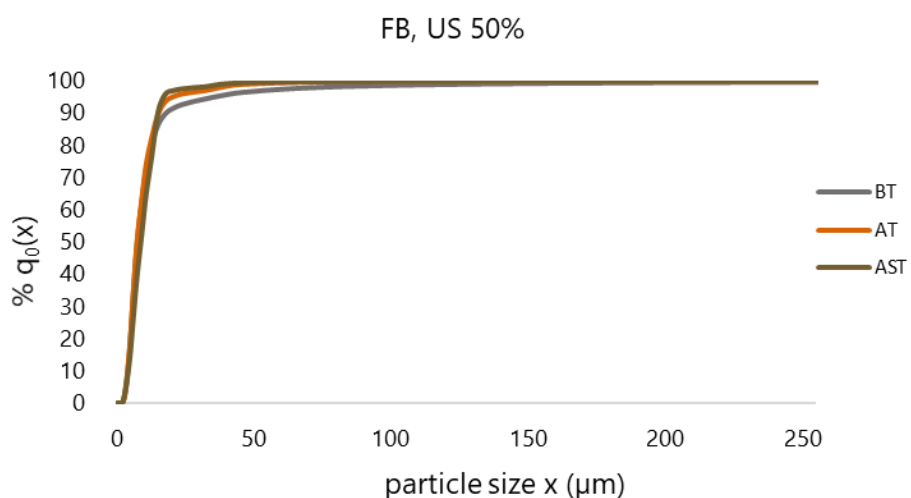


Figure 6.38: Diagram showing the cumulative curves before (BT) and after (AT) continuous-flow ultrasonification pre-treatment step on PF (at 50% amplitude, for 2 min).

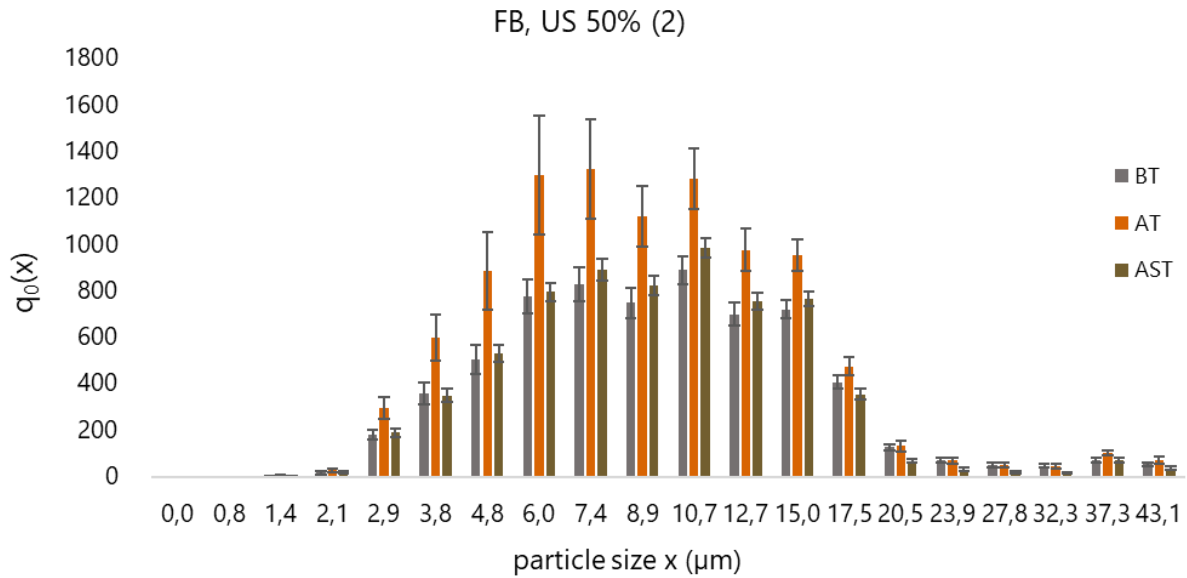


Figure 6.39: Quantity of particles $q_0(x)$ intercepted by the probe with a certain diameter-range before (BT) and after (AT) continuous flow-ultrasonification step on PF (at 50% amplitude, for 2 min), second experiment.

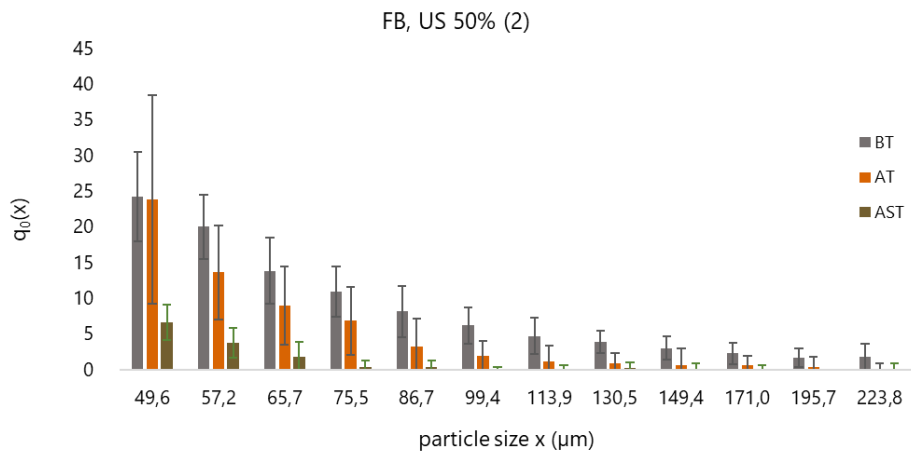


Figure 6.40: Zoom on diameters bigger than $49,6 \mu\text{m}$.

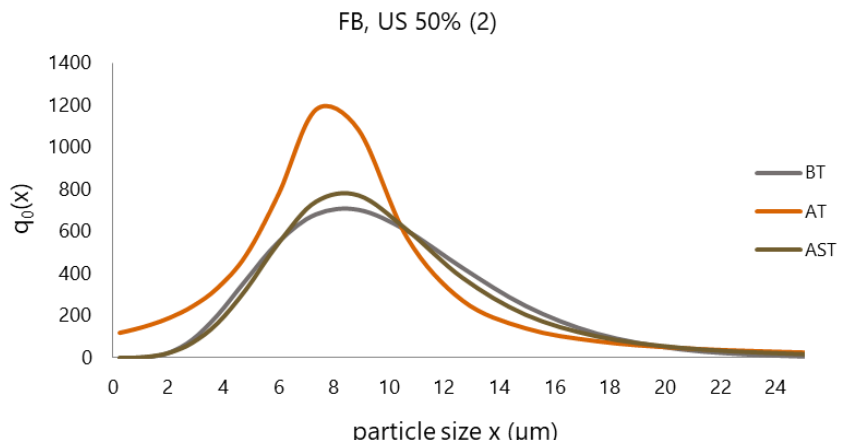


Figure 6.41: Diagram showing the distribution curves before (BT) and after (AT) continuous-flow ultrasonification pre-treatment step on FB (at 50% amplitude, for 2 min), second experiment.

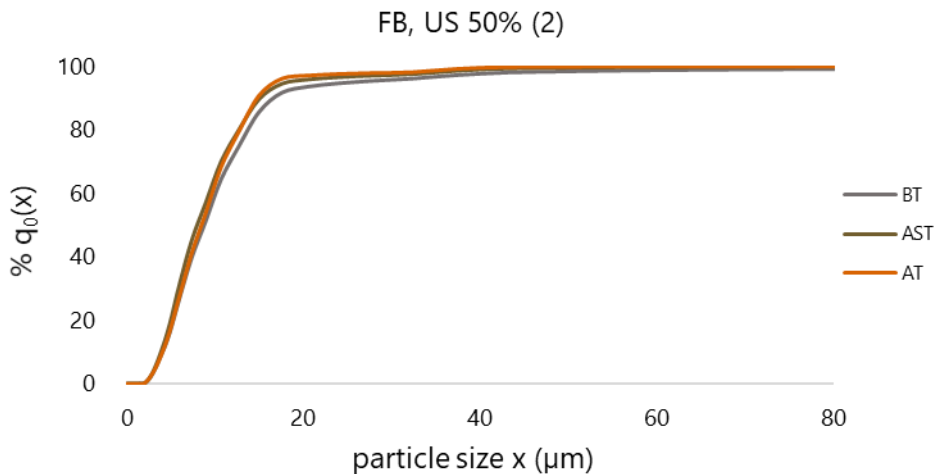


Figure 6.42: Diagram showing the cumulative curves before (BT) and after (AT) continuous-flow ultrasonification pre-treatment step on FB (at 50% amplitude, for 2 min), second experiment.

Table 6.7: Continuous ultrasonification on FB (at 50% amplitude, for 2 min): parameters of the distribution curves (mean \pm standard deviation); D50 and D90 extracted from the cumulative curves; total number of particles calculated with the Sequip-software.

		mean \pm st. deviation	D50 (µm)	D90 (µm)
<i>First experiment</i>	BT	7,02 \pm 2,04	7,30	17,54
	AT	6,52 \pm 1,33	7,27	15,06
	AST	9,30 \pm 2,75	8,67	14,89
<i>Second experiment</i>	BT	6,12 \pm 1,63	8,73	16,67
	AT	7,94 \pm 2,51	7,99	14,95
	AST	9,37 \pm 4,14	8,45	14,78

6.2.4.2 Continuous ultra-sonification at 20% of Amplitude on FB

In this case, observing the D50 (Table 6.8), it decreases of 6% (first experiment) and 16% (second experiment) after the first pre-treatment and of 14% (first experiment) and 23% (second experiment) after the second pre-treatment.

For the 20%-amplitude case, unlikely for 50%-amplitude one, the D90 values (Table 6.7) do not have a clear behaviour. In the first experiment it decreases of 10% with the first pre-treatment (and stays constant with the second pre-treatment step) and in the second experiment it stays constant with both pre-treatment steps.

These results can be explained in two ways. The amplitude value was in this experiment of 20%, unlike in the previous one (50%), so it is reasonable to think that, due to the small amplitude, the treatment did not have a significant effect on the FB sample of both experiments (as in Chapters 6.2.1.2 and 6.2.2.2). Alternatively, the pre-treatment with 20% amplitude can be seen as affecting the D0-D50 cut, unlikely the one with 50% amplitude that was seen affecting the D50-D100 cut. According to both philosophies, the pre-treatment with 50% is more suitable to use with fermentation broth.

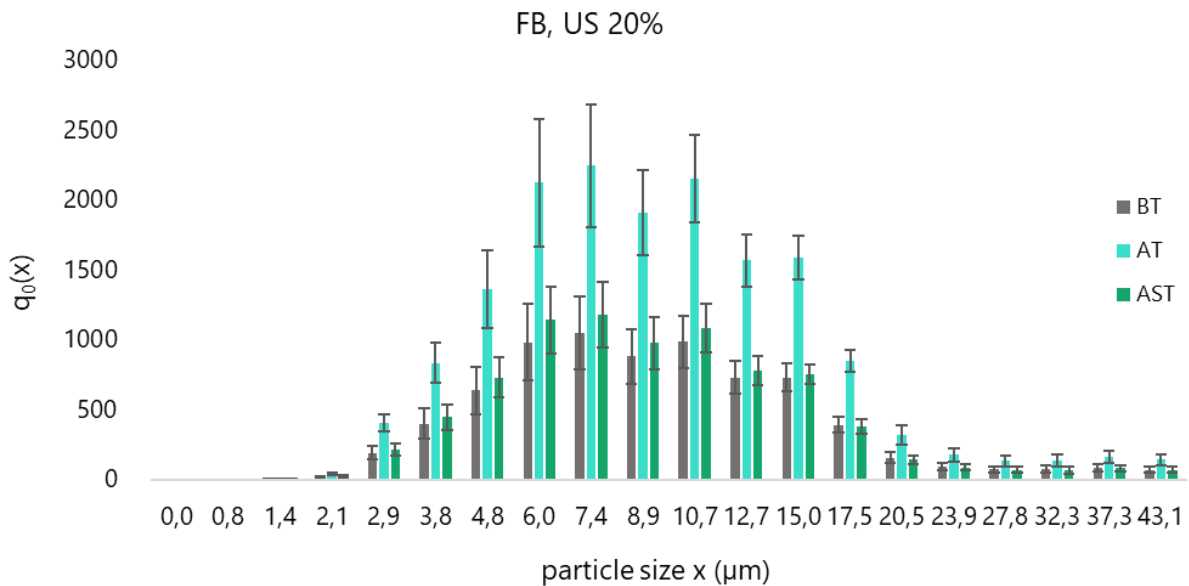


Figure 6.43: Quantity of particles $q_0(x)$ intercepted by the probe with a certain diameter-range before (BT) and after (AT) continuous flow-ultrasonification step on PF (at 20% amplitude, for 2 min).

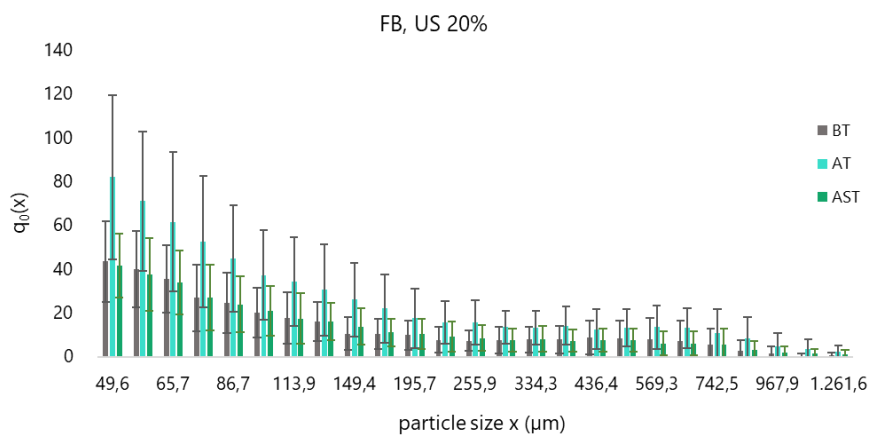


Figure 6.44: Zoom on diameters bigger than 49,6 μm .

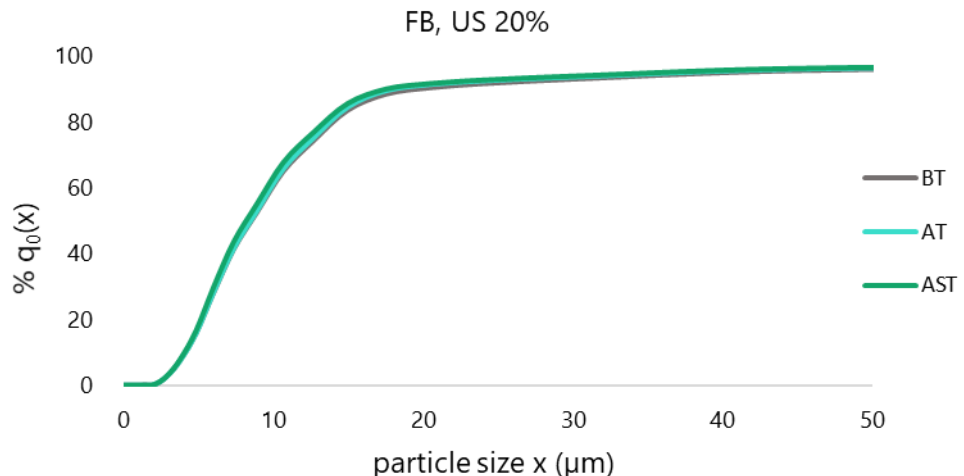


Figure 6.45: Diagram showing the cumulative curves before (BT) and after (AT) continuous-flow ultrasonification pre-treatment step on FB (at 20% amplitude, for 2 min).

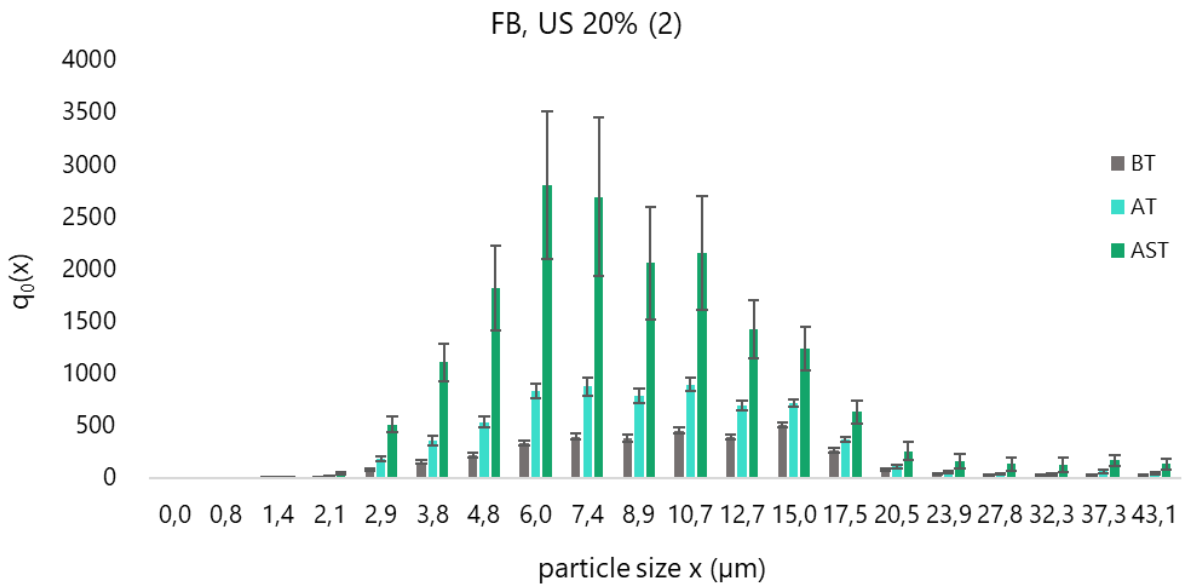


Figure 6.46: Quantity of particles $q_0(x)$ intercepted by the probe with a certain diameter-range before (BT) and after (AT) continuous flow-ultrasonification step on PF (at 20% amplitude, for 2 min), second experiment.

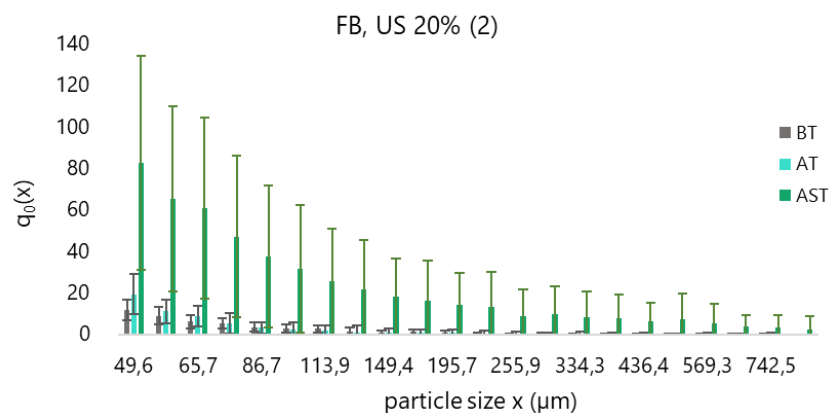


Figure 6.47: Zoom on diameters bigger than 49,6 μm .

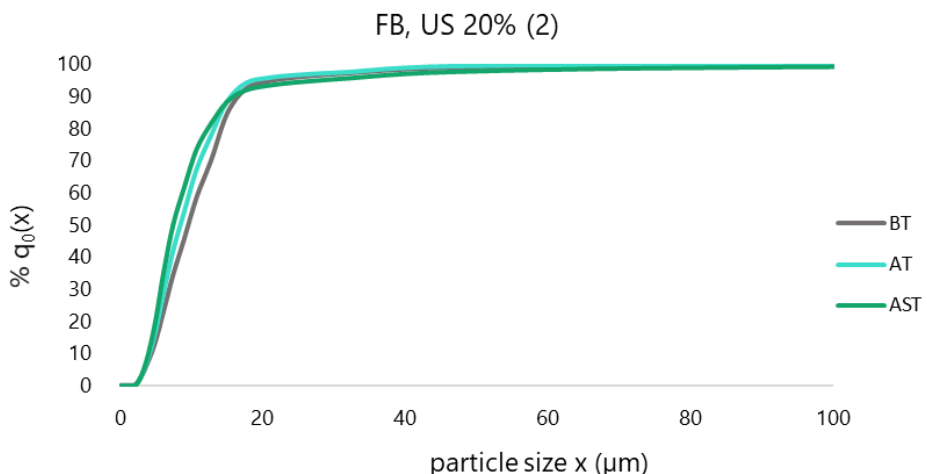


Figure 6.48: Diagram showing the cumulative curves before (BT) and after (AT) continuous-flow ultrasonification pre-treatment step on FB (at 20% amplitude, for 2 min), second experiment.

Table 6.8: Continous ultrasonification on FB (20% amplitude, for 2 min): parameters of the distribution curves (mean±standard deviation); D50 and D90 extracted from the cumulative curves; total number of particles calculated with the Sequip-software.

		D50 (μm)	D90 (μm)
<i>First experiment</i>	BT	8,52	19,40
	AT	8,47	17,54
	AST	7,36	17,54
<i>Second experiment</i>	BT	9,52	16,78
	AT	8,02	17,54
	AST	7,36	17,54

6.3 Energetical analysis

6.3.1 Comparison between technologies

The energy required to produce a change Δx of 1 μm in the particles size has been calculated for PF and FB to be able to do a comparison between technologies. The calculation has been done as follow:

$$E = \frac{\int W dt}{(-\Delta x)} \quad (1.11)$$

Where

- W is the average power consumption of the machine without feeding materials (Watt);
- t is the cycle time (s);
- Δx is the difference between the D50 or D90 value after the treatment and the value before the treatment;

The results are reported in Table 6.9. Comparing the specific energies required for a change Δx of 1 μm in the D90, the continuous ultrasonification pre-treatment is the highest one, followed by bead mill and, last, ultrasonification. Also, the energy requirement changes significantly from one technology to the other: around 13.000 J/ μm for continuous ultrasonification, around 7.000 J/ μm for bead mill and around 100 J/ μm for ultrasonification.

An analysis with the D50- Δx value was not possible with the results of the experiments conducted on FB, as the pre-treatment influenced the D50-D90 cut and not the D0-D50 one (see Chapter 6.2.4.1). The specific energy consumption for size reduction in the case of ultrasonification pre-treatment is one order of magnitude bigger looking at the $\Delta D50$ than at the $\Delta D90$, but also for $\Delta D50$ smaller than for bead mill pretreatment.

Table 6.9: Energy required to produce a change Δx in the particles size per 1 gvs of PF and FB with different pre-treatment technologies.

Feedstock	Pre-treatment	gvs		J/ μm (D50)	J/ μm (D90)
Prepared feedstock	Bead mill	3,1	First experiment	21.885	3.984
			Second experiment	9.805	9.258
	Ultrasonification	0,2	First experiment	781	165
			Second experiment	370	27
Fermentation broth	Continuous ultrasonification	1,2	First experiment		10.398
			Second experiment		14.923

6.3.2 Energetical balance

The energy required to treat 1 gvs of PF and FB has been calculated and also related to the LHV of the feedstock to be able to understand if the investigated pre-treatments are energetically sustainable. The calculation has been done collecting some data from the literature, between them some are shown in Table 6.10.

Table 6.10: Sonication operation conditions from the literature.

Reference	Batch /cont.	Time	Power	Specific energy consumption	Frequency	Reactor volume	Power density
[43], [44]	Batch	0-10 min	225 W	280 J/mL			
[43]	Cont. (lab. Scale)				20 kHz	0,1-1 L	0,4-3 W/mL
This work	Batch	2 min	200 W				
This work	Cont. (lab. Scale)				20 kHz	16 mL	

The formula used is the following one:

$$E [J/g_{VS}] = \frac{V \int \hat{W} dt}{S} \quad (1.12)$$

Where

- \hat{W} is the specific power consumption (W/mL), reported in table 6.10;
- V is the pre-treated feedstock's volume (1 mL);
- S is the number of volatile solids contained in the pre-treated feedstock's volume (0,2 g).

For continuous ultrasonification:

$$E [J/g_{VS}] = \frac{\dot{V}\tau \int \hat{W} dt}{S} \quad (1.13)$$

Where

- \hat{W} is the specific power consumption (W/mL), reported in table 6.10;
- \dot{V} is the pre-treated feedstock's flow rate (8 mL/min);
- τ is the residence time in the ultrasonicator's chamber (s), reported in table 6.10;
- S is the number of volatile solids contained in the volume of feedstock pre-treated (1,12 g).

For bead mill the specific energy consumption (J/gvs) was found to be around 0,47 (kWh/kg_{DW}) for biomass' particle diameter of around 0,3 mm [45].

Finally, the percentage of LHV has been obtained using an LHV value of 14,5 KJ/g equal to the one of straw [46].

The results are reported in Table 6.11. The bigger specific energy consumption is the one of continuous ultrasonification pre-treatment, followed by bead mill and, last, ultrasonification. The results replicate what has been seen in the comparison between technologies (Chapter 6.3.1) and, according to them, no pre-treatment used in this work is energetically sustainable, as this is the case of a pre-treatment that requires 1-2% of the biomass LHV.

Table 6.11: Energy required to treat 1 gvs of PF and FB and the %LHV required for the pre-treatment.

Feedstock	Pre-treatment	E (J/gVS)	% LHV
Prepared feedstock	Bead mill	1692	12
	Ultrasonification	1400	10
Fermentation broth	Continuous ultrasonification	2914	20

7. Conclusions

Mechanical pre-treatments are still widely used for a range of industrial processes. In the biotechnological field, especially in the bioenergy recovery through anaerobic digestion, pre-treatments play a key role in the process. The influence of pre-treatments can be divided into the effect produced on the biological phase and the effect on the organic abiotic phase (i.e. substrate). However, most industrial applications require pre-treatment steps that aim at reducing the particle size of the substrate, without compromising the *viability* or *vitality* of the microbial cells that are also present in the system. In this research work, the individual effects on substrate, biomass and combined systems was tested. Moreover, the particle size distribution was studied through different techniques to quantify the influence of each pre-treatment.

First of all, pure cultures of *Clostridium acetobutylicum* and *Bacillus subtilis*, pre-treated with ultrasonification did not result affected, particularly the apparent cell viability as shown by the cells counting performed either with plating or *in situ* laser back-reflection methods. However, the cells counting does not provide a measure of the metabolic state of the cells, which could also be compromised due to application of the pre-treatments. More studies are required to further quantify the full effects on the biological phase due to pre-treatments.

Next, a heterogeneous substrate consisting of a mixture of grass fibres, small residues from bushes and soil in equal parts, diluted with deionised water to approximately 20% (*w/w*) of dry biomass (prepared feedstock) was pre-treated (separately) with bead mill and ultrasonification. In both cases a reduction of the particle size was observed through the *in-situ* laser back-reflection technic and, since this is a substrate with no biological phase in it, the aim of the pre-treatment to make the substrate more soluble was achieved. The calculated energetic requirement was around 10% of the biomass' LHV for the ultrasonification technology, while about 12% for bead mill.

Last, a complex culture broth pre-treated with ultrasonification resulted in a shift of the particle-size distribution to smaller diameters, especially marked in the cut D50-D100 for the case 50% amplitude, while at lower amplitude (i.e. 20%), the effect is less marked and affects mainly the D0-D50 slot, according to *in situ* laser back-reflection method. In this case, with the continuous-flow ultrasonification the energetic requirement reached 20% of the biomass' LHV.

It is, however, opportune to take into consideration that the average particle size changes also from sample to sample of the same pure culture, substrate or fermentation broth and therefore more experimental work is required to assess the behaviour of particular systems.

8. Acknowledgment

I would like to thank my mum to have always been there for me, no matter what.

I would like to thank Piero to have been so comprehensive with me during the exams period and to have me learnt that exams are not at all real problems in life.

I would like to thank Conny for have given to me the advices of a sister in these years.

I would like to thank my dear chemical engineering co-workers (Elga, Flavia, Melania, Fabio and Enrico) for the amazing team work and the fun, essential to survive the university hard times.

I would like to thank Politecnico di Torino for the scholarship I received that allowed me to go to Berlin to write my Master thesis.

I would like to thank Stefan to have me given the opportunity to write my thesis in the BVT Lab.

I would like to thank Professor Ruggeri to have accepted to be my mentor.

I would like to thank “Stefan’s team” (Ewa, Lara, Lucas, Klaus) for the amazing moments I spent with them in the lab, preparing the master thesis.

I would like to thank Adrian to have me given so much support in the past months between last exam, work, applications, interviews and thesis.

I would like to thank Adrian’s family to have been a family to me, offering me a harmonious place to go to in the weekend when the stress was too high.

I would like to thank Carlos for the patience, to have given a meaning to my thesis and to have been the best mentor ever.

9. References

- [1] V. Balan, “Current Challenges in Commercially Producing Biofuels from Lignocellulosic Biomass,” *ISRN Biotechnol.*, vol. 2014, pp. 1–31, May 2014.
- [2] B. Abderezzak, B. Khelidj, A. Kellaci, and M. T. Abbes, “The Smart Use of Biogas: Decision Support Tool,” *AASRI Procedia*, vol. 2, pp. 156–162, 2012.
- [3] S. Piccinini, 2017. “La filiera biogas/biometano: situazione e prospettive,” Modena, Bologna. Web.
- [4] E. C. A. Bordoni, E. Romagnoli, E. Foppa Pedretti Ester, G. Toscano, G. Rossini, 2010. “La filiera del biogas”. Ancona. Web.
- [5] A. Horbelt, M. Maciejczyk, and B. Olzem, 2011. “Biogas can do it”. Berlin, Berlin. Web.
- [6] “EBA launches 6th edition of the Statistical Report of the European Biogas Association - European Biogas AssociationEuropean Biogas Association.” <http://european-biogas.eu/2016/12/21/eba-launches-6th-edition-of-the-statistical-report-of-the-european-biogas-association/>. [Accessed: 06-Apr-2018].
- [7] M. H. Gerardi, 2003. *The Microbiology of Anaerobic Digesters*. Wiley-Interscience.
- [8] R. Conrad, “Contribution of hydrogen to methane production and control of hydrogen concentrations in methanogenic soils,” *FEMS Microb. Ecol.*, vol. 28, no. July, pp. 193–202, 1999.
- [9] P. Bajpai, 2017. *Anaerobic Technology in Pulp and Paper Industry*. SpringerBriefs in Applied Sciences and Technology.
- [10] B. Schink, “Energetics of syntrophic cooperation in methanogenic degradation,” *Microbiol. Mol. Biol. Rev.*, vol. 61, no. 2, pp. 262–280, 1997.
- [11] R. Liaquat *et al.*, “Characterizing Bacterial Consortia from an Anaerobic Digester Treating Organic Waste for Biogas Production,” *Polish J. Environ. Stud.*, vol. 26, no. 2, pp. 709–716, 2017.
- [12] B. P. Tracy, S. W. Jones, A. G. Fast, D. C. Indurthi, and E. T. Papoutsakis, “Clostridia: The importance of their exceptional substrate and metabolite diversity for biofuel and biorefinery applications,” *Curr. Opin. Biotechnol.*, vol. 23, no. 3, pp. 364–381, 2012.
- [13] N. T. Dunford, 2012. *Food and industrial bioproducts and bioprocessing*. John Wiley & Sons.
- [14] Ruggeri, B., Tommasi, T., Sanfilippo, S., 2015. *BioH2& BioCH4 Through Anaerobic Digestion From Research to Full-Scale Applications*. Springer-Verlag, London, London.
- [15] M. Scheftelowitz and D. Thrän, “Unlocking the Energy Potential of Manure—An Assessment of the Biogas Production Potential at the Farm Level in Germany,” *Agriculture*, vol. 6, no. 2, p. 20, 2016.
- [16] A. Salihu and M. Z. Alam, “Pretreatment Methods of Organic Wastes for Biogas Production,” *J. Appl. Sci.*, vol. 16, no. 3, pp. 124–137, 2016.
- [17] A. Mshandete, L. Björnsson, A. K. Kivaisi, M. S. T. Rubindamayugi, and B. Mattiasson, “Effect of particle size on biogas yield from sisal fibre waste,” *Renewable Energy*, vol. 31, no. 14, pp. 2385–2392, 2006.
- [18] C. Rodriguez, A. Alaswad, K. Y. Benyounis, and A. G. Olabi, “Pretreatment techniques

used in biogas production from grass,” *Renew. Sustain. Energy Rev.*, vol. 68, no. October 2016, pp. 1193–1204, 2017.

- [20] L. Montgomery and G. Bochmann, 2014. “Pretreatment of feedstock for enhanced biogas production,” *IEA Bioenergy*, Vienna.
- [21] “Ball Mill Loading - Dry Milling.” <http://www.pauloabbe.com/size-reduction/resources/ball-mill-loading-dry-milling>. [Accessed: 09-Apr-2018].
- [22] “Milling and Grinding :: Anton-Paar.com.” <https://www.anton-paar.com/corp-en/products/group/milling-and-grinding/>. [Accessed: 09-Apr-2018].
- [23] T. Ishii, 2018. *Nanoparticle Technology Handbook*. Elsevier.
- [24] “Cole-Parmer.” [Online]. Available: <https://www.coleparmer.com/p/ika-t-25-homogenizer-rotor-stator-generators/57887>. [Accessed: 09-Apr-2018]
- [25] S. Goldberg, 2015. “Mechanical/Physical Methods of Cell Distribution and Tissue Homogenization”. Humana Press, New York, NY.
- [26] Moisan M., 2012. “Ultrasonic Pretreatment for Anaerobic Digestion : a Study on Feedstock , Methane Yield , and Energy Balance”. Guelph. Web.
- [27] “Sonicators | Qsonica.” <https://www.sonicator.com/collections/sonicators>. [Accessed: 09-Apr-2018].
- [28] S. Antognoni *et al.*, “Potential Effects of Mechanical Pre-treatments on Methane Yield from Solid Waste Anaerobically Digested,” *Int. J. Environ. Bioremediation Biodegrad.*, vol. 1, no. 1, pp. 20–25, 2013.
- [29] “Ultrasonic liquid processors | Qsonica.” https://www.laboratory-equipment.com/uploads/tech_resources/2015_sonicator_catalog_v29_111015115129.pdf. [Accessed: 09-Apr-2018]
- [30] J. Ariunbaatar, A. Panico, G. Esposito, F. Pirozzi, and P. N. L. Lens, “Pretreatment methods to enhance anaerobic digestion of organic solid waste,” *Appl. Energy*, vol. 123, pp. 143–156, 2014.
- [31] A. Mudhoo, 2012. *Biogas Production: Pretreatment Methods in Anaerobic Digestion*. Wiley, 2012.
- [32] S. Pilli, S. Yan, R. D. Tyagi, and R. Y. Surampalli, “Thermal Pretreatment of Sewage Sludge to Enhance Anaerobic Digestion: A Review,” *Crit. Rev. Environ. Sci. Technol.*, vol. 45, no. 6, pp. 669–702, Mar. 2015.
- [33] H. Li, C. Li, W. Liu, and S. Zou, “Optimized alkaline pretreatment of sludge before anaerobic digestion,” *Bioresour. Technol.*, vol. 123, pp. 189–194, Nov. 2012.
- [34] J. Ariunbaatar, A. Panico, G. Esposito, F. Pirozzi, and P. N. L. Lens, “Pretreatment methods to enhance anaerobic digestion of organic solid waste,” *Appl. Energy*, vol. 123, pp. 143–156, 2014.
- [35] T. V. Fernandes, G. J. Klaasse Bos, G. Zeeman, J. P. M. Sanders, and J. B. van Lier, “Effects of thermo-chemical pre-treatment on anaerobic biodegradability and hydrolysis of lignocellulosic biomass,” *Bioresour. Technol.*, vol. 100, no. 9, pp. 2575–2579, May 2009.
- [36] Y. Chen, J. J. Cheng, and K. S. Creamer, “Inhibition of anaerobic digestion process: A review,” *Bioresour. Technol.*, vol. 99, no. 10, pp. 4044–4064, Jul. 2008.

- [37] D. Deublein and A. Steinhauser, 2011. *Biogas from Waste and Renewable Resources: An Introduction*. Wiley.
- [38] A. K. Kumar and S. Sharma, “Recent updates on different methods of pretreatment of lignocellulosic feedstocks: a review.,” *Bioresour. Bioprocess.*, vol. 4, no. 1, p. 7, 2017.
- [39] A. C. Luongo Malave’, M. Bernardi, D. Fino, and B. Ruggeri, “Multistep anaerobic digestion (MAD) as a tool to increase energy production via H₂ + CH₄,” *Int. J. Hydrogen Energy*, vol. 40, no. 15, pp. 5050–5061, 2015.
- [40] E. Gill and F. S L Brinkman, “The proportional lack of archaeal pathogens: Do viruses/phages hold the key?,” *Bioessays*, vol. 33, pp. 248–254, 2011.
- [41] A. Brognaux, J. Bugge, F. H. Schwartz, P. Thonart, S. Telek, and F. Delvigne, “Real-time monitoring of cell viability and cell density on the basis of a three dimensional optical reflectance method (3D-ORM): Investigation of the effect of sub-lethal and lethal injuries,” *J. Ind. Microbiol. Biotechnol.*, vol. 40, no. 7, pp. 679–686, 2013.
- [42] L. Mancini, S. Rosemann, C. Puccinelli, S. Ciadamidaro, S. Marcheggiani, and F. A. Aulicino, “Microbiological indicators and sediment management,” *Ann. Ist. Super. Sanita*, vol. 44, no. 3, pp. 268–272, 2008.
- [43] S. Pérez-Elvira, M. Fdz-Polanco, F. I. Plaza, G. Garralón, and F. Fdz-Polanco, “Ultrasound pre-treatment for anaerobic digestion improvement.,” *Water science and technology*, vol. 60, no. 6, pp. 1525–1532, 2009.
- [44] C. Bougrier, H. Carrère, and J. P. Delgenès, “Solubilisation of waste-activated sludge by ultrasonic treatment,” *Chem. Eng. J.*, vol. 106, no. 2, pp. 163–169, Feb. 2005.
- [45] P. R. Postma *et al.*, “Energy efficient bead milling of microalgae: Effect of bead size on disintegration and release of proteins and carbohydrates,” *Bioresour. Technol.*, vol. 224, pp. 670–679, 2017.
- [46] K. Anker, Thyö and H. Wenzel, “Life Cycle Assessment of Biogas from Maize silage and from Manure,” *Development*, p. 47, 2007.